UNIVERSITY OF CALIFORNIA,
IRVINE

Virus Fate and Transport During Field-Scale Infiltration

DISSERTATION

submitted in partial satisfaction of the requirements for the degree of

DOCTOR OF PHILOSOPHY

in Civil Engineering

by

Robert Anders

Dissertation Committee:
Professor Constantinos V. Chrysikopoulos, Chair
Professor Brett F. Sanders
Professor Jan Scherfig

2006

The dissertation of Robert Anders
is approved and is acceptable in quality
and form for publication on microfilm:

Committee Chair

University of California, Irvine
2006

Table of Contents

List of Figures

List of Tables

Nomenclature

a_T	specific liquid-solid interface area, L^2/L^3
$a_T^\diamond$	specific air-liquid interface area, L^2/L^3
A	pre-exponential factor.
A_s	Happel sphere-in-cell model correction factor, defined in (3.23).
b	empirical constant.
C	concentration of virus in suspension, M/L^3.
$C^\diamond$	absorbed virus concentration at the air-liquid interface, M/L^3
C°	concentration of non-infective viruses, M/L^3.
C^*	sorbed virus concentration (virus mass/solid mass), M/M.
$C^\bullet$	concentration of suspended viruses in an activated state, M/L^3.
C_g	concentration of viruses in direct contact with solids, M/L^3.
C_0	source concentration of virus in suspension, M/L^3.
C_T	concentration of bromide, M/L^3.
C_{T_0}	source concentration of bromide, M/L^3.
d_p	diameter of grain particle, L.
d_v	diameter of virus, L .
D	hydrodynamic dispersion coefficient, L^2/t.
$\mathcal{D}$	molecular diffusion coefficient, L^2/t.
$\mathcal{D}_e$	effective diffusion coefficient, L^2/t.
D_z	vertical hydrodynamic dispersion coefficient, L^2/t
E_a	activation energy, kJ/mol.
g	acceleration due to gravity, L/t^2.
h	height of recycled water in the test basin, L.
$\hbar$	Planck's constant, 6.626×10^{-34} J/sec.
h_0	air-entry value, L.
H	Hamaker constant, $(M\cdot L^2)/t^2$.
k	liquid to liquid-solid interface mass transfer rate, t^{-1}
$k^\diamond$	liquid to air-liquid interface mass transfer rate, t^{-1}
$\acute{k}$	reaction rate coefficient.
k_c	clogging rate constant, t^{-1} .
k_r	declogging rate constant, t^{-1}.
k_B	Boltzman's constant, $(M\cdot L^2)/(t^2\cdot K)$.
K	unsaturated hydraulic conductivity, L/t
K_d	partition or distribution coefficient, L^3/M
$K^\bullet$	equilibrium constant for the formation of the activated complex.
K_s	saturated hydraulic conductivity, L/t
ℓ_z	distance between injection and sampling locations, L.
m	sub-pulse number indicator .
m_1	first normalized absolute moment.
M	number of sub-pulses.
N_G	gravity group, defined in (**??**.
N_{Lo}	London group, defined in (3.24).
N_{Pe}	Peclet number, defined in (3.27).
N_R	relative size group, defined in (3.25).
q	specific discharge, L/t.
q_0	prescribed specific discharge, L/t.

r_0	effective pore radius at air entry, L.
r_p	average radius of soil particles, L.
r^2	coefficient of determination.
r_1	forward rate coefficient, t^{-1} .
r_2	reverse rate coefficient, $M/(L^3 \cdot t)$.
R	gas constant, 8.314 J/K·mol.
t	time, t.
t_p	duration of the solute pulse, t.
$t_{p(m)}$	time period of a sub-pulse m, t .
T	temperature, in Kelvin.
U	average interstitial velocity, ($U = q/\theta_m$), L/t.
x	spatial coordinate in the horizontal direction, L.
z	spatial coordinate in the vertical direction, L.
Greek Letters	
α	collision efficiency.
α_r	resistivity coefficient, t^{-1}.
α_z	vertical dispersivity, L/t.
α_L	longitudinal dispersivity, L/t.
γ	exponent.
Δt	duration of the breakthrough, t.
$\Delta H^\bullet$	enthalpy of activation, kJ/mol.
$\Delta G^\bullet$	Gibb's free energy of activation, kJ/mol.
$\Delta S^\bullet$	entropy of activation, J/mol·K.
ε	equal to $(1-\theta)^{1/3}$.
ζ	dummy integration variable.
ζ	empirical coefficient.
η	single collector efficiency.
η_0	single collector efficiency for favorable deposition.
θ	porosity of soil (liquid volume/porous medium volume), L^3/L^3.
θ_m	moisture content (liquid volume/porous medium volume), L^3/L^3.
θ_r	residual volumetric moisture content, L^3/L^3.
θ_s	volumetric water content of a saturated porous medium, L^3/L^3.
κ	liquid to liquid-solid interface mass transfer coefficient, L/t.
$\kappa^\diamond$	liquid to air-liquid interface mass transfer coefficient, L/t.
λ	inactivation rate coefficient of suspended viruses, t^{-1}.
λ^*	inactivation rate coefficient of sorbed viruses at the liquid-solid interface, t^{-1}.
$\lambda^\diamond$	inactivation rate coefficient of sorbed viruses at the air-liquid interface, t^{-1}.
$\lambda(t)$	time-dependent inactivation rate coefficient of suspended viruses, t^{-1}.
λ_0	initial inactivation rate coefficient, t^{-1}.
Ω	slope of the Arrhenius plot.
μ	viscosity of the liquid, $M/(L \cdot t)$.
ρ_b	bulk density of the solid matrix (solids mass/aquifer volume), M/L^3.
ρ_f	density of the liquid, M/L^3.
ρ_w	density of water, M/L^3.
ρ_v	density of the virus, M/L^3.
σ	surface tension of water, M/t^2.
τ	dummy integration variable.
τ^*	tortuosity (≥ 1).

ϕ	filter coefficient, L^{-1}.
Φ	defined in (3.19), M/L^3 .

Abbreviations

ATCC	American type culture collection.
CSDLAC	County Sanitation Districts of Los Angeles County.
DOHS	California Department of Health Services.
HG	Harvey and Garabedian [1991] method.
MPN	Most probable number.
PBS	Phosphate buffered saline.
PFU	Plaque forming units.
RB	Relative breakthrough.
TSA	Trypticase soy agar.
TSB	Trypticase soy broth.
USGS	U.S. Geological Survey.
WRD	Water Replenishment District

Acknowledgments

I wish to express sincere appreciation to my graduate advisor Professor Constantinos V. Chrysikopoulos for his support and guidance. I also appreciate the contributions from my other dissertation committee members, Professor Brett Sanders and Professor Jan Scherfig. I would also wish to acknowledge two people who had a significant impact on my academic career. Dr. Roy A. Schroeder, my supervisor at the U.S. Geological Survey (USGS) until his retirement. Roy allowed me the necessary flexibility at work to pursue my research interests. The other was William A. Yanko from the County Sanitation Districts of Los Angeles County (CSDLAC). Bill saw the merit in this research and assisted me, along with James L. Leserman and Hoover Hg from the Water Replenishment District of Southern California, in obtaining the funds for a majority of this work as part of the Soil Aquifer Treatment for Sustainable Water Reuse research program. I am also grateful to other CSDLAC and USGS personnel for their assistance in conducting the field-scale experiments, especially the folks at the Virology Laboratory including Shawn, Jim, Alan, Letty, and Mila. I also wish to thank my university colleagues Dr. Eric T. Vogler, Dr. Dave Jaffe, and Matt Thomas for their friendships at the university.

I must not forget my wife Patty for her unwavering patience and encouragement throughout my time at UC Irvine. Thank you for allowing me to put our lives on hold while I pursued a personnel dream. To my son, Tyler, I tried to set the bar high. Now I will spend my life helping you get over it.

Curriculum Vitae

Robert Anders, Hydrologist
UNITED STATES GEOLOGICAL SURVEY
California Water Science Center, San Diego Projects Office
4165 Spruance Road, Suite 200
San Diego CA 92101-0812
(619) 225-6155 [phone]
(619) 225-6101 [fax]
randers@usgs.gov [email]

Academic Essentials

Education

Ph.D.:	Civil Engineering (Water Resources), 2006 UNIVERSITY OF CALIFORNIA, IRVINE
Master of Science:	Geological Science, 1997 SAN DIEGO STATE UNIVERSITY
Bachelor of Science:	Geological Science, 1991 SAN DIEGO STATE UNIVERSITY

Employment History

(1997 –) HYDROLOGIST, USGS, San Diego, California.
(1991 – 97) PHYSICAL SCIENTIST, USGS, San Diego, California.

Awards and Honors

USGS Special Achievement Cash Awards, 1997, 1998, 2003
UCI Regents Fellow 2004, 2005

Scientific Society Memberships

American Geophysical Union (AGU)

List of Publications

Professional Papers:

ANDERS, R., and C.V. CHRYSIKOPOULOS, Transport of bacteriophage (MS2 and PRD1) through variably saturated packed sand columns, in preparation.

ANDERS, R., and C.V. CHRYSIKOPOULOS, Evaluation of the factors controlling the time-dependent inactivation rate coefficients of bacteriophage MS2 and PRD1: Environmental Science & Technology, accepted.

ANDERS, R., and C.V. CHRYSIKOPOULOS, Virus fate and transport during artifical recharge with recycled water: Water Resources Research, 41, W10415, doi:10.1029/2004WR003419.

ANDERS, R., W.A. YANKO, R.A. SCHROEDER, and J.L. JACKSON, Virus fate and transport during recharge using recycled water at a research field site in the Montebello Forebay, Los Angeles County, California, 1997-2000: U.S. Geological Survey Scientific Investigation Report 2004-5161, 65 p., 2004.

ANDERS, R., and R.A. SCHROEDER, Use of water-quality indicators and environmental tracers to determine the fate and transport of recycled water in Los Angeles County, California: U.S. Geological Survey Water-Resources Investigations Report 03-4279, 104 p. 2003.

SCHROEDER, R.A., R. ANDERS, L.B. BARBER, II, J.A. LEENHEER, T.I. NOYES, R.T. RATHBUN, K.A. THORN, and S.J. YOUNGER, Water-quality changes and organic-carbon characterization during recharge with recycled water at a recharge basin in Montebello Forebay, Los Angeles County, California: U.S. Geological Survey Water-Resources Investigations Report, 260 p. 2003.

LEENHEER, J.A., C.E. ROSTAD, L.B. BARBER, R.A. SCHROEDER, R. ANDERS, and M.L. DAVISSSON, Nature and chlorine reactivity of organic constituents from reclaimed water in groundwater, Los Angeles, County, California: Environmental Science & Technology, v. 35, p. 3869-3876, 2001.

Proceedings Papers:

ANDERS, R., and C.V. CHRYSIKOPOULOS, Evaluation of the factors controlling the time-dependent inactivation rate coefficients of bacteriophage MS2 and PRD1, Proceedings of the 3rd European Bioremediation Conference, Chania, Crete, Greece, p. 136, 2005.

ANDERS, R., and C.V. CHRYSIKOPOULOS, Transport of bacteriophage (MS2 and PRD1) during field-scale infiltration: Proceedings of the 2nd European Bioremediation Conference, Chania, Crete, Greece, pp. 49-52, 2003.

SCHROEDER, R.A., R. ANDERS, Transport and fate of water-quality indicators after 40 Years of artificial recharge with treated municipal wastewater to the Central Ground-Water Basin in Los Angeles County: U.S. Geological Survey Artificial Recharge Workshop Proceedings, Sacramento, California, April 2-4, 2002: U.S. Geological Survey Open-File Report 02-89, p. [tk], 2002.

ANDERS, R., and R.A. SCHROEDER, Water-quality changes during recharge with recycled water at a research basin in the Montebello Forebay, Los Angeles County, California, in Proceedings of the AWRA 33rd National Meeting on Symposium on Conjunctive Use of Water Resources: Aquifer Storage and Recovery, California American Water Resources Association, TPS-97-2, 285-296, 1997.

SCHROEDER, R.A., R. ANDERS, J.K. BÖHLKE, R.L. MICHEL, and D.W. METGE, Water quality at production wells near artificial-recharge basins in Montebello Forebay, Los Angeles County, in Proceedings of the AWRA 33rd National Meeting on Symposium on Conjunctive Use of Water Resources: Aquifer Storage and Recovery, California American Water Resources Association, TPS-97-2, 273-284, 1997.

Conference Papers:

ANDERS, R., and C.V. CHRYSIKOPOULOS, A comparison of transport parameters for viruses and colloidal-sized microspheres during flow through variably-saturated porous media: American Geophysical Union, Fall Meeting, Supplement, San Francisco, California, December 5-9, 2005, H21E-1385, 2005.

ANDERS, R., and C.V. CHRYSIKOPOULOS, Transport parameters for bacteriophage (MS2 and PRD1) and colloidal-sized microspheres during flow through variably saturated porous media (abs.): Joint International Symposia for Subsurface Microbiology (ISSM 2005) and Environmental Biogeochemistry (ISEB XVII), August 15-19, 2005, Jackson Hole, Wyoming, p. 109-110, 2005.

ANDERS, R., and C.V. CHRYSIKOPOULOS, Evaluation of the factors controlling the time-dependent inactivation rate coefficients of bacteriophage MS2 and PRD1, Proceedings of the 3rd European Bioremediation Conference, Chania, Crete, Greece, p. 136, 2005.

ANDERS, R., and C.V. CHRYSIKOPOULOS, Transport parameters for bacteriophage (MS2 and PRD1) and colloidal-sized microspheres during flow through variably-saturated porous media: American Chemical Society, 229th ACS National Meeting, San Diego, California, March 13-17, 2005, Program, Abstract no. Coll 69, 2005.

ANDERS, R., and C.V. CHRYSIKOPOULOS, Evaluation of the factors that control the time-dependent inactivation rate coefficients of bacteriophage MS2 and PRD1: American Geophysical Union Fall Meeting, San Francisco, December 13-17, 2004, EOS Transactions Supplement, v. 85, no. 47, Abstract no. H21A-1000, 2004.

ANDERS, R., and C.V. CHRYSIKOPOULOS, Fate and transport of bacteriophage (MS2 and PRD1) during field-scale infiltration: American Geophysical Union Fall Meeting, San Francisco, December 8-11, 2003, EOS Transactions supplement, v. 84, no. 46, Abstract no. H11G-0930, 2003.

ANDERS, R., W.A. YANKO, R.A. SCHROEDER, and J.L. JACKSON, Attenuation rates for bacteriophage MS2 and PRD1 during field-scale infiltration: Boulder, Colorado, The Geological Society of America, 2002 Annual Meeting and Exposition, Denver, Colorado, Final Program, Abstracts, Paper 69-6, 2002.

ANDERS, R., and R.A. SCHROEDER, Using environmental tracers to determine long-term effects of recharging recycled water in the Central Ground Water Basin, Los Angeles County, California: Eos, Transaction of the American Geophysical Union, v. 82, no. 47, Suppl., Abstract no. H51C-0338, 2001.

ANDERS, R., W.A. YANKO, R.A. SCHROEDER, and J.L. JACKSON, Attenuation rates for PRD1 and MS2 during artificial recharge with recycled water at a research basin in Los Angeles County: American Geophysical Union Spring Meeting, Washington, D.C., May 30-June 3, 2000, EOS Transactions supplement, v. 81, no. 19, Abstract no. H41C-04, p. S226-S227, 2000.

ANDERS, R., W.A. YANKO, R.A. SCHROEDER, and J.L. JACKSON, Attenuation of PRD1 and MS2 during recharge at a constructed research basin in Los Angeles County: 4th International Symposium on Subsurface Microbiology, Vail, Colorado, August 22-27, 1999, Programs and abstracts, p. 28, 1999.

Abstract of the Dissertation

Virus Fate and Transport During Field-Scale Infiltration

by

Robert Anders

Doctor of Philosophy in Civil Engineering

University of California, Irvine, 2006

Constantinos V. Chrysikopoulos, Chair

The use of treated municipal wastewater effluent (recycled water) for artificial recharge of groundwater is increasing, especially in the southwestern United States. In many areas artificial recharge is accomplished by delivering large amounts of water, including recycled water, to large holding ponds, or spreading grounds. One concern with using recycled water is that active/infective human enteric viruses might be delivered with the recycled water to the spreading grounds. Therefore, an accurate determination of adequate soil-retention time and distance requirements are necessary to avoid possible ground-water contamination by these microorganisms.

To investigate the complex mechanisms governing the fate and transport of viruses during infiltration, a field-scale experiment was conducted at a research site using bacterial viruses (bacteriophage) MS2 and PRD1 as surrogates for human viruses, bromide as a conservative tracer, and tertiary-treated municipal wastewater (recycled water). Observed virus concentrations were fitted using a mathematical model that simulates virus transport in one-dimensional, homogeneous, water-saturated porous media accounting for virus sorption (or filtration), virus inactivation, and time-dependent source concentration. The fitted time-dependent clogging rate constants were used to estimate the collision efficiencies for bacteriophage MS2 and PRD1 during vertical fully-saturated flow.

Static and dynamic batch experiments were conducted to study the effects of temperature and the presence of sand on the inactivation of bacteriophage MS2 and PRD1. The experimental data suggested that the inactivation process can be satisfactorily represented by a pseudo first-order

expression with time-dependent rate coefficients. The time-dependent rate coefficients were used to determine pertinent thermodynamic properties required for the analysis of the molecular processes involved in the inactivation of each bacteriophage. A combination of high temperature and the presence of sand appears to produce the greatest disruption to the surrounding protein coat of MS2. However, the lower activation energies for PRD1 indicate a weaker dependence of the inactivation rate on temperature. Instead, the presence of air-liquid and air-solid interfaces appears to produce the greatest damage to specific viral components that are related to infection.

Laboratory-scale transport experiments were conducted in columns packed with sand under saturated and unsaturated conditions. The viruses employed were the male-specific RNA coliphage, MS2, and the *Salmonella typhimurium* phage, PRD1. A mathematical model developed to quantify the processes responsible for removal of viruses during vertical transport in one-dimensional, unsaturated porous media that accounts for virus sorption and inactivation was used to fit the data collected from the laboratory experiments. The liquid to liquid-solid and liquid to air-liquid interface mass transfer rates used to simulate the concentration histories were shown to increase for both bacteriophage as saturation levels were reduced. The experimental results indicate that even for unfavorable attachment conditions within a sand column, saturation fluctuations can dramatically affect virus transport through porous media.

Chapter 1

Introduction

1.1 Significance of Research

Managers of planned ground-water recharge programs facing water shortages intentionally recharge groundwater using treated municipal wastewater effluent (recycled water) to supplement the existing water supply. As a result, the use of recycled water for artificial recharge of ground water is increasing, especially in the southwestern United States. The practice of artificially recharging ground-water basins is accomplished by delivering water, including recycled water, into large holding ponds or spreading grounds, where the water infiltrates through the unsaturated zone to the water table and moves downgradient to drinking-water aquifers. During the practice of artificial recharge using recycled water, the soil is considered the final step in a multi-barrier treatment system to protect public health [National Research Council, 1994].

In California, the Department of Health Services (DOHS) governs the recharge of ground water with recycled water under Title 22 of the California Administrative Code [Barclays California Code of Regulations, 1978; California Department of Health Services, 1978]. In addition to ensuring compliance with the common drinking-water standards for all constituents, these regulations state that the proportion of recycled water in the total recharge to an area is limited to 50 percent annually and to 35 percent within three contiguous years. However, as the demand for drinking

water continues to increase, water agencies are seeking to increase the percent of recycled water currently permitted for artificial recharge. Recently, the DOHS proposed new regulations for increasing the recycled water contribution for ground-water recharge projects in California. These new regulations limit the amount of nitrogen compounds to 3 mg/L total nitrogen in the recycled water used for ground-water recharge and sets an unregulated- and unknown-contaminant control level at 0.5 mg/L total organic carbon [R. Hultquist, DOHS, oral commun., 2002]. Furthermore, these new regulations establish a new compliance point at the mound formed beneath the infiltration basin during recharge, eliminating any removal of nitrogen or organic carbon during subsurface transport as part of the consideration to meet the newly established contaminant levels. These new regulations being proposed are due partially to the lack of information on the fate and transport of wastewater constituents as they travel from the point of recharge to points of withdrawal or the long-term effects that artificial recharge with recycled water has on the quality of the ground water in the basin. Because of the possibility that human enteric viruses might make it to the spreading grounds, these draft regulations state that the applied recycled water used for a surface-spreading project shall be retained underground for a minimum of 6 months prior to extraction for use as a drinking water supply, and shall not be extracted within 500 feet (152 m) of the point of recharge [Hultquist et al., 1991; Asano and Cotruvo, 2004]. These provisions are intended to protect ground-water resources by ensuring that adequate soil-retention time and distance requirements are met for pathogen removal. Therefore, a better understanding is needed to quantify how to make effective use of the soil to protect public health in planned water-reuse programs. Such an understanding would provide regulatory agencies with the information necessary to determine allowable limits on amounts of recycled water that can be used for replenishment purposes while ensuring that adequate soil-retention time and distance requirements for pathogen removal are being met.

Several laboratory- or field-scale experiments have been conducted to investigate the magnitude of adsorption and inactivation of viruses under saturated conditions [Bales and others, 1997; Jin and others, 1997; Pieper and others, 1997; Deborde and others, 1999; Ryan and others, 1999; Schi-

jven and others, 1999]. Although laboratory experiments and mathematical modeling can provide partial understanding of virus transport in the subsurface, they have some important limitations [Yates, 1995]. These limitations are due, in large part, to the high degree of uncertainty associated with site-specific information on the virus inactivation rate and adsorption to soil. This is because many of the factors controlling virus transport and inactivation are interrelated. Furthermore, during artificial recharge, the subsurface beneath spreading grounds can exhibit significant changes in water flux and hydraulic conditions over time due to the presence of trapped air, sealing of the soil surface, and the effect of biofilms sealing the pores within the wetted zones [Faybishenko, 1995] conditions difficult to replicate in controlled laboratory experiments. For instance, reversible sorption and inactivation of viruses in laboratory-scale column experiments are typically negligible due to short residence times [Tufenkji et al., 2003]. However, any attempt to evaluate field-scale virus transport under water saturated flow conditions requires the determination of desorption rate constants as well as inactivation constants of suspended and sorbed viruses [Schijven et al., 2003]. Therefore, field-scale experiments using surrogates for human viruses also are needed to more accurately determine the influence of distance and time on virus attenuation during subsurface transport under actual recharge conditions.

1.2 Prior Recharge Studies

In Los Angles County approximately 60 km^3 of recycled water is delivered annually to the Montebello Forebay in the northern part of the Central Ground-Water Basin. The recycled water, along with imported water and local runoff, is applied to two large spreading grounds and a portion of an unlined downstream river channel that have a total area of recharge of almost 3.5 km^2. The recharged water moves down and laterally from the area of the spreading grounds southwest in the direction of regional ground-water flow [Reichard et al., 2003]. Aquifer material beneath the spreading grounds consists of alluvial deposits of nearly all sands and gravels, with some relatively fine-grained materials of possibly limited extent [Bookman-Edmonston Engineering Inc., 1994].

A research field site was constructed at the north end of the San Gabriel River Coastal Basin Spreading Grounds in the Montebello Forebay, Los Angeles County to better understand the chemical and microbiological processes that contribute to the changes in the quality of the recycled water during artificial recharge. A map of the research field site location is shown in Figure 1.1.

Tertiary-treated effluent from the San Jose Creek Water Reclamation Plant, which has undergone chlorination-dechlorination and either mono- (anthracite only) or dual-media (anthracite and sand) filtration, is delivered through a 2.4-m-diameter culvert to the spreading grounds. A portion of the flow can be diverted on demand to the research field site through a 15.2-cm pipeline using a 1,100-m^3/d pump installed in the culvert. During construction of the research field site, overlying fine-grained soil was excavated from the desilting basin to expose a well-sorted sand and gravel unit about 3 m below the local land surface. The excavated silty soil was used to construct a berm around the test basin to isolate it from the desilting basin in the adjacent large spreading grounds. Construction exposed an effective percolation area of about 500 m^2 at a maximum operating water depth of about 2.4 m.

Three recharge experiments were conducted at the research field site in August 1993; April-June, 1994; and in July 1995. Although the primary focus of analyses during the recharge experiments was on a broad suite of inorganic, isotopic, and organic constituents, some analyses also were done for microorganisms. These recharge experiments showed: (1) reduction of nitrogen was slightly greater than one-third, although actual removal rates can vary under different environmental and operational conditions; (2) reduction of organic carbon was about one-third regardless of pre-existing conditions at the research field site; and (3) the total and fecal coliform bacteria distributions in subsurface water samples from beneath the research field site increased from nondetectable levels immediately before recharge with recycled water. Complete results of the inorganic, isotopic, organic, and microbiological analyses from the three recharge experiments are presented in other reports [Anders and Schroeder, 1997; Schroeder et al., 2003].

A more comprehensive study of inorganic, isotopic, and organic analyses at 23 production wells

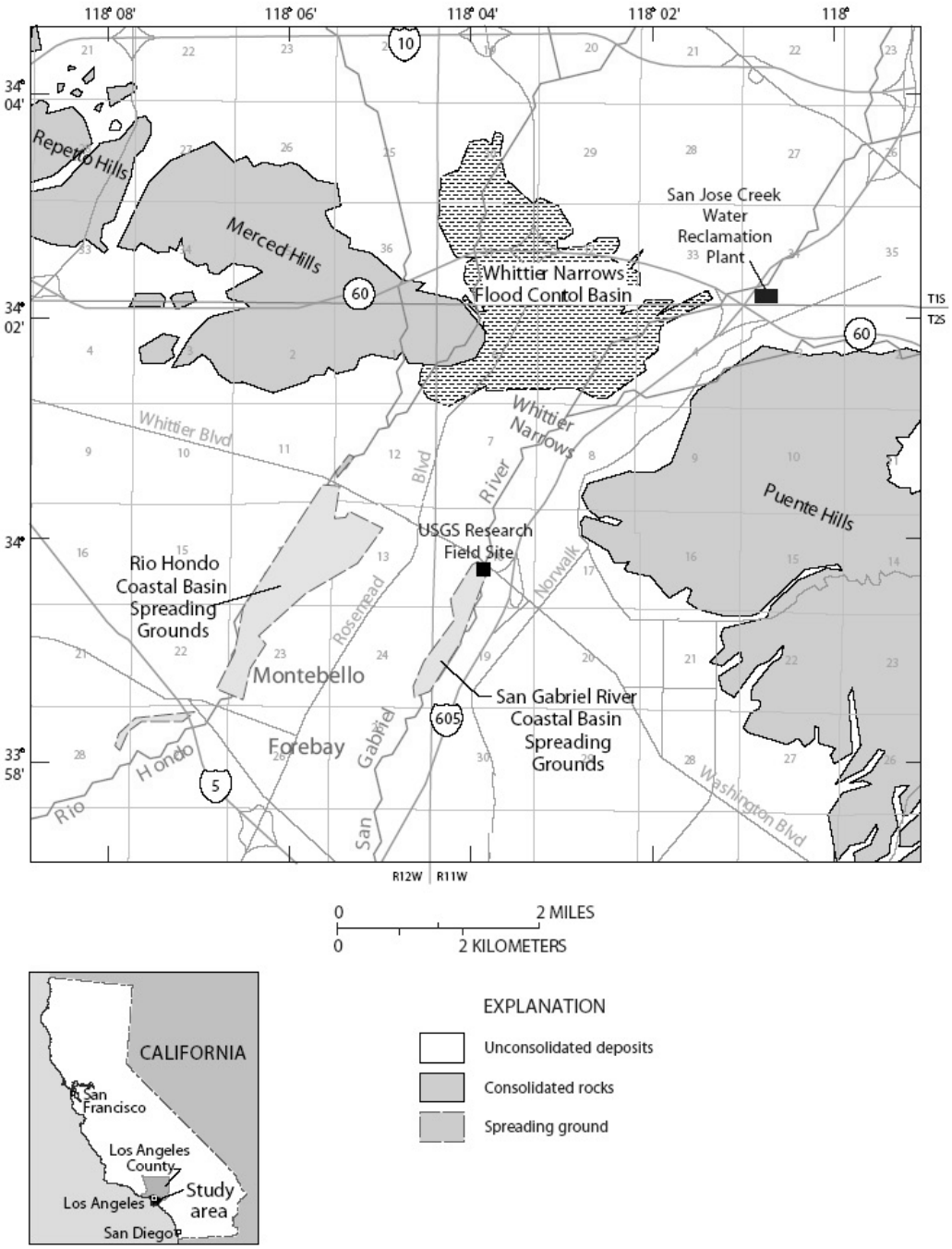

Figure 1.1: Location of the research field site in Los Angeles County, California.

within 500 ft (152 m) of the San Gabriel and Rio Hondo Coastal Basin Spreading Grounds in the Montebello Forebay located in Los Angeles County was conducted to ascertain which constituents of wastewater origin could be identified and used as tracers to determine the presence and estimate the percent of recycled water [Barber et al., 1997; Schroeder et al., Anders et al., 2003]. No completely quantitative tracer was identified although chloride, boron, ultraviolet absorbance at 254 nanometers, and excitation-emission fluorescence seemed to yield the most reasonable estimates.

Leenheer et al., [2001] focused on the nature and chlorine reactivity of organic constituents in recycled water before, during, and after recharge at the Montebello Forebay in Los Angeles County. They found that the dissolved organic matter (DOM) in the recycled water was altered, or selected fractions were preferentially degraded, into less polar constituents in the reducing ground-water environment. Furthermore, the mixing of recycled water with ground water does not appear to degrade the ground-water quality with respect to the production of chlorinated disinfection byproducts in drinking water. Finally, the major components of DOM in recycled water are sulfonic acid metabolites of anionic surfactants. The sulfonic acid metabolites are the only specific organic compounds that survived long-distance transport and are found in the 23 production wells.

Tritium-helium ($^3H/^3He$), chlorofluorocarbons (CFCs), dissolved gases, and nitrogen isotopes were analyzed in five multilevel monitoring wells along a 10-mile flow path extending from just upgradient of the spreading grounds southward through the Central Basin to investigate the long-term effects that artificial recharge using recycled water has on the quality of the ground-water basin [Anders et al., 2003]. Tritium-helium age determinations indicated that sampled groundwater samples range in age from less than 2 to more than 50 years. Chloride and boron concentrations, along with $^3H/^3He$ age determinations, indicate more rapid recharge and/or displacement of pre-existing ground water at the San Gabriel Coastal Basin Spreading Grounds than at the Rio Hondo Coastal Basin Spreading Grounds. Nitrogen-15 enrichment of the ground-water nitrate and dissolved nitrogen indicates that denitrification, an important process for the removal of nitrate at the shallower depths beneath the spreading grounds, continues to occur even at times and distances from the

spreading grounds of many years and over several miles. Analysis of dissolved gases shows that areas that contain recycled water have no detectable methane, whereas methane is present in the native ground water older than 50 years. The absence of methane in the younger ground water suggests that artificial recharge using recycled water has the desirable effect of increasing slightly the redox potential of the ground-water basin. Finally, measured chlorofluorocarbon concentrations and tritium-helium age determinations indicate that chlorofluorocarbon concentrations are markedly elevated above atmosphere-water equilibrium in ground water older than about 20 years but still young enough to contain recycled water.

Evidence that bacteria can move through the soil along with the percolating recycled water during artificial recharge occurring over intervals of several days and vertical and horizontal distances of about 10 m formed the basis for three field-scale tracer experiments [Anders et al., 2004]. The tracer experiments were conducted during August 1997; August-September 1998; and August 2000 to determine the fate and transport of viruses released into the environment during artificial recharge using recycled water. The specific goal of the first experiment was to establish the feasibility of conducting field-scale tracer experiments under actual artificial recharge conditions using recycled water seeded (augmented) with high concentrations of bacteriophage and bromide as tracers. On the basis of the results of the first tracer experiment, a second tracer experiment was designed to measure more precisely the fate and transport of surrogates for human viruses under actual recharge conditions. The third tracer experiment was done during the summer of 2000 to confirm the results obtained from the second tracer experiment. These experiments indicated that rapid reduction occurs in the concentration of bacterial viruses released into the environment with recycled water during aquifer recharge. Furthermore, these tracer experiments suggest that adsorption, not inactivation, is the predominant removal mechanism for viruses during aquifer recharge. However, these tracer experiments were conducted under saturated conditions. But if the source of groundwater contamination is from artificial recharge with recycled water, the pathogenic viruses that are present in the source water might infiltrate through an unsaturated zone before reaching

the water table. Therefore, since it has been shown that the presence of air-water interfaces serve as sorption sites for viruses and enhance inactivation, an attempt to predict the degree of virus attenuation during vertical transport through unsaturated soil would need to include the relationship between moisture content, sorption, and inactivation of viruses at the air-water interface as well as the solid-liquid interface.

1.3 Research Objectives

The overall objective of this research is to understand fully the complex mechanisms governing the transport and fate of viruses during field-scale infiltration. To accomplish this, numerical simulations will be performed with a newly developed mathematical model using data collected from a recently completed field-scale virus transport experiments. Furthermore, static and dynamic batch experiments will be performed to compare the effects of temperature and the presence of soil on the inactivation process of viruses. Finally, carefully controlled bench-scale virus transport column experiments will be conducted under saturated and unsaturated conditions to quantify the processes responsible for removal of viruses during vertical transport through unsaturated porous media. The specific objectives of the proposed research are:

- to estimate the collision efficiencies for bacteriophage MS2 and PRD1 during vertical fully-saturated flow;
- to determine the inactivation rate coefficients of viruses in the liquid phase, viruses sorbed at the liquid-solid interface, and viruses sorbed at the air-liquid interface;
- to measure virus liquid to liquid-solid and liquid to air-liquid interface mass transfer rate coefficients.

1.4 Organization of Dissertation

This dissertation is divided into 7 chapters. Chapter 1 is an introduction containing previous recharge studies conducted at the research field site and an outline of the specific objectives of this research. Chapter 2 provides the literature review.

Chapter 3 presents fitted clogging and declogging rate constants as well as the inactivation constants of suspended and sorbed viruses obtained from a newly developed mathematical model that simulates virus transport in one-dimensional, homogeneous, water-saturated porous media accounting for virus sorption (or filtration), virus inactivation, and time-dependent source concentration. The fitted time-dependent clogging rate constants were used to estimate the collision efficiencies of bacteriophage MS2 and PRD1 during vertical fully water-saturated flow.

Chapter 4 presents the effects of temperature and the presence of sand on bacteriophage MS2 and PRD1 inactivation. The inactivation process was satisfactorily represented by a pseudo first-order expression with time-dependent rate coefficients.

Chapter 5 presents the calibrated liquid to liquid-solid and liquid to air-liquid interface mass transfer rates for virus concentration data collected from laboratory experiments conducted with packed sand columns under saturated and unsaturated conditions.

The significance of the results of this research is presented in Chapter 6 along with possible applications. Chapter 7 summarizes and presents the major conclusions of this research with recommendation for future research.

Chapter 2

Literature Review

2.1 Virus Transport in Saturated Porous Media

2.1.1 Virus Sorption

The degree of virus sorption during subsurface transport is affected by several factors including viral surface properties, groundwater quality, and sediment surface charges [Gerba, 1984]. Since these small virus particles are of a colloidal nature due to their very small size relative to the porous media grain size, it is expected that theories describing colloidal behavior are applicable to viruses in dispersion medium [Gerba, 1984]. Virus particles behave as small proteinaceous colloids having coats or capsids either totally or partially composed of polypeptides. The presence of amino acids in the polypeptides introduce weakly acidic and basic groups to the viral capsid, and the virus particle develops a charge by protonation and deprotonation of these exposed ionizable groups. To maintain the electrically neutral system, the charge of the virus particle immersed in an electrolyte solution is compensated by an equivalent but opposite charge absorbed at the aqueous side of the interface. This separation of charge into two planes produce the so-called double layer. If the bulk solution of oppositely charged ions increases by addition of cationic salts or increasing pH, the thickness of this layer decreases because less volume is required to contain enough oppositely charged ions to neutralize the surface charge. The reduction of the thickness of this layer facilitates

the approach of the two surfaces, allowing van der Waals forces to have an effect. These interactions between two particles in a dispersion resulting from an attempt to obtain a balance between repulsive double-layer interactions and attractive van de Waals forces is described by the Derjaguin-Landau-Verwey-Overbeek (DLVO) theory of colloidal stability. Each ionizing group in the polypeptide has a characteristic dissociation constant, and the spread of these dissociation constants ensures that most viruses have net charges that vary continuously with pH. At a characteristic pH, defined as the isoelectric point (pH_{iep}), ionization is such that the virus particle exists in a state of zero net charge. Although the surface properties vary from virus to virus, if their pH_{iep}s are known, much of their behavior in dilute electrolytes can be predicted.

Taylor and Bosman [1982] and Moore et al. [1982] investigated the electrokinetic behavior of reovirus type 3 suspended in dilute aqueous suspensions of simple electrolytes by laser-illuminated whole-particle microelectrophoresis. They describe the interaction of viruses with the porous media as a charged colloid approaching a like-charged solid surface and adsorption would only occur if there were attractive interactions between the virus and the solid that exceeded the repulsive forces from overlay of double layers at each surface. Several others have applied the DLVO theory of colloidal stability to describe the interaction of viruses with the porous media [Grosser, 1984; Tim and Mostaghimi, 1991; Park et al., 1992; Vilker et al., 1978; Sim and Chrysikopoulos, 1996, 1998, 1999; Chrysikopoulos and Sim, 1996].

Realizing many factors control the adsorption of viruses to soils, different techniques have been developed to determine the appropriate rate expressions. Vilker and Burger [1980] identified the adsorption process as either irreversible, where no detachment occurs, or reversible, and applied mass transfer models to represent the non-equilibrium adsorption process of viruses during subsurface transport. Mass transfer adsorption models account for the transfer of viruses from the bulk liquid to a liquid-solid interface by virus diffusion through an outer liquid layer surrounding the soil particle whose thickness depends on local hydrodynamic conditions.

Other investigators described the physical and chemical factors that influence the adsorption

process of colloids and viruses to a surface by the colloid-filtration model [Bales et al., 1991; Kinsohita et al., 1993; Sim and Chrysikopoulos, 1995; Penrod et al., 1996; Pieper et al., 1997; Redman et al., 1997; DeBorde et al., 1999; Ryan et al., 1999; Schijven et al., 1999], commonly used to describe the removal of colloidal particles during pack-bed filtration in water-treatment applications [Yao et al., 1971]. The different physical-chemical mechanisms which play a role in particle removal are straining, gravitational sedimentation, interception, and Brownian diffusion [McDowell-Boyer et al., 1986]. The colloid filtration model assumes that particle attachment is governed by the collision efficiency which represents the ratio of the rate of collisions resulting in attachment to the total number of collisions [Rajagopalan and Tien, 1976; Tufenkji and Elimelech, 2003]. The magnitude of adsorption of viruses through packed columns was also investigated by fitting experimental breakthrough curves to different one-dimensional advection-dispersion models [Bales et al., 1991; Jin et al., 1997; Bales et al., 1997]. Lastly, analytical solutions were also developed for virus transport in one- and three-dimensional saturated, homogeneous porous media, accounting for virus sorption and inactivation [Sim and Chrysikopoulos, 1995; Sim and Chrysikopoulos, 1998].

2.1.2 Inactivation

The other major process controlling the ability of viruses to travel long distances through the subsurface, besides sorption, is their rate of inactivation [Gerba and Keswick, 1981; Chrysikopoulos and Sim, 1996]. Inactivation of liquid phase as well as sorbed or attached viruses is due to degradation of the viral capsid. In general, inactivation of viruses is influenced by the specific virus type, nature of the soil, and the climate (especially rainfall and temperature) of the environment, although the exact mechanisms whereby these factors affect the inactivation of viruses are not fully understood [Yates et al., 1985].

Hurst et al. (1980) produced bivariate scatter diagrams to statistically evaluated the effects of several environmental factors on virus survival in one system. Individual factors on virus survival indicated the following: (1) the survival slopes and incubation temperatures showed a statistically

significant reciprocal correlation, indicating that virus survival decreased with increasing temperature; and (2) the concentration of sewage effluent used to wet the soil did not correlate with virus survival. Similarly, Yates et al., [1985; 1988] found the single important factor controlling the degree of virus inactivation in the subsurface is temperature. Yahya et al. [1993] evaluated the survival of two bacteriophage which are potentially useful models for studying the fate and transport of pathogenic enteric viruses and other biocolloids through soil and groundwater. These studies have found that groundwater temperature is highly correlated with the inactivation rate of viruses in groundwater.

However, protection against inactivation by adsorption to soil and mineral particulates has also been reported in the literature. Sobsey et al. [1980] concluded that these soil-protective effects suggest that viruses in saturated soils may remain infectious for considerable periods of time, even at a moderate temperature of 20oC where the soil is microbially active. Yates and Ouyang [1992] suggested that the solid matrix provides a protective effect by reducing the inactivation rate coefficients of viruses sorbed onto the liquid-solid interface.

2.2 Virus Transport in Unsaturated Porous Media

Investigations by Lance and Gerba [1984] reported that a reduction in soil moisture content enhances virus sorption as well by forcing viruses to move into a thin film of water surrounding soil particles. Others have noted that virus sorption is strongly correlated with the degree of soil moisture due to the presence of solid-water and air-water interfaces in unsaturated porous media [Powelson et al. 1990; Wan and Wilson, 1994]. By conducting well-controlled studies under unsaturated conditions, Jin et al. [2000] contributed the presence of an air-water interface for the observed increase in the removal of two bacteriophage. Chu et al. [2001] suggested the water content effect heavily depends upon the properties of the solid surface and the virus type, and in the absence of a reactive solid-water interface the reactions at the air-water interface may become more pronounced and be accentuated at low water contents.

Besides virus sorption, soil moisture content is an important controlling factor for virus inactivation in unsaturated porous media. Trouwborst et al. [1974] reported that when viruses are adsorbed at air-water interfaces, the interfacial tension along a virus particle creates a deforming force, which results in disruption of coat protein of viruses, and consequently enhances virus inactivation. Further investigation by Thompson et al. [1998] and Thompson and Yates [1999] suggested that the presence of the air-liquid-solid interfacial forces caused the increased inactivation of a relatively hydrophobic virus in tubes composed of hydrophobic solid surfaces but not in tubes which had hydrophilic solid surfaces. Therefore, virus inactivation resulting from interfacial tension at the air-liquid interface is clearly distinguishable from thermoinactivation (due to temperature effect).

Chapter 3

Virus Fate and Transport During Artificial Recharge with Recycled Water

In this work,, virus concentrations measured during a field-scale tracer experiment were fitted using a newly developed mathematical model that simulates virus transport in one-dimensional, homogeneous, water-saturated porous media accounting for virus sorption (or filtration) and inactivation. The analytical solution is also applicable to the special case of time-dependent source concentration. The fitted clogging and declogging rate constants as well as the inactivation constants of suspended and sorbed viruses were used to estimate the collision efficiency of bacteriophage MS2 and PRD1 during vertical fully water-saturated flow. Finally, the development of an optimal management scenario that can maximize the amount of recycled water applied to the spreading grounds while still maintaining favorable attachment conditions for virus retention is discussed.

3.1 Materials and Methods

3.1.1 Field preparation

Prior to starting the field-scale experiment, the soil surface of the test basin was tilled to breakup any hardpan that might have remained from previous spreading operations. Throughout the experiment, temperature, pH, and specific conductance were periodically measured in order to monitor possible water quality changes in the test basin itself and in the subsurface beneath the test basin. Field measurements of pH and specific conductance were made using portable pH meter (Orion model 250A) with a pH combination electrode (Orion model 9106) and a portable temperature-compensated conductivity meter (Orion model 124), respectively. Water temperatures were measured using a hand-held alcohol-filled thermometer.

The well points were purged prior to water sample collection by removing three casing volumes with a submersible SP-300R sampling pump system (Fultz Pumps, Inc., Lewistown, PA). As soon as the specific conductance, pH, and temperature measurements had stabilized, 0.6 cm PFE-Teflon tubing was inserted into the casing of each well point at depths of 1.5 m (WP1) and 3.0 m (WP2) beneath the floor of the test basin to allow for low-flow ($\sim$ 200 mL/min) continuous sampling with peristaltic pumps.

3.1.2 Bromide analysis

Bromide, in the form of potassium bromide (Ameribrom Inc., New York, NY, photo grade), was chosen as the conservative tracer to track the recharge front and to estimate dilution of the recycled water by soil moisture and/or ground water during recharge. It should be noted that alkali halides are the most commonly used salts for subsurface fluid tracing [Chrysikopoulos, 1993]. All water samples for bromide analysis were collected into 125 mL polyethylene bottles and bromide concentrations were measured at the USGS National Water Quality Laboratory (Denver, CO) using ion chromatography.

3.1.3 Bacteriophage assays

The male-specific RNA coliphage, MS2, and the *Salmonella typhimurium* phage, PRD1, bacterial viruses representative of those found in treated municipal wastewater and in recycled water [Yanko et al., 1999], were used as surrogates for human viruses for the field experiment. These bacteriophage have been used extensively in subsurface virus transport studies and are considered to be good model viruses because they behave more conservatively (attach less) than many pathogenic viruses and are relatively persistent during transport through the subsurface [Bales et al., 1997; Jin et al., 1997; Ryan et al., 1999; Schijven et al., 1999]. Water samples for bacteriophage analyzes were collected into sterile bottles and stored at 4°C until the bacteriophage concentrations were measured at the County Sanitation Districts of Los Angeles County (CSDLAC) virology laboratory.

Bacteriophage concentrations were measured using either the double agar layer assay [Adams, 1959] or MPN procedure [Kott, 1966]. Trypticase soy broth (TSB) (Difco), TSB (Difco) soft agar (containing 0.05% 1N $CaCl_2$) and TSA (Difco) bottom agar were used for analyzing PRD1 bacteriophage using *Salmonella typhimurium* LT2 (ATCC #15277) as the host bacteria, and for analyzing MS2 bacteriophage using *E. coli* F^-amp (ATCC #700891) as the host bacteria with the same concentration of antibiotics as described by Debartolomeis and Cabelli [1991]. The double agar layer assay was estimated to have a detection limit of 0.5 PFU/mL, whereas the MPN method employed in this study was estimated to have a detection limit of 0.02 MPN PFU/mL.

3.1.4 Tracer injection

Recycled water was delivered from the culvert to the test basin at a rate of about 1,063 m^3/d for several days. Eventually, a mound was established and the test basin began to fill with recycled water. At the start of the experiment, the depth and volume of recycled water in the test basin was about 1.2 m and 473 m^3, respectively. Because direct sunlight may significantly affect the inactivation rates of bacteria and bacteriophage [Sinton et al., 1999], PRD1 and MS2 were introduced into the test basin during the evening or early morning when inactivation from ultraviolet radiation or photolysis

would be minimal. The initial seeding was accomplished by spraying the surface of the water in the test basin with solutions containing 8.5×10^{11} PFU of PRD1, 8.5×10^{13} PFU of MS2, and 72.9 kg of potassium bromide (49 kg of Br). After completion of the initial seeding of the test basin, 4.7×10^{12} PFU of PRD1, 6.0×10^{13} PFU of MS2, and 16.4 kg of potassium bromide (11 kg of Br), were injected with peristaltic pumps directly into the feed pipe delivering recycled water to the test basin. After completion of the injection process, the delivery of recycled water to the test basin was halted for 16 hours, and subsequently resumed without addition of bacteriophage and bromide. Water samples were collected at 1.5 and 3.0 m beneath the floor of the test basin (sampling points WP1 and WP2) and from the test basin itself for a period of 9 days.

3.1.5 Model Development

One-dimensional virus transport in homogeneous, saturated porous media accounting for virus sorption (or filtration) and inactivation is governed by the following partial differential equation [Sim and Chrysikopoulos, 1995]

$$\frac{\partial C(t,z)}{\partial t}+\frac{\rho}{\theta}\frac{\partial C^*(t,z)}{\partial t}=D\frac{\partial^2 C(t,z)}{\partial z^2}-U\frac{\partial C(t,z)}{\partial z}-\lambda C(t,z)-\lambda^*\frac{\rho_b}{\theta}C^*(t,z), \tag{3.1}$$

where C is the concentration of virus in suspension; C^* is the concentration of virus sorbed on the solid matrix; D is the hydrodynamic dispersion coefficient; U is the average interstitial velocity; ρ_b is the bulk density of the solid matrix; λ is the inactivation rate constant of suspended viruses; λ^* is the inactivation rate constant of sorbed viruses; θ is the porosity of porous medium; t is time; and z is the coordinate in the direction of flow. The left hand side of (3.1) consists of the accumulation terms, and the last two terms represent the inactivation of suspended and adsorbed viruses, respectively. The rate of virus attachment onto the solid matrix is described by the following generalized expression

$$\frac{\rho}{\theta}\frac{\partial C^*(t,z)}{\partial t}=r_1C(t,z)-r_2C^*(t,z), \tag{3.2}$$

where r_1 and r_2 are the forward and the reverse rate coefficients.

The desired expression for C^* is obtained by solving (3.2) subject to an initial condition of zero sorbed (or filtered) virus concentration ($C^*(0,z)=0$) as

$$C^*(t,z)=\frac{r_1\theta}{\rho_b}\int_0^t C(\tau,z)\exp\left[-\frac{r_2\theta}{\rho_b}(t-\tau)\right]d\tau. \tag{3.3}$$

In the view of (3.2) and (3.3) the governing equation (3.1) can be written as

$$\frac{\partial C(t,z)}{\partial t}=D\frac{\partial^2 C(t,z)}{\partial z^2}-U\frac{\partial C(t,z)}{\partial z}-\mathcal{A}C(t,z)-\mathcal{B}\int_0^t C(\tau,z)e^{-\mathcal{H}(t-\tau)}d\tau, \tag{3.4}$$

where the following substitutions have been employed

$$\mathcal{A}=r_1+\lambda, \tag{3.5}$$

$$\mathcal{B}=r_1(\lambda^*-\mathcal{H}), \tag{3.6}$$

$$\mathcal{H}=\frac{\theta r_2}{\rho_b}. \tag{3.7}$$

For a semi-infinite, one-dimensional porous medium in the presence of a broad pulse input of viruses, the appropriate initial and boundary conditions are:

$$C(0,z)=0, \tag{3.8}$$

$$-D\frac{\partial C(t,0)}{\partial z}+UC(t,0)=\begin{cases}UC_0(t) & 0<t\le t_p,\\ 0 & t>t_p,\end{cases} \tag{3.9}$$

$$\frac{\partial C(t,\infty)}{\partial z}=0, \tag{3.10}$$

where $C_0(t)$ is the time-dependent source concentration, and t_p is the duration of the solute pulse. The condition (3.8) establishes that there is no initial virus concentration within the porous medium. The constant flux boundary condition (3.9) implies virus concentration discontinuity at the inlet and that the source concentration is not constant during the broad pulse. The downstream boundary condition (3.10) preserves concentration continuity for a semi-infinite system.

An analytical solution to the problem described by the governing partial differential equation (3.4) subject to initial and boundary conditions (3.8)–(3.10) has been derived by Sim and Chrysikopoulos [1995] for the case of continuous and time-invariant (constant) source concentration.

The Sim and Chrysikopoulos [1995] model was modified by Keller et al. [2004] to account for the special case of a single, time-invariant broad-pulse source concentration. For the general case of a time-dependent broad-pulse source concentration described in this study, an analytical solution can be obtained with application of the principle of superposition, as suggested by Chrysikopoulos et al. [1990] and Chrysikopoulos and Lee [1998]. Assuming that the broad pulse t_p consists of several sub-pulses

$$t_p = t_{p(1)} + t_{p(2)} + \cdots + t_{p(M)}, \tag{3.11}$$

where $t_{p(m)}$ $(m = 1,\ 2,\ \ldots,\ M)$ represents the time period of sub-pulse m. For the duration of each sub-pulse the source concentration, $C_{0(m)}$, is assumed to remain constant. The solution is expressed as:

$$C(t,z) = \sum_{m=1}^{M} C_{0(m)}(t)\Big[\Phi\big(t-\widehat{t}_{m-1},z\big) - \Phi\big(t-\widehat{t}_{m},z\big)\Big], \qquad (t > t_p), \tag{3.12}$$

where

$$\widehat{t}_{m-1} = \sum_{i=1}^{m-1} t_{p(i)}, \tag{3.13}$$

$$\widehat{t}_{m} = \sum_{i=1}^{m} t_{p(i)}, \tag{3.14}$$

$$\begin{aligned}\Phi(t,z) = \frac{U}{D^{1/2}}\exp\left[\frac{Uz}{2D}\right]\Bigg\{\int_0^t\int_0^\tau \mathcal{H}e^{-\mathcal{H}\tau}J_0\Big[2\big(\mathcal{B}\zeta(\tau-\zeta)\big)^{1/2}\Big] \\ \times\Bigg\{\frac{1}{(\pi\zeta)^{1/2}}\exp\left[\frac{-z^2}{4D\zeta}+\left(\mathcal{H}-\mathcal{A}-\frac{U^2}{4D}\right)\zeta\right] \\ -\frac{U}{2D^{1/2}}\exp\Big[\frac{Uz}{2D}+(\mathcal{H}-\mathcal{A})\zeta\Big]\operatorname{erfc}\left[\frac{z}{2(D\zeta)^{1/2}}+\frac{U}{2}\left(\frac{\zeta}{D}\right)^{1/2}\right]\Bigg\}d\zeta d\tau \\ +e^{-\mathcal{H}t}\int_0^t J_0\Big[2\big(\mathcal{B}\zeta(t-\zeta)\big)^{1/2}\Big]\Bigg\{\frac{1}{(\pi\zeta)^{1/2}}\exp\left[\frac{-z^2}{4D\zeta}+\left(\mathcal{H}-\mathcal{A}-\frac{U^2}{4D}\right)\zeta\right] \\ -\frac{U}{2D^{1/2}}\exp\Big[\frac{Uz}{2D}+(\mathcal{H}-\mathcal{A})\zeta\Big]\operatorname{erfc}\left[\frac{z}{2(D\zeta)^{1/2}}+\frac{U}{2}\left(\frac{\zeta}{D}\right)^{1/2}\right]\Bigg\}d\zeta\end{aligned} \tag{3.15}$$

The Bessel function relationship $I_0(x) = J_0(ix)$, where I_0 is the modified Bessel function of the first kind of zeroth order and x is an arbitrary argument [Abramowitz and Stegun, 1972], can

be used for the evaluation of $J_0(ix)$ with complex argument. The solution (3.12) can also be used for early times ($t < t_p$); however, if $\widehat{t}_{m-1} < t < \widehat{t}_m$ then $\Phi(t - \widehat{t}_m) = 0$. It should be noted that for the derivation of (3.12) the superposition principle can be employed because the governing partial differential equation (3.1) is linear with respect to the aqueous phase concentration.

For this work, COLLOIDFIT, a program written in FORTRAN, was develop to fit the virus transport model (3.12) to the experimental data. COLLOIDFIT utilizes subroutine *mrqmin* [Press et al., 1992] for the nonlinear least squares regression, and subroutines *qdag* and *twodq* [IMSL, 1991] for the numerical evaluation of the single and double integrals, respectively, present in (3.15).

3.1.6 Determination of collision efficiency

The forward and the reverse rate coefficients presented in (3.2) are defined as [Sim and Chrysikopoulos, 1995]:

$$r_1 = k_c = U\phi F(C^*), \tag{3.16}$$

$$r_2 = \frac{\rho}{\theta}(k_r + \lambda^*), \tag{3.17}$$

respectively, where k_c is the clogging rate constant, ϕ is the filter coefficient, $F(C^*)$ is the dynamic blocking function that accounts for variations of porosity with increasing particle attachment, and k_r is the declogging rate constant. For the filtration of submicron particles such as viruses, it is assumed that $F(C^*) = 1$ and (3.16) reduces to

$$k_c = U\phi. \tag{3.18}$$

The filter coefficient is expressed as [Rajagopalan and Tien, 1976]:

$$\phi = \frac{3(1-\theta)}{2d_p}\eta, \tag{3.19}$$

where η is the single collector removal efficiency of the filter and $d_p = 0.25$ mm is the average grain diameter of the porous medium.

Note that the single collector removal efficiency presented in (3.19) is commonly expressed as [Yao et al., 1971]:

$$\eta = \alpha\eta_0, \tag{3.20}$$

where α is the collision efficiency, and η_0 is the single collector removal efficiency for favorable deposition (in the absence of double layer interaction energy). Combining (3.18), (3.19), and (3.20) yields the following expression for the collision efficiency factor

$$\alpha = \frac{k_c}{U}\frac{2d_p}{3(1-\theta)}\frac{1}{\eta_0}. \tag{3.21}$$

An approximate expression for η_0 applicable to deep-bed filtration based on the Happel sphere-in-cell porous media model is the following [Rajagopalan and Tien, 1976; Logan et al., 1995]:

$$\eta_0 = A_s \mathrm{N}_{Lo}^{1/8}\mathrm{N}_R^{15/8} + 3.375\times10^{-3}A_s\mathrm{N}_G^{1.2}\mathrm{N}_R^{-0.4} + 4A_s^{1/3}\mathrm{N}_{Pe}^{-2/3}, \tag{3.22}$$

where A_s is the porosity-dependent flow parameter defined as:

$$A_s = \frac{1-\varepsilon^5}{1-1.5\varepsilon+1.5\varepsilon^5-\varepsilon^6}, \tag{3.23}$$

(where $\varepsilon = (1-\theta)^{1/3}$), N_{Lo} is the London group:

$$\mathrm{N}_{Lo} = \frac{4H}{9\pi\mu d_v^2 q}, \tag{3.24}$$

N_R is the relative size group:

$$\mathrm{N}_R = \frac{d_v}{d_p}, \tag{3.25}$$

N_G is the gravity group:

$$\mathrm{N}_G = \frac{d_v^2(\rho_v-\rho_f)g}{18\mu q}, \tag{3.26}$$

N_{Pe} is the Peclet number:

$$\mathrm{N}_{Pe} = \frac{d_p q}{\mathcal{D}}, \tag{3.27}$$

where $q = U\theta$ is the specific discharge or the approach velocity, $\mathcal{D}$ is the virus diffusivity governed by Brownian motion and described by the Stokes-Einstein equation as [Atkins, 1990]

$$\mathcal{D} = \frac{k_B T}{3\pi\mu d_v}, \tag{3.28}$$

$k_B = 1.38\times10^{-23}$ (kg·m^2)/(s^2·K) is the Boltzman constant, $H = 6.6\times10^{-21}$ (kg·m^2)/s^2 is the Hamaker constant [Truesdail et al., 1998], d_v is the virus diameter (2.5×10^{-8} m for MS2 and 6.2×10^{-8} m for PRD1 [Kinoshita et al., 1993]), ρ_v is the virus density (assumed at near-neutral buoyancy), ρ_f is the density of water, $\mu = 8.91\times10^{-4}$ kg/(m·s) is the viscosity of water, $g = 9.81$ m/s^2 is the acceleration due to gravity, and T is the absolute temperature in Kelvin. Figure 3.1 presents the single collector removal efficiency as a function of particle size predicted by (3.22), together with the η_0 values for MS2 and PRD1 for the initial field conditions.

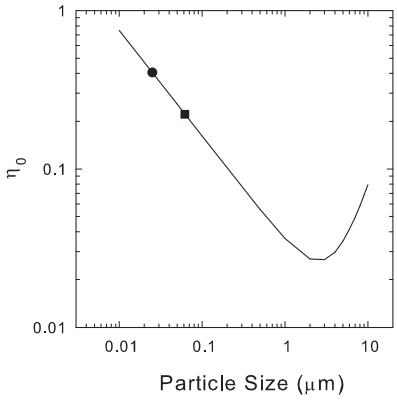

Figure 3.1: Predicted single collector removal efficiency based on (**??**h3eq22) (solid line) and η_0 values for MS2 (solid circle) and PRD1 (solid square) for the initial conditions at the field site. Here $U = 25.3$ cm/hr, $d_p = 0.25$ mm, $\theta = 0.3$, $H = 6.6\times10^{-21}$ (kg·m^2)/s^2, $\rho_v \approx \rho_f$, and $T = 298$ K.

An alternative method to calculate α has been proposed by Harvey and Garabedian [1991]. Hereafter the method will be referred to as HG. The HG method is based on the relative breakthrough, RB, defined as the ratio of the time-integrated mass of each bacteriophage relative to that of the conservative tracer

$$\mathrm{RB} = \int_0^t \frac{C(t)}{C_0}\mathrm{d}t \Bigg/ \int_0^t \frac{C_T(t)}{C_{T_0}(t)}\mathrm{d}t, \tag{3.29}$$

where C_T is the tracer concentration, and subscript 0 indicates initial concentrations in the test basin. The RB can be determined from experimental data by numerical integration of the area under the corresponding normalized breakthrough curves (i.e., trapezoid rule). Furthermore, assuming that

the bacteriophage and bromide enter the test basin as a dirac input, α is expressed as [Harvey and Garabedian, 1991]:

$$\alpha = \frac{d_p \left\{ [1 - 2(\alpha_L/\ell_z) \ln \mathrm{RB}]^2 - 1 \right\}}{6(1-\theta)\eta_0 \alpha_L}, \tag{3.30}$$

where ℓ_z is the distance from the injection point to the sampling point, and α_L is the longitudinal dispersivity defined as [*Nielsen et al.*, 1986]:

$$\alpha_L = \frac{D - \mathcal{D}_e}{|U|^\gamma}, \tag{3.31}$$

where $\mathcal{D}_e = \mathcal{D}/\tau^*$ is the effective molecular diffusion coefficient (where $\tau^* \geq 1$ is the tortuosity coefficient) and γ is an exponent that for relatively homogeneous, water-saturated systems is approximately equal to one.

3.2 Field-Scale Experiment

3.2.1 Water-quality

The initial water temperature in the test basin was 28.8°C and the specific conductance adjusted to 25°C was 1,005 μS/cm. The initial specific conductance at WP1 was 1,010 μS/cm and increased to 1,025 μS/cm during the experiment. The initial temperature at WP2 was 28.6°C and the specific conductance 992 μS/cm; both increased slightly during the experiment. The pH measured from water samples collected from beneath the test basin ranged from 7.3 to 7.6 pH units. Overall, the observed fluctuations in temperature, pH, and specific conductance were minimal; this indicates that chemical conditions changed little during the recharge experiment and were similar to those observed during other recharge experiments conducted at the research field site [Schroeder et al., 2003; Anders et al., 2004].

3.2.2 Bacteriophage inactivation

During the initial seeding and subsequent metered injection of bromide and bacteriophage, 24 grab samples were collected from four locations around the perimeter and near the center of the test

basin in order to determine the degree of mixing in the ponded water and to establish the initial concentrations. The average concentrations were: $2.4 \pm 1.4 \times 10^5$ PFU/mL for MS2, $2.4 \pm 1.1 \times 10^4$ PFU/mL for PRD1, and 107 ± 28.0 mg/L for bromide. The high standard deviations indicate incomplete mixing in the test basin during the first few hours of the experiment. Measured bromide and bacteriophage concentrations in water samples collected from the test basin during the field-scale recharge experiment are shown in Figure 3.2. The shaded area in Figure 3.2 represents the 16 hour period when no recycled water, bacteriophage, or bromide were delivered to the test basin. Figure 3.2a indicates that the bromide concentration remained essentially constant for the 16 hour period after mixing was complete and before dilution occurred as the delivery of new recycled water resumed. However, as shown in Figures 3.2b and 3.2c, bacteriophage concentrations decreased during the 16 hour period probably due to inactivation.

Assuming that virus inactivation is a first-order process [Yates et al., 1985; Chrysikopoulos and Vogler, 2004] expressed as:

$$\ln\left[\frac{C(t)}{C_0}\right] = -\lambda t \tag{3.32}$$

the rate of bacteriophage inactivation can be determined by linear regression analysis of the observed normalized bacteriophage log-concentrations. Figure 3.3 shows the bacteriophage log-concentrations for the 16 hour period and the corresponding linear regression lines. The slope of the solid line, $\lambda = 0.07$ hr^{-1} represents the inactivation rate coefficient for MS2 with a coefficient of determination $r^2 = 0.94$, and the slope of the dashed line, $\lambda = 0.02$ hr^{-1} represents the inactivation rate coefficient for PRD1 with $r^2 = 0.36$. The slopes indicate that the inactivation rate of MS2 was higher than that of PRD1, as was also reported by Yahya et al. [1993]. It should be noted that the estimated inactivation rate coefficients correspond to a water temperature of 28.8°C and are therefore higher than those reported in the literature for groundwater temperatures of 4°C [Yates et al., 1985; Powelson et al., 1990] or 7°C [Yahya et al., 1993]. In addition to temperature, Brownian coagulation of viruses [Grant, 1994] and/or microbial activity [Jansons et al., 1989] may also increase the rate of virus inactivation. However, λ values for bacteriophage MS2 and PRD1 evaluated from (3.32) can provide an estimate of

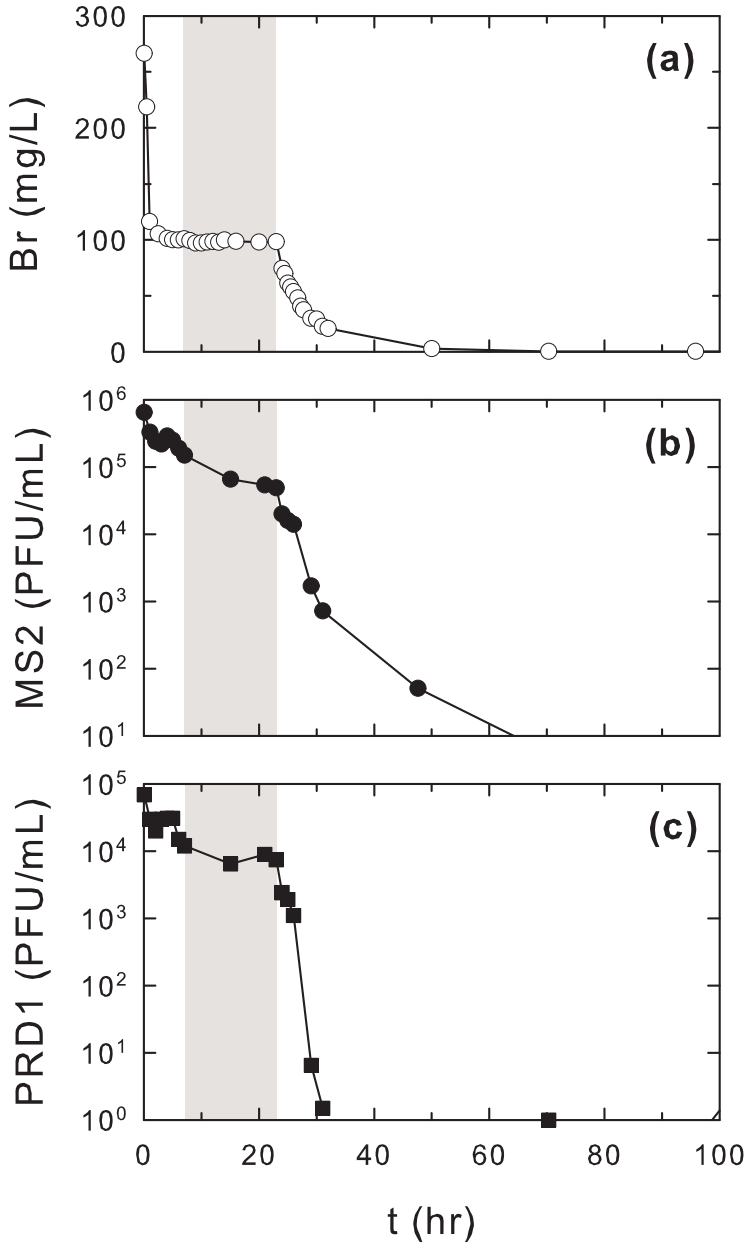

Figure 3.2: Concentrations of (a) bromide, (b) MS2, and (c) PRD1 in water samples collected from the test basin. Shaded area indicates the 16-hour period when no recycled water was delivered to the test basin.

the retention time required for adequate virus removal. For example, the estimated λ value for PRD1 in the test basin suggests that almost 38-log removal of bacteriophage would occur in 6 months. This period is equal to the underground retention time proposed by the State of California for surface spreading of municipal wastewater [Asano and Cotruvo, 2004]. It should be noted here that Sim and Chrysikopoulos [1996] have proposed that the inactivation rate coefficient should be considered as a time-dependent parameter, and suggested that virus transport data collected in the vicinity of the source of contamination at early times are more reliable for estimation of inactivation rate coefficients. Furthermore, Chrysikopoulos and Vogler [2004] have shown that temporally variable inactivation rate coefficients can significantly affect the predicted virus migration in porous media.

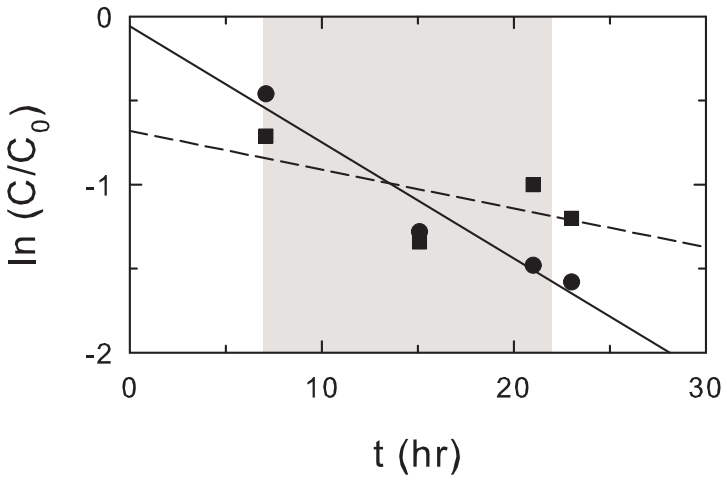

Figure 3.3: Normalized log-concentrations of MS2 (solid circles) and PRD1 (solid squares) in the test basin as a function of time. The slope of the fitted lines (solid line for MS2, and dashed line for PRD1) represent the corresponding inactivation rate coefficients. Shaded area represents the 16-hour period when no recycled water was delivered to the test basin.

3.2.3 Estimation of transport parameters

Gauge measurements shown in Figure 3.4 indicate that the height of recycled water, h, in the test basin remained at about 1.25 m during the initial seeding and injection of bacteriophage and

bromide. Furthermore, the shaded area in Figure 3.4 shows that h decreased from 1.25 m to 0.5 m during the 16 hour period when no recycled water was delivered to the test basin. Once delivery was resumed, h increased to about 1.0 m and remained at that height for the remaining period of the experiment. The recycled water did not return to the original height of 1.25 m due to operations at the spreading grounds that required draining of standing water in the desilting basin adjacent to the test basin.

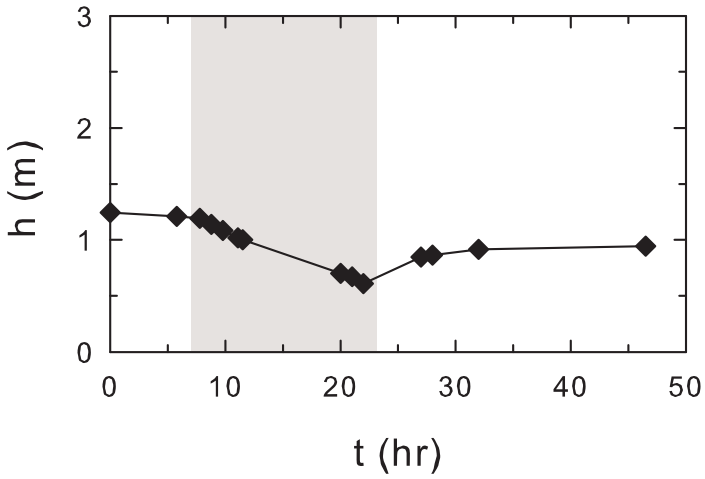

Figure 3.4: Height of recycled water in the test basin (solid diamonds) as a function of time. Shaded area represents the 16 hour period when no recycled water was delivered to the test basin.

The bromide concentrations observed at both sampling locations WP1 and WP2 are shown in Figure 3.5. A comparison of bromide concentrations at WP1 and WP2 to initial concentrations in the test basin indicate that no major dilution occurred at these shallower depths. The mean concentration arrival time for bromide at the sampling locations is defined by the first normalized absolute moment as [Valocchi, 1985]:

$$m_1 = \int_0^\infty tC_T(t,z)\mathrm{d}t \Big/ \int_0^\infty C_T(t,z)\mathrm{d}t. \tag{3.33}$$

First moment analysis of the bromide concentration data provides a mean arrival time of 25.2 hours at WP1 and 28.6 hours at WP2. Also shown in Figure 3.5 are the model simulated

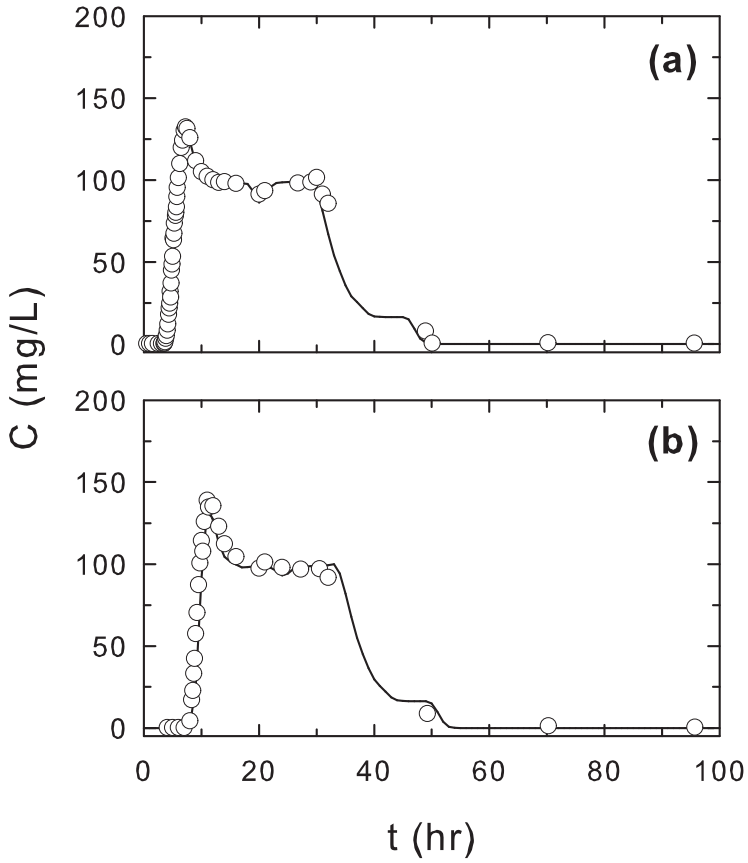

Figure 3.5: Bromide concentration breakthrough data (open circles) observed at (a) WP1 and (b) WP2, and the corresponding simulated concentration histories (solid curves).

bromide concentration history curves. These curves were constructed with $\rho_b = 1.86$ gm/cm^3 and $\theta = 0.3$ determined from the measured grain-size distribution data and $k_c = k_r = \lambda = \lambda^* = 0$. The parameter values for U and D correspond to the changes in the height of the recycled water in the test basin (vertical gradient) during the field experiment (see Figure 3.4). Clearly, the absolute minimum number of values for U and D is 4. The parameter values for U and D during the initial seeding and injection of bacteriophage and bromide were fitted by COLLOIDFIT. The remaining U and D values, during the 16 hour period when no recycled water was delivered to the test

basin and once delivery was resumed, were calculated from the measured changes in h in the test basin. The broad bromide input pulse was sub-divided into 15 sub-pulses based upon measured bromide concentrations in water samples collected from the test basin during the field-scale recharge experiment (see Figure 3.2). The time-dependent bromide source concentrations as well as the U and D values for each sub-pulse at both sampling locations are listed in Table 3.1. It should be noted that due to the relatively high interstitial velocities, D is governed mainly by mechanical dispersion and the contribution of $\mathcal{D}_e$ is very small. The dispersivity values for the data collected at WP1 and WP2, as determined by (3.31), are $\alpha_L = 1.86$ and 1.41 cm, respectively. Note that the estimated dispersivity at WP1 is greater than the one at WP2. Given that the dispersivity is a property of the porous medium, the dispersivity values obtained here indicate that the soil formation beneath the test basin is not perfectly homogeneous. The variation in dispersivity values is relatively small, suggesting that the degree of heterogeneity is slight.

The bacteriophage MS2 concentrations observed at both sampling locations WP1 and WP2 are shown in Figure 3.5. In contrast to bromide, the first moment of the arrival time for MS2 was 10.3 hours at WP1 and 14.0 hours at WP2. The early mean concentration arrival times of MS2 is attributed to a combination of mechanisms that result in faster velocities and straighter paths [Sirivithayapakorn and Keller, 2003]. These mechanisms include pore exclusion, in which the virus particles are excluded from smaller pores based on their size [Enfield at al., 1989; Abdel-Salam and Chrysikopoulos, 1995; Rehmann et al., 1999] and/or size exclusion that excludes the virus particles from streamlines near the pore walls [Ginn, 2002; Auset and Keller, 2004; Keller et al., 2004]. It should be noted that dispersivity can also be a function of colloid size at low Peclet numbers due to the size exclusion effect [Keller et al. 2004].

The bacteriophage MS2 reached a maximum concentration of 6.0×10^4 PFU/mL at WP1 and 3.4×10^4 PFU/mL at WP2. The concentration history curves for MS2 presented in Figure 3.6 were constructed using U and D values listed in Table 3.1 and $\lambda = 0.07$ hr^{-1} determined from (3.32). The broad MS2 input pulse was sub-divided into 17 sub-pulses with durations similar to those used

Table 3.1: Model Parameters for Bromide Breakthrough Data at WP1 and WP2

$t_{p(m)}$(hr)	C_{T_0}(mg/L)	U(cm/hr)	D(cm^2/hr)
WP1: $z = 152.4$ cm; $\alpha_L = 1.86$ cm			
0.25	266.5	25.8	48.1
0.75	218.6	25.8	48.1
2.0	116.4	25.8	48.1
4.0	101.1	25.8	48.1
2.0	100.1	25.5	47.5
5.0	98.0	25.5	47.5
8.0	98.7	24.3	45.3
1.0	98.1	24.3	45.3
1.0	98.3	24.7	46.0
1.0	86.4	24.7	46.0
1.0	68.4	24.7	46.0
1.0	57.7	24.7	46.0
2.0	42.0	24.7	46.0
3.0	25.7	24.7	46.0
9.0	16.4	24.7	46.0
WP2: $z = 304.8$ cm; $\alpha_L = 1.41$ cm			
0.25	266.5	30.1	42.5
0.75	218.6	30.1	42.5
2.0	116.4	30.1	42.5
4.0	101.1	30.1	42.5
2.0	100.1	29.9	42.2
5.0	98.0	29.9	42.2
8.0	98.0	29.5	41.7
1.0	98.1	29.5	41.7
1.0	98.3	29.7	41.9
1.0	86.4	29.7	41.9
1.0	68.4	29.7	41.9
1.0	57.7	29.7	41.9
2.0	42.0	29.7	41.9
3.0	25.7	29.7	41.9
9.0	16.4	29.7	41.9

for the bromide (see Figure 3.2). Two sub-pulses in addition to those employed for the bromide case were required to describe adequately the measured MS2 concentrations during the periods when no recycled water was being delivered to the test basin. Values of k_c for each sub-pulse were fitted using COLLOIDFIT. All MS2 time-dependent source concentrations as well as the fitted k_c values for each sub-pulse at both sampling locations are listed in Table 3.2. Values of k_r and λ^* were fitted using only the receding portion of experimental breakthrough data. Changes in the values of k_r and λ^* affect slightly the slope and intercept of the receding portion of the breakthrough curve, respectively. This observation has also been reported by Schijven et al. [1999]. Consequently, these parameters were assumed to remain constant with time but to vary with depth (temporally-invariant but spatially-variable).

The solid curve in Figure 3.6a represents the model simulated MS2 breakthrough curve at WP1 with fitted values for $\lambda^* = 0.025$ hr^{-1} and $k_r = 5\times10^{-4}$hr^{-1}. The initial value of k_c at WP1 was 0.3 hr^{-1}; however, when the delivery of recycled water to the test basin was halted, the value of k_c increased to 1.2 hr^{-1}. After delivery of recycled water was resumed, k_c values decreased slightly for the remaining period of the experiment. The model simulated MS2 breakthrough curve at WP2 is indicated by the solid curve in Figure 3.6b, and it was constructed with fixed value of $\lambda^* = 0.025$ hr^{-1} and fitted $k_r = 5\times10^{-5}$hr^{-1}. For MS2 at WP2, the initial k_c was 0.2 hr^{-1}, this value increased to 0.5 hr^{-1} when the delivery of recycled water to the test basin was halted, and then k_c values increased to 0.8 hr^{-1} for the remaining period of the experiment. The small fitted values of k_r indicate that desorption does not affect significantly the fate and transport of viruses during vertical fully water-saturated flow.

The bacteriophage PRD1 concentrations observed at both sampling locations WP1 and WP2 are shown in Figure 3.7. Note that first moment estimated the arrival times for PRD1 at WP1 and WP2 of 10.1 hours and 14.5 hours, respectively, are similar to the arrival times for bacteriophage MS2. Therefore, the transport of PRD1 exhibits similar size exclusion behavior as MS2. However, unlike the MS2 data, the peak PRD1 concentration is higher at WP2. The broad PRD1 input pulse

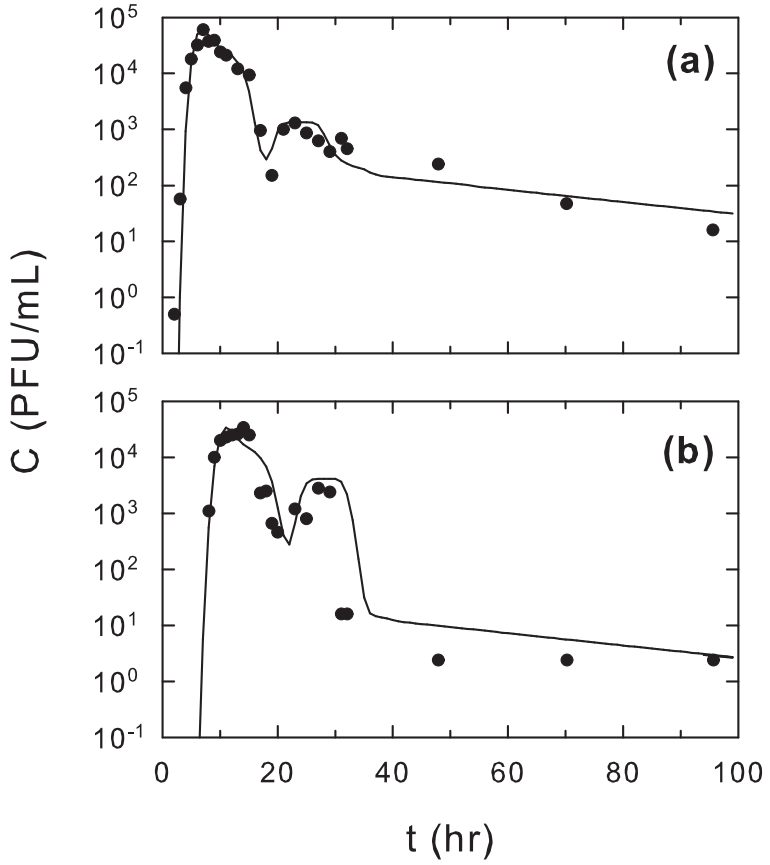

Figure 3.6: MS2 concentration breakthrough data (solid circles) observed at (a) WP1 and (b) WP2, and the corresponding simulated concentration histories (solid curves).

was sub-divided into the same 17 sub-pulses used for bacteriophage MS2. All PRD1 time-dependent source concentrations as well as the fitted k_c values for each sub-pulse at both sampling locations are listed in Table 3.3.

The concentration history curves for PRD1 presented in Figure 3.7 were constructed following the same procedure described previously for bacteriophage MS2 with $\lambda = 0.02$ hr^{-1}. The model-simulated breakthrough history at WP1 and WP2 presented in Figure 3.7 by the solid curves were constructed with $\lambda^* = 0.015$ hr^{-1} and $k_r = 1{\times}10^{-5}$ hr^{-1}. The values of k_c for PRD1 did not exhibit the same trend as that for MS2, but instead increased slightly at both depths during the recharge

Table 3.2: Model Parameters for MS2 Breakthrough Data at WP1 and WP2

$t_{p(m)}$(hr)	C_0(PFU/mL)	k_c(hr^{-1})	
		WP1	WP2
2.0	650000	0.3	0.2
1.0	330000	0.3	0.2
1.0	260000	0.3	0.2
1.0	240000	0.3	0.2
2.0	200000	0.3	0.2
2.0	110000	0.3	0.3
5.0	66000	1.2	0.5
8.0	66000	0.6	0.2
1.0	54000	0.8	0.8
1.0	49000	0.8	0.8
1.0	20000	0.8	0.8
1.0	16000	0.8	0.8
1.0	14000	0.8	0.8
3.0	7900	0.8	0.8
2.0	1200	0.8	0.8
16.0	390	0.8	0.8
23.0	2.8	0.8	0.8

experiment and indicate the attachment of PRD1 is affected less by the delivery of recycled water to the test basin. The lack of a similar trend might be explained by noting that the reverse rate coefficient for PRD1 at WP1 and WP2 is $r_2 = 9.35\times10^{-2}$ hr^{-1} which is an order-of-magnitude less than the forward rate coefficient for most sub-pulses at both sampling depths.

3.2.4 Comparison of collision efficiencies

Collision efficiencies for both bacteriophage MS2 and PRD1 were estimated with (3.21) using the fitted time-dependent k_c values and the additional model parameters listed in Table 3.4. The estimated collision efficiencies suggest more favorable attachment conditions existed for bacteriophage

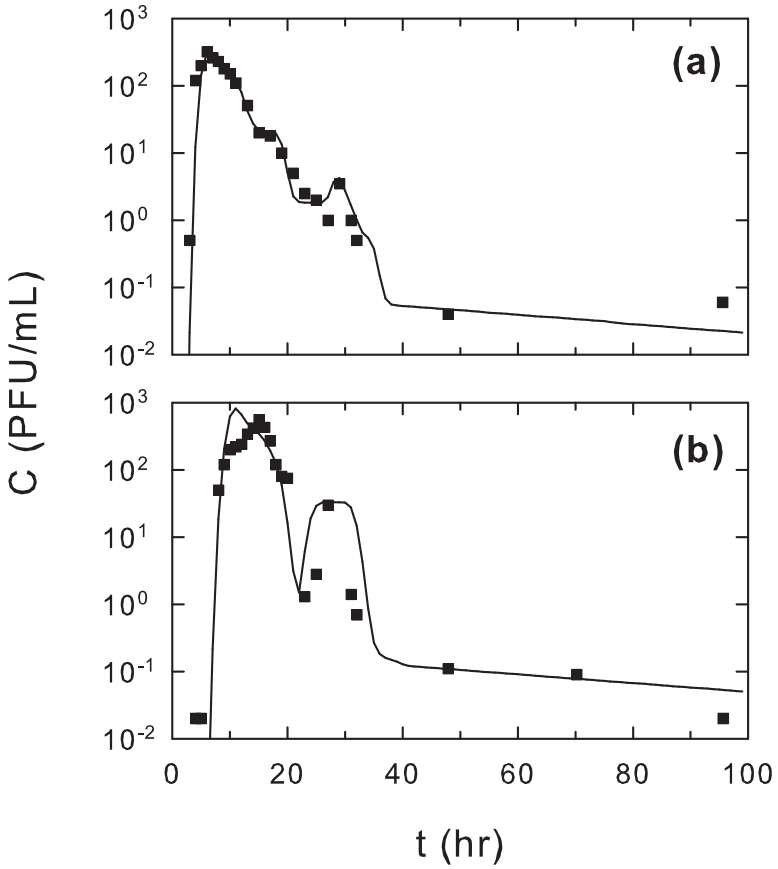

Figure 3.7: PRD1 concentration breakthrough data (solid squares) observed at (a) WP1 and (b) WP2, and the corresponding simulated concentration histories (solid curves).

PRD1 than for MS2 during the field-scale recharge experiment. The more favorable attachment conditions (higher collision efficiencies) for bacteriophage PRD1 may be due to its lipid-containing structure and higher hydrophobicity, whereas a more hydrophilic virus such as MS2 behaves more conservatively [Kinoshita et al., 1993]. Figure 3.8 shows the relationship between k_c and estimated α values for MS2 and PRD1, as well as the corresponding linear regression lines.

According to (3.21) the slope of the lines in Figure 3.8 is inversely proportional to η_0, and indicates that the soil beneath the test basin is almost twice as efficient at removing PRD1 than

Table 3.3: Model Parameters for PRD1 Breakthrough Data at WP1 and WP2

$t_{p(m)}$(hr)	C_0(PFU/mL)	k_c(hr^{-1})	
		WP1	WP2
2.0	69000	0.9	0.4
1.0	30000	0.9	0.4
1.0	27000	0.9	0.4
1.0	31000	0.9	0.4
2.0	19000	0.9	0.4
2.0	9200	1.0	0.4
5.0	6400	1.0	0.9
8.0	6400	1.4	0.5
1.0	9000	1.4	1.0
1.0	7400	1.2	1.0
1.0	2400	1.2	1.0
1.0	1900	1.2	1.0
1.0	1100	1.2	1.0
3.0	550	1.2	1.0
2.0	4.0	1.2	1.0
16.0	1.5	1.2	1.0
23.0	1.0	1.2	1.0

MS2 at the conditions present during the experiment. For comparison, the corresponding collision efficiencies were also determined with the HG method and they are listed in Table 3.5. Figure 3.9 shows the collision efficiencies as a function of time estimated by both (3.21) and the HG method. The time-dependent collision efficiencies estimated from the experimentally determined k_c values reached asymptotic values higher than those predicted by the HG method.

Note that the temporal variablity of the collision efficiencies cannot be accounted for by the HG method. Furthermore, factors such as temperature and groundwater quality that could affect the degree of attachment have been shown to change very little throughout the duration of the recharge experiment while other factors, such as viral surface properties or sediment surface charge,

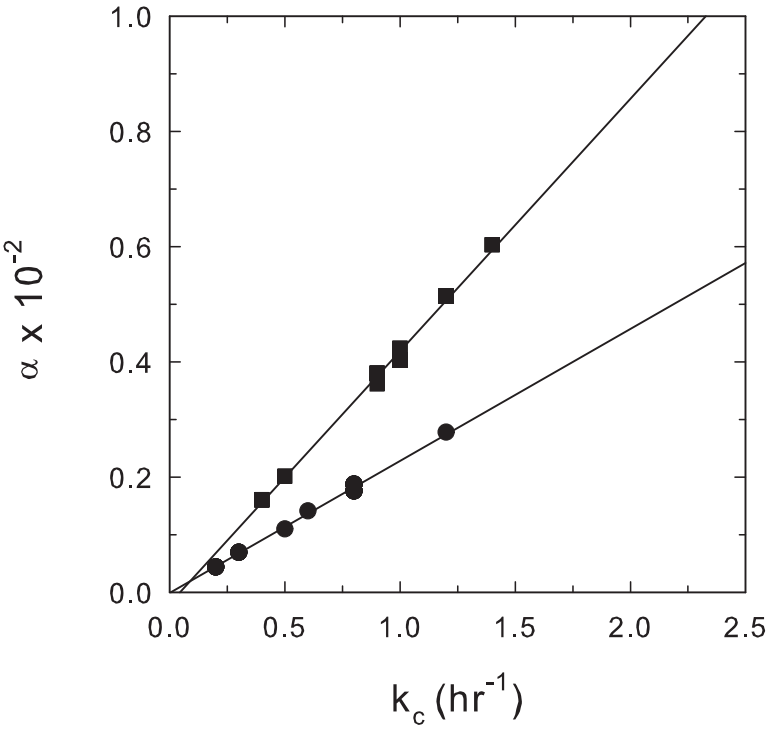

Figure 3.8: Relationship between k_c and α for MS2 (solid circles) and PRD1 (solid squares). Corresponding linear regression lines indicate $\alpha = 2.3{\times}10^{-3}k_c$ for MS2 and $\alpha = 4.4{\times}10^{-3}k_c$ for PRD1.

are not expected to vary greatly during the experiment.

The time-dependent variation in collision efficiencies may in part be attributed to fluctuations in the interstitial fluid velocity caused by changes in recycled water delivery to the test basin. Veerapaneni and Wiesner [1997] noted that flow rate influences the morphology of deposits as well as the deposit distribution of monodispersed latex particles filtered through a bed of spherical glass beads. According to Harter et al. [2000] a significant decrease in α with decreasing pore velocity indicates either η_0 does not sufficiently describe velocity dependent filtration phenomena or that chemical interactions between collector and biocolloid (represented by α) are indeed velocity dependent. Tufenkji and Elimelech [2003] developed a new empirical correlation for predicting η_0 that

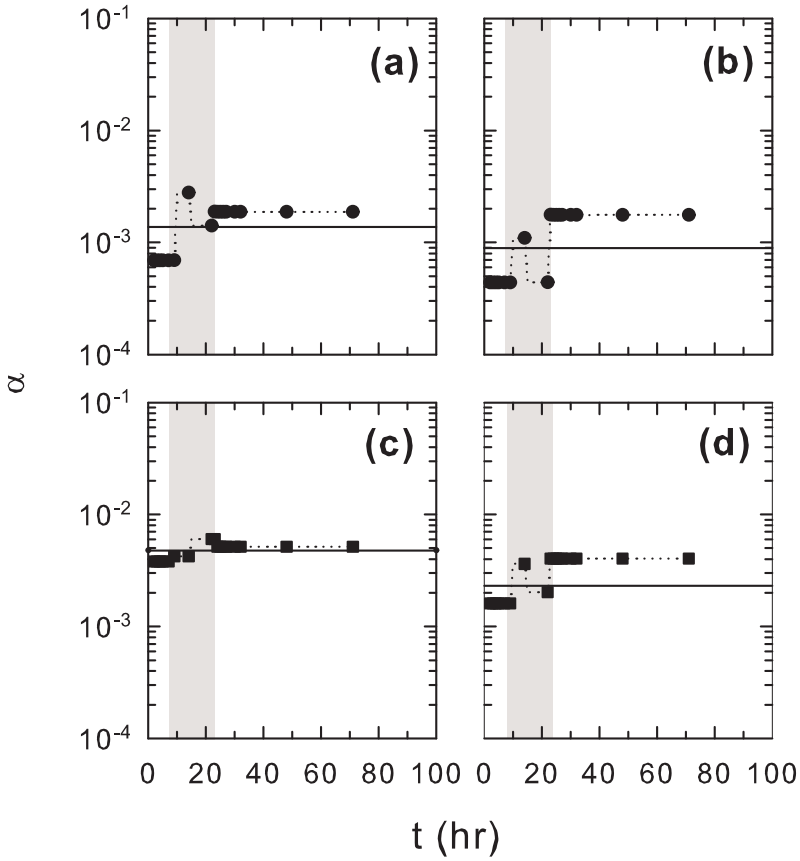

Figure 3.9: Time-dependent α values for MS2 (solid circles) at (a) WP1 and (b) WP2 and PRD1 (solid squares) at (c) WP1 and (d) WP2 together with the corresponding α values estimated by the HG method (solid lines).

Table 3.4: Model Parameters for Virus Transport Simulations

Parameter	Value	Units
A_s	75.5	...
d_p	2.5×10^{-4}	m
d_v	2.5×10^{-8} (MS2)	m
	6.2×10^{-8} (PRD1)	m
H	6.6×10^{-21}	$(\mathrm{kg\cdot m^2})/\mathrm{s^2}$
k_B	1.38×10^{-23}	$(\mathrm{kg\cdot m^2})/(\mathrm{s^2\cdot K})$
T	298	K
ε	0.89	...
μ	8.91×10^{-4}	$\mathrm{kg/(m\cdot s)}$
ρ_f	999	$\mathrm{kg/m^3}$
ρ_v	1001	$\mathrm{kg/m^3}$

better reflects the significant influence of hydrodynamic interactions on the deposition of microorganisms. However, α values estimated with (3.21) and (3.22) are only slightly higher than α values estimated with (3.21) and the new η_0 empirical relationship developed by Tufenkji and Elimelech [2003]. The slight difference indicates the retarding effect of hydrodynamic interactions counterbalances the attractive van der Waals forces experienced by both bacteriophage during the recharge experiment. Furthermore, changes in U affect differently the k_c values for bacteriophage MS2 and PRD1 during the field experiment. Therefore, interstitial velocity fluctuations alone cannot adequately explain the α values obtained during this recharge experiment. An alternative explanation is that the estimated time-dependent α values are affected by alterations in the surface structure as well as the porosity of the filtering media during the recharge experiment caused by the presence of entrapped air, sealing of the soil surface, and/or biofilms sealing the pores within the wetted zones.

Collision efficiencies evaluated by the HG method are frequently reported in the literature. Pieper et al. [1997] reported that for bacteriophage PRD1 $\alpha = 0.013$ in an uncontaminated aquifer zone and $\alpha = 0.0014$ in a contaminated zone. The lower collision efficiency (less favorable attachment

Table 3.5: Parameters for Estimation of α by the HG Method

Parameter	Value		Units	
	MS2		PRD1	
	WP1	WP2	WP1	WP2
RB	3.35×10^{-2}	1.69×10^{-2}	1.96×10^{-3}	3.43×10^{-3}
η_0	1.59×10^{-1}	1.44×10^{-1}	8.7×10^{-2}	7.86×10^{-2}
α	4.6×10^{-3}	2.7×10^{-3}	1.67×10^{-2}	7.0×10^{-3}

conditions) in the contaminated zone may be attributed to the presence of dissolved organic matter that enhances bacteriophage transport. Schroeder et al. [2003] reported dissolved organic carbon concentrations of almost 10 mg/L in recycled water at the research field site. Deborde et al. [1999] calculated that $\alpha = 0.004$ for MS2 and $\alpha = 0.014$ for PRD1 in a gravel-dominated floodplain aquifer. These α values are similar to those obtained in the present study. However, the greater d_p values of 0.00125 m (coarse sand) and 0.012 m (medium pebbles) at that particular field site indicate less favorable attachment conditions existed due to the high groundwater velocities and low specific conductance. Schijven et al. [1999] studied the passage of viruses in calcareous, fine dune sand and found that α values ranged from 0.0014 to 0.00027 for MS2 and 0.0024 to 0.00043 for PRD1. These very low α values reflect highly unfavorable conditions for attachment and are consistent with the concept that in sandy soils with relatively high pH values of 7.3-8.3, electrostatic repulsion is important in restricting attachment [Bales et al., 1993]. Considering the slight difference in pH values reported by Schijven et al. [1999] and those measured during this experiment, as well as the high velocities during aquifer recharge and the presence of organic matter in recycled water, one would expect less favorable conditions for attachment than those existing in this study.

In view of (3.18), U and k_c values for each sub-pulse can be used to obtain the corresponding

average experimental ϕ values of 2.18±1.12 m^{-1} ($M = 34$) for MS2 and 3.49±1.32 m^{-1} ($M = 34$) for PRD1 during the field experiment, with the highest values occurring when delivery of recycled water to the test basin was halted. Using the following steady-state filtration equation presented by Logan et al. [1995] to describe particle removal by isolated spheres

$$\frac{C(t)}{C_0} = \exp\left[-\frac{3(1-\theta)}{2d_p}\eta z\right], \tag{3.34}$$

and (3.19), the first-order virus filtration rate is given as:

$$\ln\left[\frac{C(t)}{C_0}\right] = -\phi z. \tag{3.35}$$

It should be noted that ϕ is the summation of individual coefficients representing all physicochemical actions that cause suspended viruses to deposit onto porous media [Craft and Eichholz, 1970]. Figure 3.10 shows a plot of $\ln(C/C_0)$ as a function of z for both MS2 and PRD1. The solid lines in Figure 3.10 are based on the average of the estimated ϕ values, whereas the dotted lines represent the lowest and highest estimated ϕ values for the conditions of the field recharge experiment. For a desired log removal of viruses, the corresponding z distance represents the appropriate retention distance. For example, using $\phi = 0.66\ m^{-1}$, the most conservative ϕ value for MS2 at the conditions of the present study, Figure 3.10a suggests that over 40-log removal of bacteriophage would occur in 153 m of passage through the subsurface formation. This distance is equal to the separation distance proposed by the State of California for surface spreading of municipal wastewater [Asano and Cotruvo, 2004]. Obviously, the λ and ϕ values reported here for bacteriophage MS2 and PRD1 are applicable to the conditions of the specific field site. Results with actual human viral pathogens and different subsurface formations are expected to vary.

3.3 Summary

Virus concentrations measured during an artificial recharge field-scale experiment were fitted using a newly developed mathematical model that simulates virus transport in one-dimensional homogeneous, water-saturated porous media accounting for virus sorption (or filtration), inactivation, and

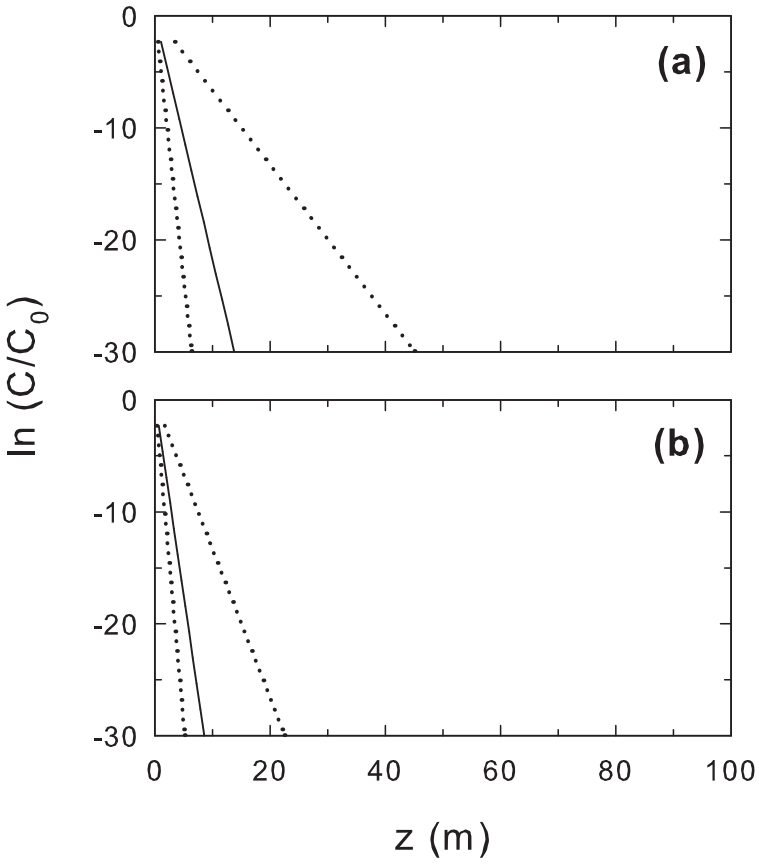

Figure 3.10: Normalized log-concentrations of (a) MS2 and (b) PRD1 in the test basin as a function of distance. The slope of the solid lines are based on the average ϕ values, and the dotted lines represent the lowest and highest estimated ϕ

time-dependent source concentration. The fitted model parameters include the clogging and declogging rate constants, and the inactivation rate constants of suspended and sorbed viruses. These fitted parameters were used to estimate the time-dependent field-scale collision efficiency factors of bacteriophage (MS2 and PRD1). The experimental results of this study can be used for the development of an optimal management scenario that can maximize the amount of recycled water applied to the spreading grounds while still maintaining favorable attachment conditions for virus retention.

Chapter 4

Evaluation of the Factors Controlling the Time-Dependent Inactivation Rate Coefficients of Bacteriophage MS2 and PRD1

In this work, the inactivation process is represented by a pseudo first-order expression with a time-dependent rate coefficient. Static and dynamic batch experiments were performed to compare the effects of temperature and the presence of soil on the time-dependent rate coefficient. Finally, the ability to more accurately predict the inactivation of viruses in groundwater using thermodynamic parameters obtained from time-dependent inactivation rate coefficients is discussed.

4.1 Materials and Methods

4.1.1 Bacteriophage assays

The single-stranded RNA male-specific coliphage, MS2, and the double-stranded DNA somatic *Salmonella typhimurium* phage, PRD1, were used as model viruses in this study. These bacterio-

phage have been used extensively in virus inactivation studies and are considered to be good model viruses because they behave more conservatively (lower sorption) than many pathogenic viruses and are capable of surviving for significant periods of time in groundwater [Yahya et al., 1993; Ryan et al., 2002; Harvey and Ryan, 2004; Anders and Chrysikopoulos, 2005]. Bacteriophage concentrations were measured using the double-agar-layer assay method [Adams, 1959]. PRD1 bacteriophage were analyzed using *Salmonella typhimurium* LT2 (ATCC #15277) as the host bacterium. For the analysis of MS2 bacteriophage, *E. coli* F^- amp (ATCC#700981) were used as the host bacterium with the same concentration of antibiotics as described by Debartolomeis and Cabelli [1991].

The double-agar-layer assay method was performed by preparing a mixture of 1.0 mL of host bacteria, 4.0 mL of molten soft agar (50°C), and 1.0 mL of sample. To ensure that all host bacteria were in log-phase growth, 0.1 mL of prepared stocks of each host were transferred to a test tube containing 10 mL of trypticase soy broth (Difco) and placed in a shaker at 37°C for 4 hours or until cultures were visibly turbid. The mixture was gently vortexed and poured onto the appropriate plating medium. Plates were incubated at 37°C for 24 hours. The concentrations were determined by counting the number of plaques on each plate. Plates were made in duplicate and the concentration was averaged from the plaques counted on each plate. The double-agar-layer assay used for this study was estimated to have a detection limit of 0.5 plaque forming units (PFU)/mL.

4.1.2 Static and dynamic batch experiments

A low-ionic-strength phosphate buffered saline (PBS) solution was prepared with 0.25 mM Na_2HPO_4, 1.2 mM NaCl, 0.037 mM KCl in UV-disinfected distilled water with a specific conductance of 17.8 μS/cm, and adjusted to a pH of 7.5 with HCl. The resulting specific conductance of the pH-adjusted PBS solution was about 200 μS/cm and corresponds to an ionic strength of 2 mM. Prepared stocks of bacteriophage MS2 and PRD1 with concentrations in excess of 10^8 PFU/mL were diluted with the PBS solution to yield bacteriophage concentrations of about 5.0×10^5 and 5.5×10^5 PFU/mL, respectively.

Over 100 oven-baked 40 mL borosilicate glass bottles were filled with 10 mL of the pH-adjusted PBS solution containing bacteriophage MS2 and PRD1. Half the bottles were filled with 10 grams of #60-sieved, pre-soaked, oven-dried Monterey sand (RMC Industries, Decatur, GA) and gently vortexed to ensure that the sand was completely wetted by the PBS solution.

The bottles were arranged into 4 groups (3 static and 1 dynamic) with 2 sets of bottles in each group. Each set consisted of 14 bottles containing virus suspensions with sand and 14 bottles containing virus suspensions without sand. For the static batch experiments one group of bottles was placed in a refrigerator at 4°C, one group was placed in a constant-temperature room at 15°C, and one group was placed in an incubator at 25°C. The dynamic batch experiment was performed with all the bottles attached to a small bench-top tube rotator (Glas-Col, Terre Haute, IN) placed in the constant-temperature room at 15°C. The bottles were rotated end-over-end allowing the sand to mix within the PBS solution containing each bacteriophage. At selected times during the experiment one bottle of each set was chosen at random. Then 1.0 mL of the PBS solution was removed, assayed for bacteriophage MS2 and PRD1 using the double-agar-layer assay method. Subsequently, the used bottles were discarded.

4.1.3 Time-dependent inactivation

Sim and Chrysikopoulos [1996] and Chrysikopoulos and Vogler [2004] have shown that experimental data from numerous batch inactivation studies can be described by a pseudo first-order expression with a time-dependent rate coefficient as follows:

$$\frac{\mathrm{d}C(t)}{\mathrm{d}t} = -\lambda(t)C(t) \tag{4.1}$$

where C is the concentration of suspended viruses in the liquid phase; t is time; and $\lambda(t)$ is the time-dependent inactivation rate coefficient of suspended viruses given by:

$$\lambda(t) = \lambda_0 e^{-\alpha_r t} \tag{4.2}$$

where λ_0 is the initial inactivation rate coefficient and α_r is the resistivity coefficient. Substituting (4.2) into (4.1) and solving the resulting expression subject to the initial condition $C(0) = C_0$, where

C_0 is the initial virus concentration, yields

$$\ln\left[\frac{C(t)}{C_0}\right] = \frac{\lambda_0}{\alpha_r}[\exp(-\alpha_r t) - 1] \tag{4.3}$$

For the limiting case where the inactivation rate coefficient is considered constant (i.e. $\lambda(t) = \lambda$) the preceding equation reduces to the form [Yates et al., 1985]:

$$\ln\left[\frac{C(t)}{C_0}\right] = -\lambda t. \tag{4.4}$$

It should be noted that the parameters λ_0 and α_r can be obtained by fitting equation (4.3), and λ by fitting (4.4) to the data collected from the static or dynamic batch virus inactivation experiments.

4.1.4 Thermodynamic parameters

The initial inactivation rate coefficient, which depends on temperature and the presence of sand, can be expressed by the empirically derived Arrhenius equation:

$$\lambda_0 = A \exp\left[\frac{-E_a}{RT}\right] \tag{4.5}$$

where E_a is the energy of activation, A is the pre-exponential factor, R=8.314 J/K·mol is the gas constant and T is temperature in Kelvin. This approach relies on the concept that a molecule must acquire, through random collisions with other molecules, a certain amount of energy, E_a, before it can undergo a reaction [Ginoza, 1968]. Consequently, the activation energy of the inactivation process can be defined as [Morel and Hering, 1993]:

$$E_a = -\Omega R \tag{4.6}$$

where Ω is the slope of the plot of ln λ_0 versus 1/T (Arrhenius plot).

Following basic reaction rate theory, the effects of temperature and the presence of sand on the virus inactivation process can be determined by assuming that a thermodynamic equilibrium exists between the concentration of infective viruses and viruses in an activated (transition) state as follows:

$$C \rightleftharpoons C^{\bullet} \rightarrow C^{\circ} \tag{4.7}$$

where $C^{\bullet}$ is the concentration of suspended viruses in an activated (transition) state and C° is the concentration of non-infective viruses. The equilibrium of suspended viruses in the liquid phase with suspended viruses in the activated (transition) state is defined by a pseudo-equilibrium (or "steady-state") constant, $K^{\bullet}$, given as:

$$K^{\bullet} = \frac{C^{\bullet}}{C} \tag{4.8}$$

Furthermore, the first-order expression for the formation of suspended viruses in the activated state can be described by

$$\frac{\mathrm{d}C(t)}{\mathrm{d}t} = -\acute{k}C^{\bullet} \tag{4.9}$$

where $\acute{k}$ is the reaction rate coefficient of the overall inactivation process, which is given by the following relationship [Aikens, 1990]:

$$\acute{k} = \frac{k_B T}{\hbar} \tag{4.10}$$

where k_B=1.381×10^{-23} J/K is Boltzman's constant, and $\hbar$=6.626×10^{-34} J/sec is Planck's constant. In view of (4.1) and (4.9), the time-dependent rate coefficient can be expressed as:

$$\lambda(t) = \acute{k}K^{\bullet} \tag{4.11}$$

Although $K^{\bullet}$ cannot be measured directly, it can be related to other standard thermodynamic parameters as follows [Ginoza, 1968]:

$$\Delta G^{\bullet} = -RT \ \ln K^{\bullet} = \Delta H^{\bullet} - T\Delta S^{\bullet} \tag{4.12}$$

where $\Delta G^{\bullet}$ is the free energy of formation of the activated (transition) state, $\Delta H^{\bullet}$ is the standard enthalpy of formation of the activated (transition) state, and $\Delta S^{\bullet}$ is the standard entropy of formation of the activated (transition) state. In view of equations (4.2), and (4.10)–(4.12), the value of the thermodynamic parameter $\Delta G^{\bullet}$ required to undergo the inactivation process can be expressed as follows:

$$\Delta G^{\bullet} = -RT \ \ln\left[\frac{\lambda_0 \ \hbar}{k_B \ T}\right]. \tag{4.13}$$

4.2 Results and Discussion

4.2.1 Model simulations

The parameters λ_0 and α_r were determined by fitting equation (4.3) to the observed normalized bacteriophage log-concentrations, whereas the λ values were determined by linear regression fit to equation (4.4) of the same experimental data. Note that equation (4.3) represents time-dependent inactivation, whereas equation (4.4) assumes that the inactivation rate is constant. Table 4.1 shows the λ_0, α_r and λ values for both MS2 and PRD1 with and without sand at 4°, 15° and 25°C. It should be noted that sand containing only trace amounts of ferric oxyhydroxide coatings or organic carbon was used in this study in order to avoid virus adsorption onto the sand grains [Murray and Laband, 1979]. Furthermore, the low ionic strength of the final PBS solution, along with the low bacteriophage concentrations in the virus suspensions, minimizes any possible loss of virus infectivity due to Brownian coagulation [Grant, 1995; Chu et al., 2000; Matsui et al., 2003].

The MS2 concentrations from the static batch experiments with and without sand at 4°, 15° and 25°C are shown in Figure 4.1. The plots indicate that MS2 inactivation is affected by the ambient temperature. It should be noted that normalized bacteriophage concentrations over 1 are due to slight variations in the initial concentration of the virus suspensions present in each bottle. Also presented in Figure 4.1 are the corresponding simulated concentration histories for both time-dependent and constant inactivation rates (based on the parameter values listed in Table 4.1, at 4°, 15° and 25°C). The simulated concentration histories for the time-dependent inactivation match the experimental data slightly better than using constant inactivation rates. Sim and Chrysikopoulos [1996] made a similar observation.

The temporal variability of the inactivation rate coefficient is attributed to multiphasic sequential inactivation caused by the presence of two or more subpopulations of bacteriophage, which exhibit different heat sensitivities [Ginoza, 1968; Grant el al., 1993; Chrysikopoulos and Vogler, 2004]. The magnitude of α_r is proportional to the resistivity of the dominant subpopulation, because the overall inactivation is controlled by the dominant subpopulation [Sim and Chrysikopoulos,

Table 4.1: Fitted Inactivation Parameters for Bacteriophage MS2 and PRD1

Conditions	$\lambda_0(\text{day}^{-1})$	α_r (day^{-1})	λ (day^{-1})
	MS2		
Static batch experiments			
4°C, sand	1.5×10^{-2}	2.5×10^{-5}	2.0×10^{-2}
4°C, no sand	2.6×10^{-2}	3.3×10^{-6}	2.7×10^{-2}
15°C, sand	6.6×10^{-2}	3.4×10^{-6}	7.6×10^{-2}
15°C, no sand	6.0×10^{-2}	6.7×10^{-6}	6.7×10^{-2}
25°C, sand	2.6×10^{-1}	4.3×10^{-5}	3.0×10^{-1}
25°C, no sand	1.2×10^{-1}	9.2×10^{-3}	7.9×10^{-2}
Dynamic batch experiments			
15°C, sand	7.1×10^{-2}	4.2×10^{-3}	7.2×10^{-2}
15°C, no sand	9.1×10^{-2}	6.7×10^{-5}	9.5×10^{-2}
	PRD1		
Static batch experiments			
4°C, sand	3.1×10^{-3}	5.3×10^{-4}	4.0×10^{-3}
4°C, no sand	6.7×10^{-3}	1.9×10^{-4}	7.7×10^{-3}
15°C, sand	2.0×10^{-3}	3.0×10^{-4}	1.9×10^{-3}
15°C, no sand	2.1×10^{-3}	3.5×10^{-5}	5.2×10^{-3}
25°C, sand	9.1×10^{-3}	6.1×10^{-5}	1.0×10^{-2}
25°C, no sand	3.3×10^{-2}	1.8×10^{-2}	1.4×10^{-2}
Dynamic batch experiments			
15°C, sand	1.2×10^{-1}	1.5×10^{-2}	5.8×10^{-2}
15°C, no sand	1.1×10^{-4}	1.2×10^{-2}	1.9×10^{-3}

1996]. Temporally variable inactivation allows for rapid inactivation of the most sensitive subpopulations and slower inactivation of the more resistive subpopulations. Note that in the presence of sand, λ_0 increases faster with increasing temperature than for the case where there is no sand present, whereas α_r is greatest at 25°C in the absence of sand.

The static batch PRD1 inactivation experimental data with and without sand as well as the corresponding simulated concentration histories for both time-dependent and constant inactivation rates, based on the parameter values listed in Table 4.1 at 4°, 15° and 25°C are shown in Figures **??**. Clearly, the temperature as well as the presence of sand have only a minor effect on PRD1 inactivation under the conditions examined in this work. Note that for PRD1 the observed greater inactivation at 4°C than at 15°C suggests a minor effect of temperature might exist during the inactivation process. It should be noted that λ_0 for PRD1 in the presence of sand is affected by temperature to a lesser extent than the case where there is no sand present. The increased α_r value for PRD1 at 25°C in the absence of sand indicates the presence of a large subpopulation which is relatively insensitive to heat.

Figure 4.3 shows the bacteriophage inactivation experimental data from the dynamic batch experiment at 15°C with and without sand, together with the corresponding simulated concentration histories for both time-dependent and constant inactivation rates. Based on the similar λ_0 and λ values for the static and dynamic batch experiments at 15°C listed in Table 4.1, the presence of an air phase has little effect on the inactivation process of the dominant MS2 subpopulation. Thompson et al. [1999] observed a similar lack of MS2 inactivation under similar batch conditions. However, there is a slight increase in α_r values during the dynamic batch experiments, especially in the presence of sand. Such an increase in the magnitude of α_r suggests that a subpopulation of MS2 bacteriophage exists with a slightly higher sensitivity to the presence of an air phase. In contrast, the increased inactivation rate for PRD1 during the dynamic batch experiment with sand, along with the increased α_r values with and without sand, suggest that the presence of air-liquid and air-solid interfaces, instead of temperature, sand, or the presence of air-liquid interfaces, are responsible for

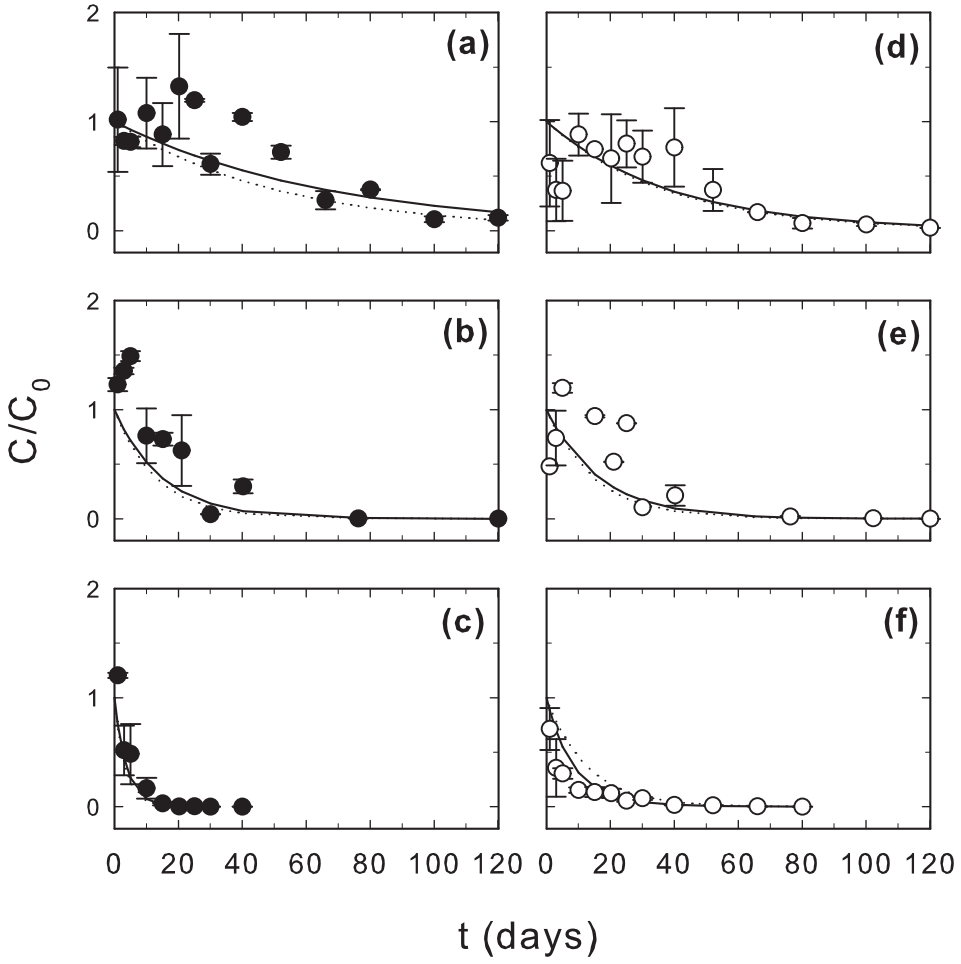

Figure 4.1: Experimental data for MS2 inactivation under static batch conditions with sand (solid circles) and without sand (open circles) at temperatures of (a, d) 4°, (b, e) 15° and (c, f) 25°C. Simulated concentration histories are based on the pseudo first-order inactivation model (solid curves) and constant rate inactivation model (dotted curves).

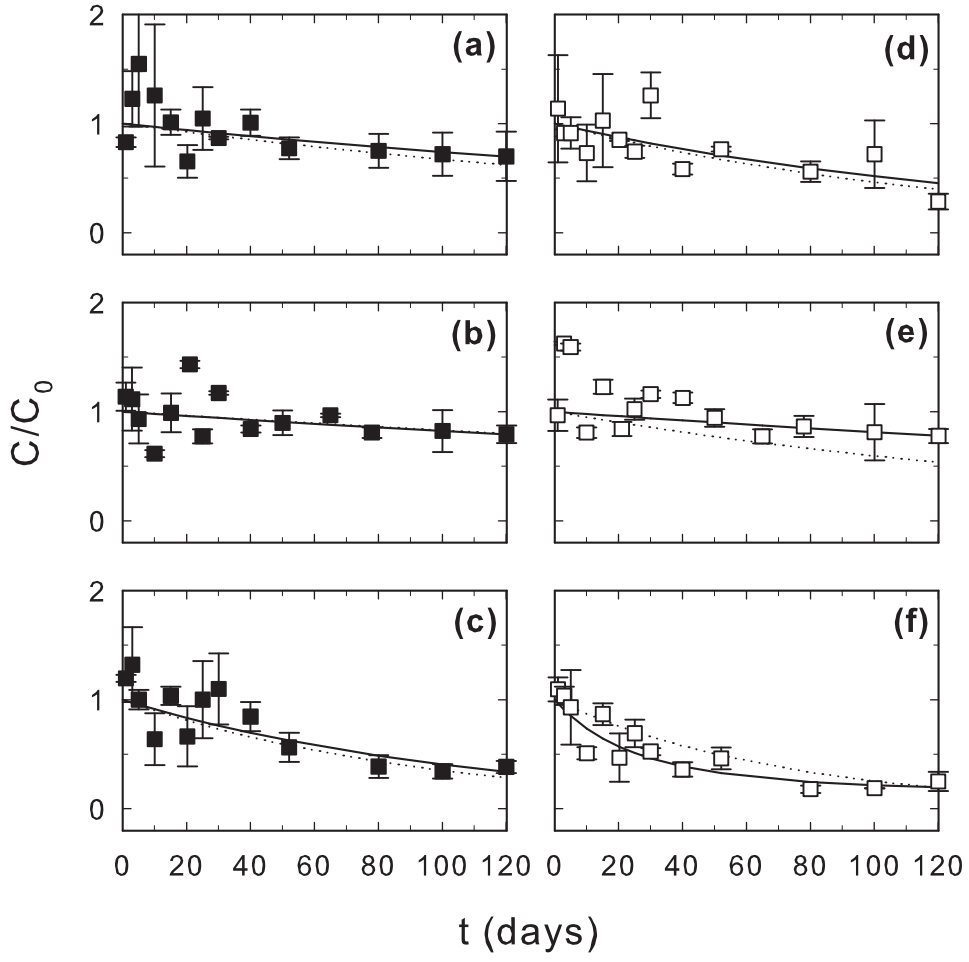

Figure 4.2: Experimental data for PRD1 inactivation under static batch conditions with sand (solid squares) and without sand (open squares) at temperatures of (a, d) 4°, (b, e) 15° and (c, f) 25°C. Simulated concentration histories are based on the pseudo first-order inactivation model (solid curves) and constant rate inactivation model (dotted curves).

the greatest damage to specific viral components that are required for infection.

4.2.2 Inactivation thermodynamics

The native structure of proteins are maintained by a complex interplay of various forces that act to fold and hold its primary structure, the polypeptide chain, in a specific conformation [Ginoza, 1968]. Therefore, the molecular process of inactivation occurs when the polypeptide chain conformation is altered or destroyed by some environmental stress and the protein molecules generally lose their ability to infect a host. To analyze the molecular processes involved in the inactivation process, the λ_0 values listed in Table 4.1 were used to determine the thermodynamic parameters E_a, $\Delta G^{\bullet}$, $\Delta H^{\bullet}$, and $\Delta S^{\bullet}$ for each of the bacteriophage considered in this study. It should be noted that these parameters describe the thermodynamics of the formation of the activated (transition) state shown in (4.7) and as such provide information on the energy requirements to undergo the inactivation process. Equilibrium values for virus inactivation are required to obtain thermodynamic parameters for the complete inactivation process shown in (4.7). However, it is not possible to obtain these values because the alteration that causes virus inactivation is irreversible or, at least, difficult to reverse [Ginoza, 1968].

Arrhenius plots for MS2 and PRD1 inactivation for the static batch experiments with and without sand using λ_0 values listed in Table 4.1 are shown in Figure 4.4. The slopes of the MS2 Arrhenius plots shown in Figure 4.4a indicate that the energies of activation (formation of the transition state that results in loss of infectivity) state required for MS2 to undergo the inactivation process under the static batch conditions were 93.9 kJ/mol in the presence of sand and 50.5 kJ/mol in the absence of sand.

Comparison of the slopes of the MS2 Arrhenius plots with and without sand shown in Figure 4.4a indicates a cross-over pattern with a greater λ_0 in the absence of sand at 4°C and 15°C, and a greater λ_0 in the presence of sand at 25°C. The slopes of the PRD1 Arrhenius plots shown in Figure **??** indicate that the energies of activation required for PRD1 to undergo the inactivation process

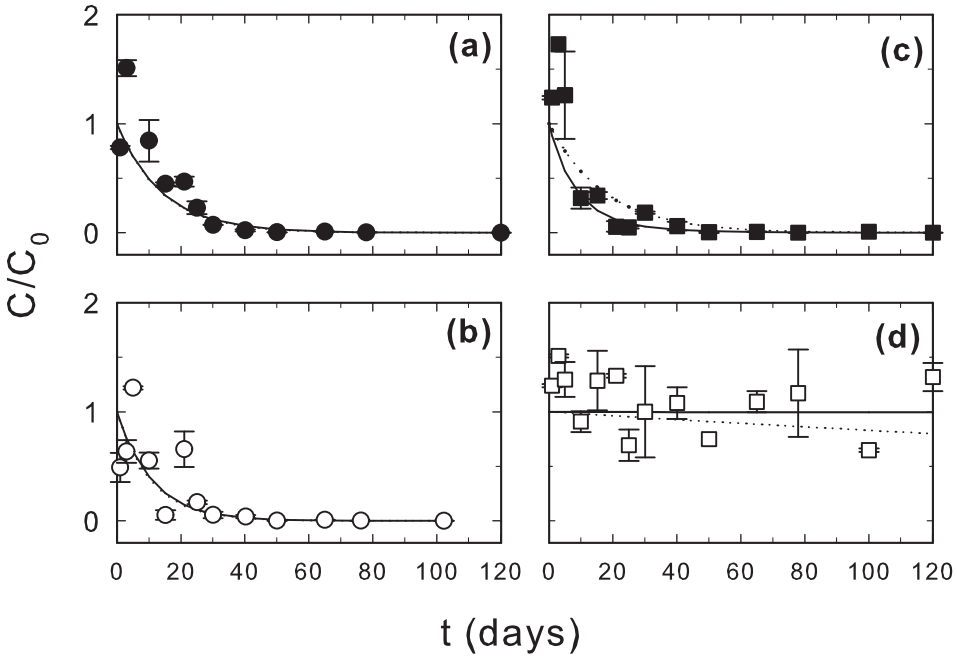

Figure 4.3: Experimental data for (a, b) MS2 and (c, d) PRD1 inactivation under dynamic batch conditions with sand (solid symbols) and without sand (open symbols) at 15°C. Simulated concentration histories are based on the time-dependent inactivation model (solid curves) and constant rate inactivation model (dotted curves).

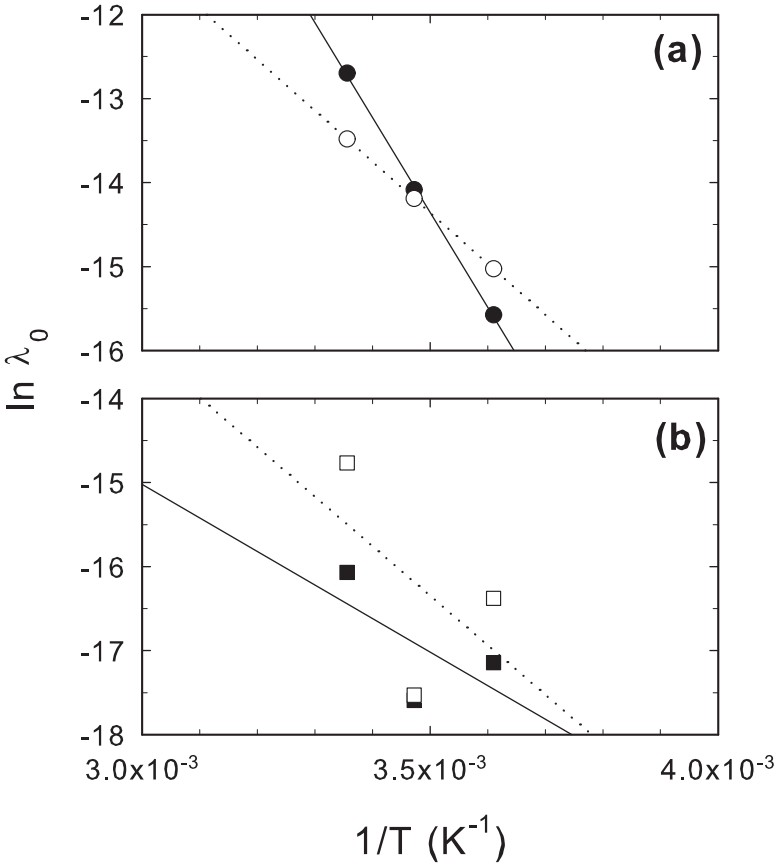

Figure 4.4: Arrhenius plots for (a) MS2 and (b) PRD1 inactivation under static batch conditions with sand (solid symbols) and without sand (open symbols). The slopes of the Arrhenius plots indicate the activation energies in the presence of sand (solid line) and in the absence of sand (dotted line).

under the static batch conditions were 33.2 kJ/mol in the presence of sand and 49.0 kJ/mol in the absence of sand. For PRD1, the λ_0 values are greater in the absence of sand for all temperatures considered in this study. The activation energies for the inactivation of both MS2 and PRD1 are listed in Table 4.2.

Table 4.2: Thermodynamic Parameters for Bacteriophage MS2 and PRD1 Inactivation

	E_a (kJ/mol)	$\Delta G^\bullet$ (kJ/mol) 4°, 15° and 25°C	$\Delta H^\bullet$ (kJ/mol)	$\Delta S^\bullet$ (J/mol·K)
		MS2		
sand	93.9	103.5, 104.2, 104.4	91.6	43.3
no sand	50.5	102.3, 104.4, 106.4	48.1	195.5
		PRD1		
sand	33.2	107.2, 112.6, 112.8	32.4	272.5
no sand	49.0	105.4, 112.42, 109.6	49.8	206.2

Preston and Farrah [1988] reported that low activation energies ($E_a < 160$ kJ/mol; 1 calorie = 4.184 J) indicate that virus adsorption is a physical process rather than a chemical process ($E_a >$ 160 kJ/mol). The low activation energies for both bacteriophage employed in this study suggest that electrostatic and/or hydrodynamic interactions play a significant role in virus inactivation as well. However, the standard entropy of formation of the activated state is also an important factor in determining the magnitude of the inactivation rate coefficient [Ginoza, 1968].

In view of relationship (4.12), it is clear that the standard entropy of formation of the activated (transition) state, $\Delta S^\bullet$, can be determined directly from the change in $\Delta G^\bullet$ values as a function of

temperature, where the y-intercepts indicate the standard enthalpy of formation of the activation (transition) state, $\Delta H^{\bullet}$. The $\Delta G^{\bullet}$ values for the inactivation of both MS2 and PRD1 under static batch conditions at 4°, 15° and 25°C were determined from (4.13) and they are listed in Table 4.2. Figure 4.5 presents the free energy plots for MS2 and PRD1 inactivation with and without sand. For MS2 it was determined from the slope of the free energy plot shown in Figure 4.5a that $\Delta S^{\bullet}$ is equal to 43.3 J/mol·K in the presence of sand and 195.5 J/mol·K in the absence of sand. For PRD1 it was determined from Figure 4.5b that $\Delta S^{\bullet}$ is equal to 272.5 J/mol·K in the presence of sand and 206.1 J/mol·K in the absence of sand.

The $\Delta S^{\bullet}$ values listed in Table 4.2 indicate the presence of sand has a greater effect on increasing disorder of the activated (transition) state for PRD1 (value is more positive) than it is for MS2. This results in lower $\Delta G^{\bullet}$ values for MS2 and allows the inactivation process to proceed at a faster rate than PRD1. In contrast, the absence of sand has the effect of decreasing slightly the $\Delta S^{\bullet}$ value for PRD1. It should be noted here that the results of this study provide similar $\Delta S^{\bullet}$ and $\Delta H^{\bullet}$ values to those reported by Ginoza [1968] at higher temperatures and suggest that protein denaturation is the predominant mechanism involved in the inactivation process of viruses.

The results from the dynamic batch experiments suggest that the presence of air-liquid and air-solid interfaces has the effect of decreasing $\Delta S^{\bullet}$ values for PRD1 during the inactivation process as well. However, it is not clear from the kinetic data collected during the dynamic batch experiments whether protein denaturation is the cause of inactivation. Using thermodynamic parameters based on the time-dependent inactivation model provides a better method to predict the inactivation of viruses in groundwater. Furthermore, the observed temporal variation of the inactivation rate coefficients suggest that virus subpopulations may remain infective in porous media for an extended period of time and continue to migrate downstream to points of withdrawal.

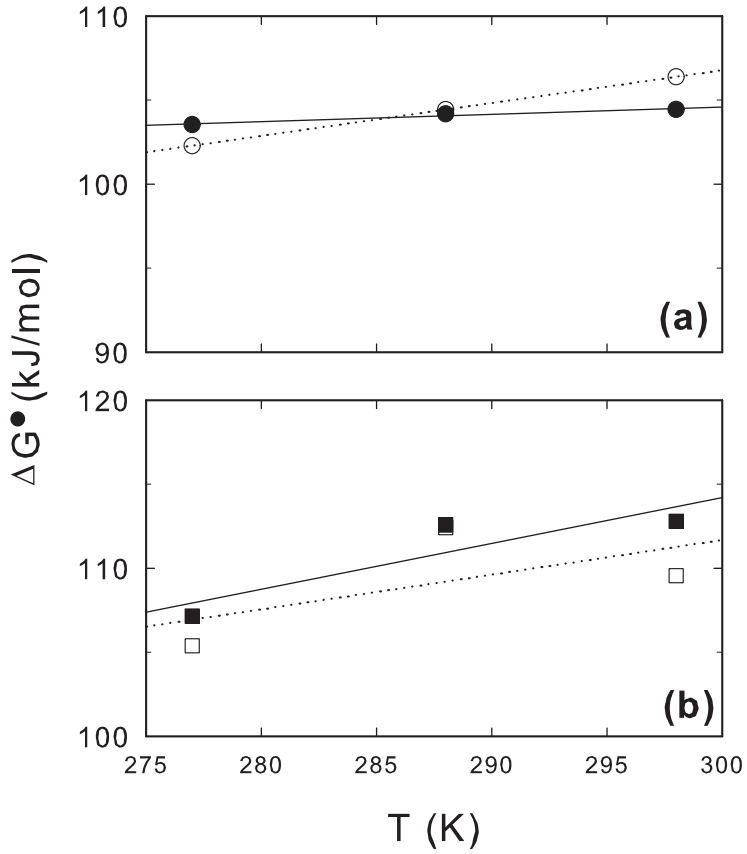

Figure 4.5: Free energy of formation of the activated state, $\Delta G^{\bullet}$, as a function of temperature for (a) MS2 and (b) PRD1 inactivation under static batch conditions with sand (solid symbols) and without sand (open symbols). The slopes of the free energy plots indicate the standard entropy of formation of the activated state, $\Delta S^{\bullet}$, and the y-intercepts indicate the standard enthalpy of formation of the transition state, $\Delta H^{\bullet}$, in the presence of sand (solid line) and in the absence of sand (dotted line).

4.3 Summary

Static and dynamic batch experiments were conducted to study the effects of temperature and the presence of sand on the inactivation of bacteriophage MS2 and PRD1. The experimental data suggested that the inactivation process can be satisfactorily represented by a pseudo first-order expression with time-dependent rate coefficients. The time-dependent rate coefficients were used to determine pertinent thermodynamic properties required for the analysis of the molecular processes involved in the inactivation of each bacteriophage. A combination of high temperature and the presence of sand appears to produce the greatest disruption to the surrounding protein coat of MS2. However, the lower activation energies for PRD1 indicate a weaker dependence of the inactivation rate on temperature. Instead, the presence of air-liquid and air-solid interfaces appears to produce the greatest damage to specific viral components that are related to infection. These results indicate the importance of using thermodynamic parameters based on the time-dependent inactivation model to better predict the inactivation of viruses in groundwater.

Chapter 5

Transport of Bacteriophage (MS2 and PRD1) Through Variably Saturated Packed Sand Columns

in this work, laboratory-scale transport experiments were conducted in columns packed with sand under saturated and unsaturated conditions. The viruses employed were the male-specific RNA coliphage, MS2, and the *Salmonella typhimurium* phage, PRD1. A mathematical model developed to quantify the processes responsible for removal of viruses during vertical transport in one-dimensional, unsaturated porous media that accounts for virus sorption and inactivation was used to fit the data collected from the laboratory experiments. The liquid to liquid-solid and liquid to air-liquid interface mass transfer rates were shown to increase for both bacteriophage as saturation levels were reduced. The experimental results indicate that even for unfavorable attachment conditions within a sand column, saturation fluctuations can dramatically affect virus transport through porous media.

5.1 Materials and Methods

5.1.1 Bacteriophage assays

The model viruses employed for this study were MS2 and PRD1. MS2 is an icosahedral, single-stranded RNA male-specific coliphage with an average diameter of ∼25 nm and an isoelectric point (pH_{iep}) of 3.9 [Zerda, 1982]. PRD1 is an icosahedral, double-stranded DNA somatic *Salmonella typhimurium* phage, 62 nm in diameter, with pH_{iep} ∼4.5 measure in a calcium phosphate buffer solution containing 10^{-4} M calcium [Bales et al., 1991]. These bacteriophage have been used extensively in virus transport and inactivation studies and are considered to be good model viruses because they behave more conservatively (attach poorly) than many pathogenic viruses and are relatively persistent during transport through the subsurface [Hurst et al., 1980; Yates et al., 1985; Yahya et al., 1993; Bales et al., 1997; Ryan et al., 1999; Schijven et al., 1999; Ryan et al., 2002; Harvey and Ryan, 2004; Anders and Chrysikopoulos, 2005].

The effluent concentrations of each bacteriophage were measured using the double-agar-layer assay method [Adams, 1959]. Trypticase soy broth (TSB) (Difco), TSB (Difco) soft agar (containing 0.05% 1N $CaCl_2$) and trypticase soy agar (TSA) (Difco) bottom agar were used for analyzing PRD1 bacteriophage using *Salmonella typhimurium* LT2 (ATCC #15277) as the host bacterium. For the analysis of MS2 bacteriophage, *E. coli* F^- amp (ATCC #700981) were used as the host bacterium with the same concentration of antibiotics as described by Debartolomeis and Cabelli [1991]. To ensure that all host bacteria were in log-phase growth, 0.1 mL of prepared stocks of each host were transferred to a test tube containing 10 mL of TSB and placed in a shaker at 37°C for 4 hours or until cultures were visibly turbid. The mixture was gently vortexed and poured onto the appropriate plating medium. Plates were incubated at 37°C for 24 hours. The concentrations were determined by counting the number of plaques on each plate. Plates were made in duplicate and the concentration was averaged from the plaques counted on each plate. The double-agar-layer assay used for this study was estimated to have a detection limit of 0.5 plaque forming units (PFU)/mL.

5.1.2 Bromide analysis

Bromide, in the form of sodium bromide, was chosen as the non-reactive tracer for the transport column experiments. It should be noted that alkali halides are the most commonly used salts for subsurface fluid tracing [Chrysikopoulos, 1993]. All effluent samples for bromide were collected into borosilicate test tubes. Bromide concentrations were measured using ion chromatography (ICS-1500, Dionex Corp., Sunnyvale, CA).

5.1.3 Sand preparation

Clean, graded, kiln-dried Monterey sand (RMC Industries, Decatur, GA) was used in this study. The sand was sieved using a 250 micron mesh, soaked in UV-disinfected distilled water for several days to remove any salts, and oven-dried for 24 hours at 105°C. The sand was placed in sterile containers to reduce the possibility of microbial contamination.

Analysis by X-ray powder diffractometry found the sand to be composed of quartz as the major phase ($>$ 25% by weight) with minor amounts (between 5 and 25% by weight) of microcline and albite and trace amounts ($<$ 5% by weight) of muscovite and phlogopite. Reflectance spectroscopic analysis over the visible to near-infrared wavelength range (0.4 - 2.5 μm) using a halogen lamp for illumination identified hematite coatings on the grains. Total carbon was measured by an automated carbon analyzer and found to be less than 0.05 mg/g of sand.

5.1.4 Preparation of virus suspension

An aliquot of stock suspensions of both bacteriophage was diluted with a low-ionic-strength phosphate buffered saline (PBS) solution. The PBS solution was prepared with 0.25 mM Na_2HPO_4, 1.2 mM NaCl, 0.037 mM KCl in UV-disinfected distilled water with a specific conductance of 17.8 μS/cm, and adjusted to a pH of 7.5 with HCl. The final virus suspension was prepared by combining the diluted stock suspensions with the non-reactive tracer. The resulting virus suspension contained bacteriophage MS2 and PRD1 concentrations of 5.0×10^5 and 5.5×10^5 PFU/mL, respec-

tively. The specific conductance of the final virus suspension was 212 μS/cm and corresponds to an ionic strength of about 2 mM. This is an ionic strength low enough to ensure unfavorable attachment conditions.

5.1.5 Transport experiments

The transport column experiments were conducted under saturated conditions and under decreasing amounts of moisture content. For each experiment, the pre-washed sand was packed into 5.1-cm in diameter by 15.2-cm in length Plexiglass columns. The columns were filled from the bottom with the PBS solution at a rate of 1 mL/min to avoid the capture of air bubbles. The porosity and bulk density of each column were determined by noting the weight difference before and after each column was completely saturated with the PBS solution. Initial bacteriophage concentrations were measured from samples collected through the tubing before the tubing was attached to the column. The saturated transport experiments were conducted using a peristaltic pump. The virus suspension was introduced from the bottom of the column and effluent samples were collected after they exited from the top of the column.

For the unsaturated experiments, the packed columns were attached to a special apparatus (Soil Measurement Systems, Tucson, AZ) that allowed for various levels of water saturation. The special apparatus consists of a fraction collector placed inside a vacuum chamber while the packed column is placed above the vacuum chamber with its lower outlet connected to the vacuum chamber. The virus suspension was applied at a rate that created a constant water potential throughout the packed column. The water potential was measured by tensiometers placed into the upper and lower end of each packed column and recorded with a datalogger (Campbell Scientific, Inc., Logan, UT). Liquid samples were collected over regular time intervals from the column effluent in small fractions by using the automatic fraction collector placed inside the vacuum chamber. The pressure inside the vacuum chamber was monitored by a hand-held tensiometer. After the completion of each experiment, the Plexiglas column apparatus was disassembled, cleaned, and reassembled to avoid

any carry-over of bacteriophage or bromide.

5.2 Model Development

5.2.1 Virus transport in unsaturated porous media

The transport of viruses in one-dimensional, unsaturated porous media accounting for virus sorption and inactivation is governed by the following partial differential equation [Sim and Chrysikopoulos, 2000]

$$\frac{\partial}{\partial t}\left(\theta_m C\right) + \rho\frac{\partial C^*}{\partial t} + \frac{\partial}{\partial t}\left(\theta_m C^\diamond\right) = \frac{\partial}{\partial z}\left(D_z\theta_m\frac{\partial C}{\partial z}\right) - \frac{\partial}{\partial z}\left(qC\right) - \lambda\theta_m C - \lambda^*\rho C^* - \lambda^\diamond\theta_m C^\diamond, \quad (5.1)$$

where C is the virus concentration in the liquid phase; C^* is the deposited virus concentration at the liquid-solid interface; $C^\diamond$ is the adsorbed virus concentration at the air-liquid interface; q is the specific discharge (Darcian fluid flux); θ_m is the volumetric moisture content (moisture volume divided by the total volume of the porous medium); λ, λ^*, and $\lambda^\diamond$ are the inactivation rate coefficients of viruses suspended in the liquid phase, viruses sorbed at the liquid-solid interface, and viruses sorbed at the air-liquid interface, respectively; ρ is the bulk density of the solid matrix; t is time; and the vertical spatial coordinate z is positive downward. The last three terms on the right-hand side of (5.1) represent the inactivation of liquid phase viruses, viruses sorbed at the liquid-solid interface, and viruses sorbed at the air-liquid interface, respectively. Furthermore, the second and third terms on the left-hand side of (5.1) represent virus accumulation at the liquid-solid and air-liquid interfaces, respectively. The vertical hydrodynamic dispersion coefficient D_z is defined as [Nielsen et al., 1986]

$$D_z = \alpha_z\frac{q}{\theta_m} + \mathcal{D}_e, \quad (5.2)$$

where $\mathcal{D}_e = \mathcal{D}/\tau$ is the effective molecular diffusion coefficient in the unsaturated porous medium (where $\mathcal{D}$ is the molecular diffusion coefficient and $\tau \geq 1$ is the tortuosity coefficient); and α_z is the vertical dispersivity. Virus diffusivity, $\mathcal{D}$, is governed by Brownian motion and is described by the

Stokes-Einstein equation as [Atkins, 1990]

$$\mathcal{D} = \frac{k_B T}{3\pi\mu d_v}, \tag{5.3}$$

where $k_B = 1.38\times10^{-23}$ (kg·m^2)/(s^2·K) is the Boltzman constant, d_v is the virus diameter, $\mu = 8.91\times10^{-4}$ kg/(m·s) is the viscosity of water, and T is the absolute temperature in Kelvin.

The initial and boundary conditions present for the transport system examined here are

$$C(0,z) = C^*(0,z) = C^\diamond(0,z) = 0, \tag{5.4}$$

$$-D_z\theta_m\frac{\partial C(t,0)}{\partial z} + q(t,0)C(t,0) = \begin{cases} q(t,0)C_0, & 0 \le t \le t_p \\ 0 & t_p \le t \end{cases} \tag{5.5}$$

$$\frac{\partial C(t,\infty)}{\partial z} = 0, \tag{5.6}$$

where C_0 is the pulse-type source concentration, and t_p is the duration of the pulse. The condition (5.4) establishes that there is no initial liquid phase and adsorbed virus concentrations within the porous medium. The flux-type boundary condition (5.5) for pulse injection implies concentration discontinuity at the ground surface (inlet) and leads to material balance conservation [Parker and van Genuchten, 1984; Chrysikopoulos et al., 1990]. The downstream boundary condition (5.6) preserves concentration continuity for a vertical, semi-infinite porous medium.

5.2.2 Virus sorption onto interfaces

The accumulation of deposited viruses at solid-liquid and air-liquid interfaces is described by the following expressions [Sim and Chrysikopoulos, 1999]

$$\rho\frac{\partial C^*}{\partial t} = k\theta_m\big(C - C_g\big) - \lambda^*\rho C^*, \tag{5.7}$$

$$\frac{\partial}{\partial t}\big(\theta_m C^\diamond\big) = k^\diamond\theta_m C - \lambda^\diamond\theta_m C^\diamond, \tag{5.8}$$

where k and $k^\diamond$ are the liquid to liquid-solid and liquid to air-liquid interface mass transfer rates, respectively; and $C_g(t,z)$ is the liquid phase concentration of viruses in direct contact with solids. It

is assumed that the following linear equilibrium relationship is valid [Sim and Chrysikopoulos, 1996]

$$C^* = K_d C_g, \tag{5.9}$$

where K_d is the partition or distribution coefficient and implies that virus sorption onto solids occurs if $C > C_g$, whereas desorption occurs when $C < C_g$.

The liquid to liquid-solid interface mass transfer rate is expressed as

$$k = \kappa a_T, \tag{5.10}$$

where κ is the liquid to liquid-solid interface mass transfer coefficient; and a_T is the specific liquid-solid interface area. It should be noted that the transfer of viruses from the bulk liquid to a liquid-solid interface is assumed to be governed by virus diffusion through an outer liquid layer surrounding the soil particle, the thickness of which depends on local hydrodynamic conditions [Vilker and Burge, 1980; Folger, 1992].

The liquid to air-liquid interface mass transfer rate is defined as

$$k^\diamond = \kappa^\diamond a_T^\diamond, \tag{5.11}$$

where $\kappa^\diamond$ is the liquid to air-liquid interface mass transfer coefficient; and $a_T^\diamond$ is the specific air-liquid interface area. It should be noted that for a given moisture content the accumulation of viruses at air-liquid interfaces, as described by (5.8), is governed by irreversible virus sorption onto the air-water interface and subsequent virus inactivation.

5.2.3 Transport parameter estimation

There are several approaches available for parameter estimation [Beck and Arnold, 1977]. This work employed the Levenberg-Marquardt nonlinear least squares regression method was employed [Levenberg, 1944, Marquardt, 1963]. The objective of the nonlinear least squares method is to calculate values of the model parameters that minimize the residual sum of squares between simulated and observed data. Values of U and D_z for each saturated experiment were obtained by fitting the

standard advection-dispersion equation to the bromide breakthrough response. Furthermore, the values of k and K_d were obtained by fitting the virus transport model for saturated flow conditions to the observed bacteriophage concentrations by using the previously estimated values of U and D_z. The parameter $k^{\diamond}$ was set to zero because at 100% water saturation there is no air-liquid interfaces present in the packed columns.

The liquid to liquid-solid interface mass transfer coefficient, κ, was calculated by defining the specific liquid-solid interface area, a_T, as the ratio of total surface area of soil particles to the bulk volume of the porous medium [Fogler, 1992]

$$a_T = \frac{3(1-\theta_s)}{r_p}, \tag{5.12}$$

where r_p represents the average radius of soil particles; and $\theta_m = \theta_s$ is the water content of the saturated porous medium.

Water flow in unsaturated or variably saturated, homogeneous, rigid porous media is traditionally described with the Richards equation [Philip, 1969; Bear, 1972, p. 511]. However, in this study all unsaturated column experiments were conducted only after a constant water potential was achieved throughout the packed column. By allowing the complete redistribution of soil moisture, the unknown values of U and D_z for the unsaturated column experiments were estimated by using the same procedure as described above for the saturated column experiments. The remaining unknown parameters for the unsaturated column experiments, k, K_d, and $k^{\diamond}$, were obtained by fitting the virus transport model to the observed bacteriophage breakthrough concentrations.

The capillary tube model by Cary [1994], which relies on experimental capillary pressure-saturation relations to estimate the pore-size distribution, was used to calculate the specific air-liquid interface area. This model defines the specific air-liquid interface area, $a_T^{\diamond}$, as the ratio of the total air-liquid interface area to the bulk volume of the porous medium

$$a_T^{\diamond}(\theta_m) = \frac{2\theta_s^b}{r_0}\left[\zeta\theta_r\frac{\theta_s^{-b}-\theta_m^{-b}}{-b} + \frac{\theta_s^{1-b}-\theta_m^{1-b}}{1-b}\right], \tag{5.13}$$

where ζ and b are empirical, soil type specific constants; θ_r is the residual or monolayer moisture

content; and r_0 is the effective pore radius at air-entry which can be evaluated by the capillary rise equation with zero contact angle as follows [Guymon, 1994, p. 43]

$$r_0 = \frac{2\sigma}{\rho_w g h_0}, \tag{5.14}$$

where σ is the surface tension of water; ρ_w is the density of water; g is the gravitational constant; and h_0 is the air-entry value, defined as the pore water head where air begins to enter water-saturated pores [Guymon, 1994]. It should be noted that the inverse of this ratio is the effective water film thickness in the porous media (averaged over both true water thickness and pendular water around grain-grain contacts) during the unsaturated column experiments [Wan and Tokunaga, 1998].

5.3 Results and Discussion

5.3.1 First moment analysis

A set of 4 column experiments were completed using the virus suspension (bacteriophage/bromide solution); two saturated and two unsaturated. Shown in Figure 5.1 are the normalized bromide concentrations observed during experiment 1 at 100% water saturation (Figure 5.1a), experiment 2 at 100% water saturation (Figure 5.1b), experiment 3 at 76% water saturation (Figure 5.1c) and experiment 4 at 54% water saturation (Figure 5.1d).

Clearly, the bromide concentration response curves shown in Figure 5.1 indicate that there was no detectable retention (behaved conservatively) of bromide in the columns. The mean concentration arrival time for bromide during each experiment is defined by the first normalized absolute moment as [Valocchi, 1985]:

$$m_1 = \int_0^\infty t C_T(t,z)\mathrm{d}t \Big/ \int_0^\infty C_T(t,z)\mathrm{d}t. \tag{5.15}$$

The mean arrival times provided by first moment analysis of the bromide concentration data is listed in Table 5.1. The mean arrival times for the saturated column experiments were 0.77 and 0.71 hours and indicate that these experiments were conducted under similar interstitial velocities. Furthermore, the mean arrival times increased to 1.04 hours at 76% water saturation, and continue to

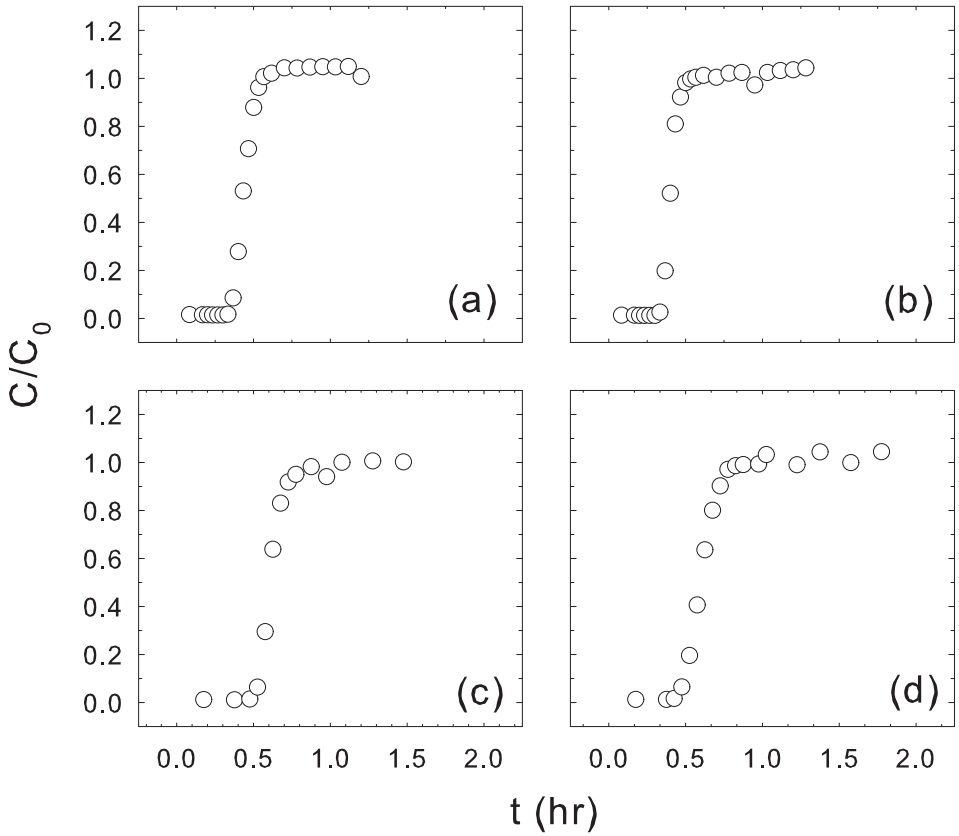

Figure 5.1: Bromide concentration breakthrough data for (a) experiment 1 at 100% water saturation, (b) experiment 2 at 100% water saturation, (c) experiment 3 at 76% water saturation and (d) experiment 4 at 54% water saturation.

increase to 1.08 hours at 54% water saturation. The higher mean arrival times for the unsaturated column experiments correspond to reduced application rates of the virus suspension which was necessary to maintain a constant water potential throughout the packed column.

Table 5.1: First Moment Analysis for Bacteriophage MS2 and PRD1 and Bromide at 100%, 76%, and 54% Water Saturation

Tracer	Exp 1	Exp 2	Exp 3	Exp 4
	100%		76%	54%
MS2	0.80	···	1.05	1.21
PRD1	···	0.77	1.05	1.18
Br	0.77	0.71	1.04	1.08

Shown in Figure 5.2 are the normalized bacteriophage MS2 (solid circle) and PRD1 (solid square) observed concentrations for the saturated (Figures 5.2a, 5.2b) and unsaturated (Figures 5.2c, 5.2d, 5.2e, 5.2f) column experiments. The mean arrival times provided by first moment analysis of the bacteriophage concentration data and listed in Table 5.1 indicate that the mean arrival times of 0.80 and 0.77 hours for bacteriophage MS2 and PRD1, respectively, at saturation levels of 100% are slightly greater than the times for the conservative tracer. Similarly, the mean arrival time of 1.05 hours for both bacteriophage MS2 and PRD1 at 76% water saturation is only slightly greater than the arrival time for the conservative tracer. However, at a saturation level of 54%, the mean arrival times for bacteriophage MS2 and PRD1 are 1.21 and 1.18 hours, respectively. The later mean concentration arrival times of both bacteriophage are attributed to increased retention as saturation levels decrease from fully water saturated to 54% water saturation.

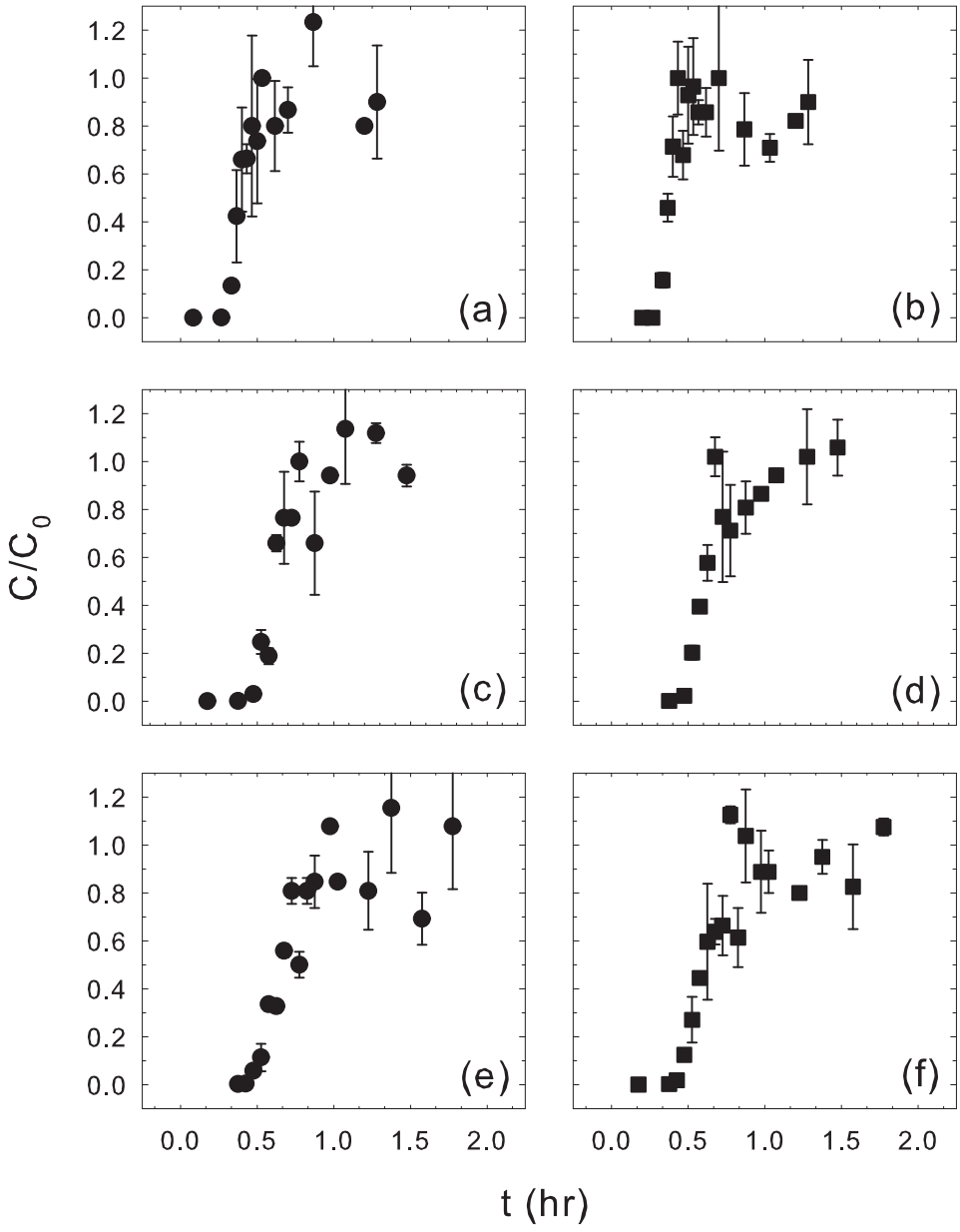

Figure 5.2: Concentration breakthrough data for bacteriophage MS2 (solid circles) and PRD1 (solid squares) at (a, b) 100% water saturation, (c, d) 76% water saturation and (e, f) 54% water saturation.

5.3.2 Model simulations

All fixed model parameter values for the model simulations are listed in Table 5.2. The values for the empirical coefficients ζ and b for sand are adopted from Cary [1994]. The unsaturated hydraulic parameters h_0 and θ_r were obtained from a soil-water retention curve generated for the sand used to pack the columns [van Genuchten et. al., 1992]. The virus inactivation rate coefficients λ, λ^*, and $\lambda^\diamond$ used to simulate the observed bacteriophage concentrations were obtained from static and dynamic batch experiments conducted to study the effects of temperature and the presence of sand on bacteriophage MS2 and PRD1 inactivation [Anders and Chrysikopoulos, 2006]. It should be noted here that although virus inactivation rate coefficients are time- and temperature-dependent [Sim and Chrysikopoulos, 1996; Chrysikopoulos and Vogler, 2004], in this study they were assumed to be constant.

Table 5.2: Fixed Model Parameters for Simulations

Parameter	Value	Units
r_p	1.25×10^{-2}	cm
ρ	1.65	g/cm^3
θ_r	0.003	cm^3/cm^3
h_0	29.94	cm
b	2	$\cdots$
ζ	160	$\cdots$
σ	72.8×10^{-3}	N/m
g	980	cm/s^2

Model transport parameters corresponding to the experimental data for bacteriophage MS2 and PRD1 during the saturated and unsaturated column experiments are listed in Table 5.3. It should be noted that the slightly different a_T values, obtained from (5.12), are due to differences in porosity of the column that occurred reassembling the column apparatus between each experiment.

Values of $a_T^{\diamond}$, calculated from (5.13), increased from 95.3 cm^{-1} to 311.1 cm^{-1} as the water saturation level was reduced from 76% to 54%.

Shown in Figure 5.3 are the model simulated bacteriophage MS2 concentration history curves (solid curves) for the saturated (Figure 5.3a) and unsaturated (Figures 5.3b, 5.3c) column experiments. The estimated values of K_d for bacteriophage MS2 varied from 33.72 cm^3/g at 100% water saturation to 380.9 cm^3/g at 76% water saturation, with an intermediate value of 136.7 at 54% water saturation. The range of K_d values suggests that a reduction in soil moisture content can enhance virus sorption by forcing viruses to move into a thin film of water surrounding soil particles. The estimated parameter k increased from 3.68×10^{-4} hr^{-1} at 100% saturation to 3.31×10^{-3} hr^{-1} at 76% water saturation and increased further to 7.59×10^{-3} hr^{-1} at 54% water saturation. In contrast, the estimated $k^{\diamond}$ value at 76% water saturation is 1.18×10^{-2} hr^{-1} and increased to 1.80×10^{-1} hr^{-1} at 54% water saturation. Studies suggesting that colloidal particles are sorbed more strongly onto air-liquid interfaces than onto liquid-solid interfaces have been reported by other investigators [Wan and Wilson, 1994].

Shown in Figure 5.4 are the model simulated bacteriophage PRD1 concentration history curves (solid curves) for the saturated (Figure 5.4a) and unsaturated (Figures 5.4b, 5.4c) column experiments. The estimated values of K_d for bacteriophage PRD1 ranged from 36.17 cm^3/g at 100% water saturation to 311.9 cm^3/g at 76% water saturation and confirms that the amount of viruses in direct contact with solids is significant under the conditions present during the unsaturated column experiments. The estimated parameter k increased from 3.20×10^{-5} hr^{-1} at 100% saturation to 1.59×10^{-3} hr^{-1} at 76% water saturation and increased further to 1.23×10^{-2} hr^{-1} at 54% water saturation. The greater influence of saturation levels on k values for bacteriophage PRD1 is due possibly to its lipid-containing structure and high hydrophobicity [Kinoshita et al., 1993]. However, the estimated $k^{\diamond}$ values of 3.51×10^{-3} hr^{-1} and 9.96×10^{-2} hr^{-1} at 76% and 54% water saturation, respectively, are less than the $k^{\diamond}$ values estimated for bacteriophage MS2 for the same saturation levels. Therefore, the degree of adsorption of bacteriophage PRD1 to air-liquid interfaces appears to

Table 5.3: Model Parameters Corresponding to the Experimental Data for Bacteriophage MS2 and PRD1

Parameter	Exp 1	Exp 2	Exp 3	Exp 4	Units
	100%		76%	54%	
θ_s	0.41	0.40	0.42	0.37	cm^3/cm^3
θ_m	···	···	0.32	0.20	cm^3/cm^3
U	37.8	41.4	24.6	25.2	cm/h
D_z	5.46	2.92	2.20	4.27	cm^2/h
a_T	141.6	144.0	139.2	151.2	cm^{-1}
$a_T^\diamond$	···	···	95.3	311.1	cm^{-1}
		MS2			
k	3.68×10^{-4}	···	3.31×10^{-3}	7.59×10^{-3}	h^{-1}
K_d	33.72	···	380.9	136.7	cm^3/g
$k^\diamond$	···	···	1.18×10^{-2}	0.18	h^{-1}
		PRD1			
k	···	3.20×10^{-5}	1.59×10^{-3}	1.23×10^{-2}	h^{-1}
K_d	···	36.17	311.9	40.75	cm^3/g
$k^\diamond$	···	···	3.51×10^{-3}	9.96×10^{-2}	h^{-1}

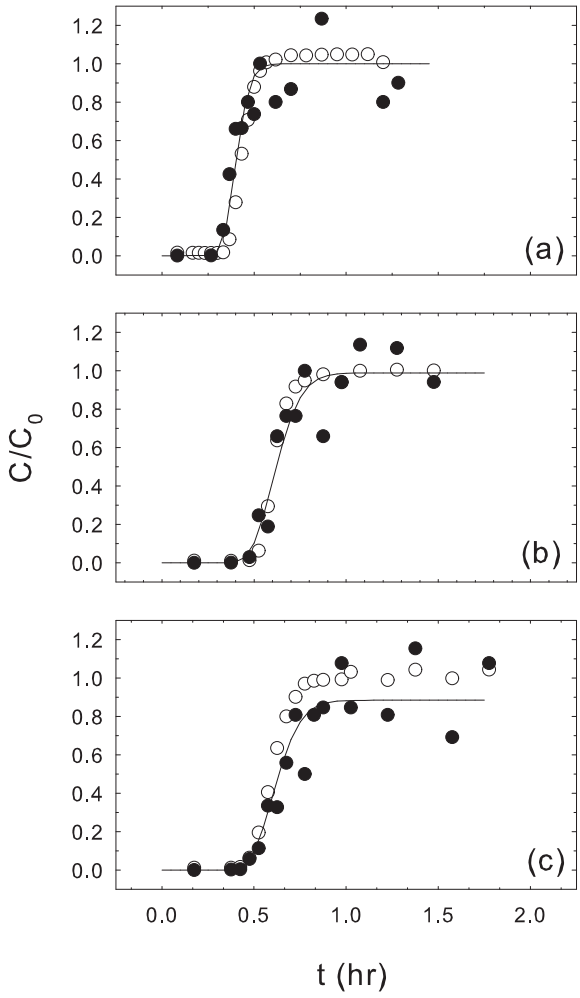

Figure 5.3: Simulated concentration histories (solid curves) for bacteriophage MS2 at (a) 100% water saturation, (b) 76% water saturation and (c) 54% water saturation. Also shown are corresponding bromide (open circles) and bacteriophage MS2 (solid circles) concentration breakthrough data. Here $r_p = 1.25\times10^{-2}$ cm, $\rho = 1.65$ g/cm^3, $\theta_r = 0.003$ cm^3/cm^3, $h_0 = 29.94$ cm, $b = 2$, $\zeta = 160$, $\sigma = 72.8\times10^{-3}$ N/m, g = 980 cm/s^2.

be limited by the inability to overcome the repulsive barrier necessary for deposition due to overall negative surface charge of both viruses and porous media [Zevi et al., 2005]. Instead, the increased k values without corresponding increases in $k^{\diamond}$ values suggest that some film straining occured as saturation levels were reduced due to the larger size of bacteriophage PRD1. It should be noted that the saturation levels achieved during experiments conducted in this study never exceeded the critical saturation levels necessary to produce film straining of bacteriophage MS2 [Wan and Tokunaga, 1997].

The model simulated normalized bacteriophage MS2 and PRD1 concentration history curves for the saturated and unsaturated column experiments are shown in Figure 5.5. Recall the later mean concentration arrival times of both bacteriophage are attributed to increased retention as saturation levels decrease from fully water saturated to 54% water saturation (see Table 5.1). However, bacteriophage MS2 and PRD1 exhibit size exclusion behavior during transport under unsaturated conditions which can be attributed to a combination of mechanisms that result in faster velocities and straighter paths.

5.3.3 Air-liquid-solid interface mass transfer coefficients

Figure 5.6 shows the calculated liquid to liquid-solid and liquid to air-liquid interface mass transfer coefficients for bacteriophage MS2 and PRD1 by employing (5.10) and (5.11) and parameters listed in Table 5.3. For bacteriophage MS2, values of κ increased from 2.60×10^{-6} cm/h to 5.02×10^{-5} cm/h as the water saturation is reduced to 54% even as the a_T values are fairly constant throughout the saturated and unsaturated experiments. The $\kappa^{\diamond}$ values increase from 1.23×10^{-4} cm/h to 5.98×10^{-4} cm/h. Therefore, the reduction in water saturation not only has the effect of increasing $\kappa^{\diamond}$ values but also increasing values of κ as well. The calculated value of $\kappa^{\diamond}$ is approximately 5 times larger than the one for κ at 76% water saturation, and increased to about 12 times larger at 54% water saturation. The $\kappa^{\diamond}$ to κ ratio increase suggests that bacteriophage MS2 are sorbed more strongly onto air-liquid interfaces than onto liquid-solid interfaces. This phenomenom provides a plausible

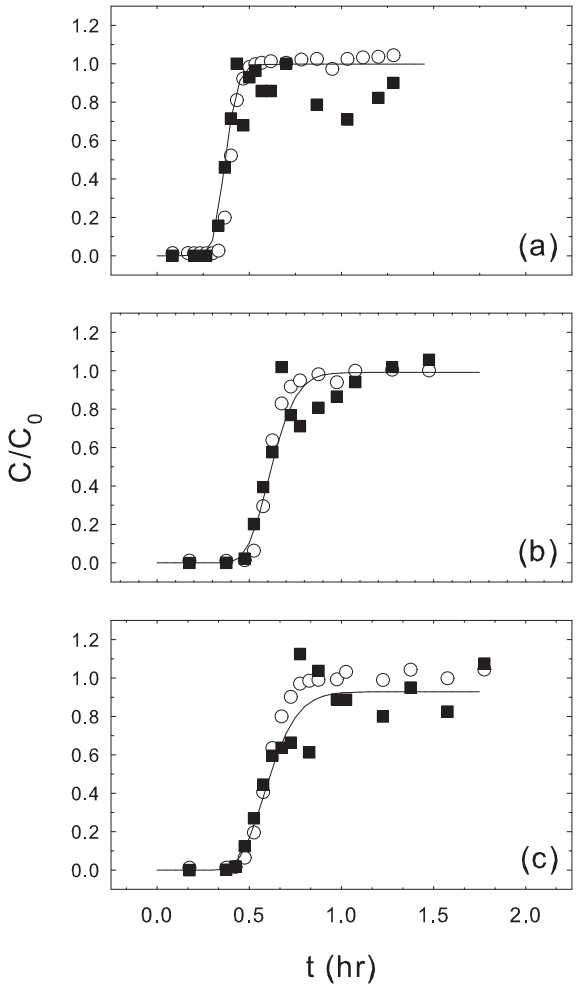

Figure 5.4: Simulated concentration histories (solid curves) for bacteriophage PRD1 at (a) 100% water saturation, (b) 76% water saturation and (c) 54% water saturation. Also shown are corresponding bromide (open circles) and bacteriophage PRD1 (solid squares) concentration breakthrough data. Here $r_p = 1.25\times10^{-2}$ cm, $\rho = 1.65$ g/cm^3, $\theta_r = 0.003$ cm^3/cm^3, $h_0 = 29.94$ cm, $b = 2$, $\zeta = 160$, $\sigma = 72.8\times10^{-3}$ N/m, g = 980 cm/s^2.

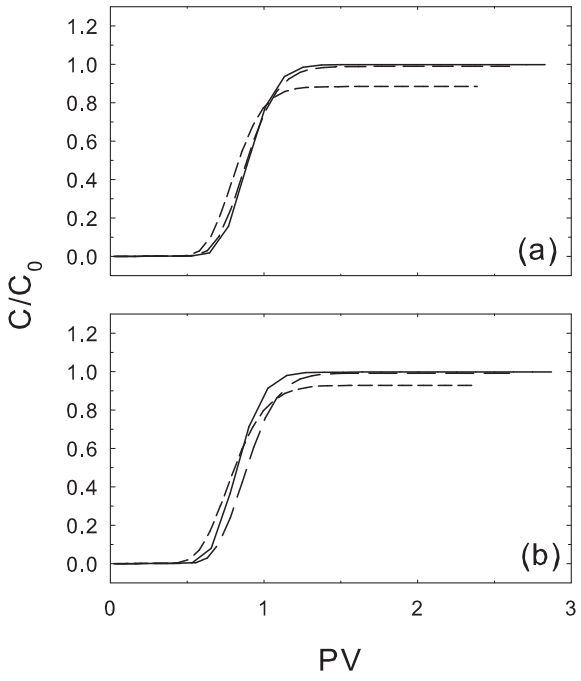

Figure 5.5: Simulated concentration histories normalized to injection rates for bacteriophage (a) MS2 and (b) PRD1 at 100% water saturation (solid curves), 76% water saturation (dash curves) and 54% water saturation (dotted curves). Here $r_p = 1.25\times10^{-2}$ cm, $\rho = 1.65$ g/cm^3, $\theta_r = 0.003$ cm^3/cm^3, $h_0 = 29.94$ cm, $b = 2$, $\zeta = 160$, $\sigma = 72.8\times10^{-3}$ N/m, g = 980 cm/s^2.

explanation for the rapid removal of viruses observed during periods of minor changes of water saturation levels in porous media during artificial recharge [Anders et al., 2004].

For bacteriophage PRD1 κ values shown in Figure 5.6 increase from 2.22×10^{-7} cm/h to 8.16×10^{-5} cm/h and $\kappa^{\diamond}$ values increase from 3.68×10^{-5} cm/h to 3.20×10^{-4} cm/h as water saturation levels are reduced from 76% to 54%. These κ and $\kappa^{\diamond}$ values are slightly less than the corresponding parameter values for bacteriophage MS2 at 76% and 54% water saturation. PRD1 exhibits a calculated $\kappa^{\diamond}$ to κ ratio of 3 and 4 at 76% and 54% water saturation, respectively. Anders and Chrysikopoulos [2006] reported that for bacteriophage PRD1 the presence of air-liquid and air-solid interfaces appeared to cause greater damage to specific viral components that are related

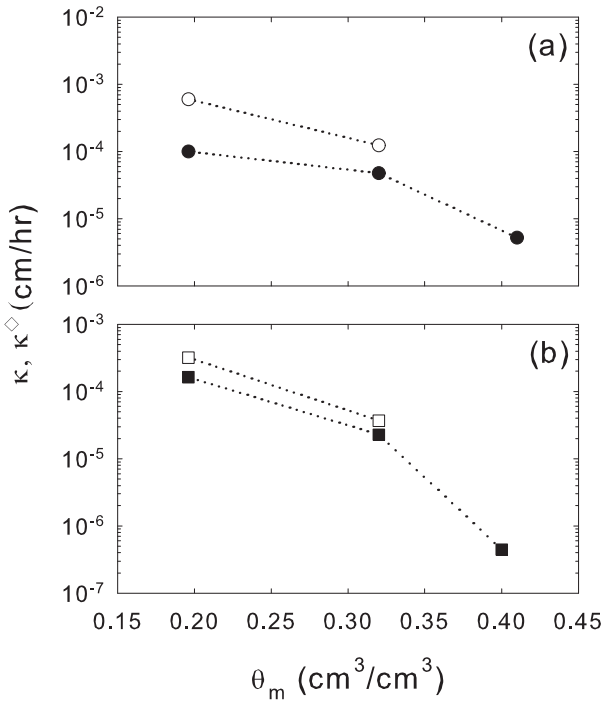

Figure 5.6: Calculated values of liquid to liquid-solid interface mass transfer coefficients (solid symbols) and liquid to air-liquid interface mass transfer coefficients (open symbols) for bacteriophage (a) MS2 and (b) PRD1 employing (5.10) and (5.11) and parameters listed in Table 5.3.

to infection than was observed for bacteriophage MS2. Therefore, for bacteriophage PRD1 it is the combination of film straining and the increased value of $\lambda^{\diamond}$ under unsaturated conditions that contributes to the lower effluent concentrations at 54% water saturation.

5.4 Summary

Laboratory-scale transport experiments were conducted in packed sand columns under saturated and unsaturated conditions using the male-specific RNA coliphage, MS2 and the *Salmonella typhimurium* phage, PRD1 as model viruses. A previously developed mathematical model was used to quantify the processes responsible for removal of viruses during vertical transport in one-dimensional, unsaturated porous media. Liquid to liquid-solid and liquid to air-liquid interface mass transfer rates were

obtained by fitting the virus transport model to the experimental data. The estimated liquid to liquid-solid and liquid to air-liquid interface mass transfer rates increased for both bacteriophage as saturation levels were reduced from 100% to 54%. It was observed that bacteriophage MS2 are sorbed more strongly onto air-liquid interfaces than onto liquid-solid interfaces. For bacteriophage PRD1 it is the combination of several processes that contributes to the lower effluent concentrations at 54% water saturation. Therefore, even under unfavorable attachment conditions within a sand column (eg., lacking organic matter; pH = 7.5; ionic strength = 2 mM), saturation fluctuations can dramatically affect virus transport through porous media.

Chapter 6

Application and Engineering Significance of Results

The newly developed virus transport model presented in Chapter 3 successfully simulated observed concentration data collected from a field-scale recharge experiment. The most conservative ϕ value for MS2 suggests that over 40-log removal of bacteriophage would occur in 153 m of passage through the subsurface formation. Furthermore, the estimated λ value for PRD1 in the test basin suggests that almost 38-log removal of bacteriophage would occur in 6 months. Having a transport model that considers virus removal by attachment and/or inactivation is necessary to determine adequate soil-retention time and distance requirements for pathogen removal during the design of groundwater recharge programs. This work also illustrates the importance of conducting field-scale tracer experiments at a specific site under actual recharge conditions with recycled water using surrogates for human viruses to verify established setback requirements.

The pseudo first-order inactivation model presented in Chapter 4 successfully described the inactivation process of bacteriophage MS2 and PRD1 in static and dynamic batch experiments. The analysis of the thermodynamic properties determined from the time-dependent inactivation rates provides a methodology to predict the effects of temperature and the presence of sand on the inactivation process of other viruses in groundwater. Furthermore, the observed temporal variation

of the inactivation rate coefficients suggest that virus subpopulations may remain infective in porous media for an extended period of time and continue to migrate downstream to points of withdrawal.

A mathematical model developed to quantify the processes responsible for removal of viruses during vertical transport in unsaturated porous media successfully simulated bacteriophage MS2 and PRD1 concentration breakthrough data obtained from laboratory-scale transport experiments. The ability to obtain calibrated liquid to liquid-solid and liquid to air-liquid interface mass transfer rates provides insight into the processes responsible for the retention of viruses in unsaturated porous media.

The methods developed in this research quantify how to make effective use of the soil to protect public health in planned water-reuse programs. The results provide the information necessary to determine allowable limits on amounts of recycled water that can be used for replenishment purposes while ensuring that adequate soil-retention time and distance requirements for pathogen removal are being met. Such information could be used by regulatory agencies to determine the permissible limits on the amount of recycled water that can be used for replenishment purposes while ensuring that necessary retention times for pathogen removal are being met.

Chapter 7

Conclusions and Future Research

7.1 Conclusions

Firstly, virus concentrations measured during an artificial recharge field-scale experiment were fitted using a newly developed mathematical model that simulates virus transport in one-dimensional homogeneous, water-saturated porous media accounting for virus sorption (or filtration), inactivation, and time-dependent source concentration. The fitted model parameters include the clogging and declogging rate constants, and the inactivation rate constants of suspended and sorbed viruses. These fitted parameters were used to estimate the time-dependent field-scale collision efficiency factors of bacteriophage (MS2 and PRD1). The experimental results of this research can be used for the development of an optimal management scenario that can maximize the amount of recycled water applied to the spreading grounds while still maintaining favorable attachment conditions for virus retention.

Secondly, static and dynamic batch experiments were conducted to study the effects of temperature and the presence of sand on the inactivation of bacteriophage MS2 and PRD1. The experimental data suggested that the inactivation process can be satisfactorily represented by a pseudo first-order expression with time-dependent rate coefficients. The time-dependent rate coefficients were used to determine pertinent thermodynamic properties required for the analysis of the molecu-

lar processes involved in the inactivation of each bacteriophage. A combination of high temperature and the presence of sand appears to produce the greatest disruption to the surrounding protein coat of MS2. However, the lower activation energies for PRD1 indicate a weaker dependence of the inactivation rate on temperature. Instead, the presence of air-liquid and air-solid interfaces appears to produce the greatest damage to specific viral components that are related to infection. These results indicate the importance of using thermodynamic parameters based on the time-dependent inactivation model to better predict the inactivation of viruses in groundwater.

Thirdly, laboratory-scale transport experiments were conducted in packed sand columns under saturated and unsaturated conditions using the male-specific RNA coliphage, MS2 and the *Salmonella typhimurium* phage, PRD1 as model viruses. A mathematical model developed to quantify the processes responsible for removal of viruses during vertical transport in one-dimensional, unsaturated porous media that accounts for virus sorption and inactivation was used to analyze the data collected from the column experiments. Liquid to liquid-solid and liquid to air-liquid interface mass transfer rates for the mathematical model were obtained by fitting the experimental data with a nonlinear least squares regression method. The calibrated liquid to liquid-solid and liquid to air-liquid interface mass transfer rates used to simulate the concentration histories increased for both bacteriophage as saturation levels were reduced from 100% to 54%. Therefore, even under unfavorable attachment conditions within a sand column (eg., lacking organic matter; pH = 7.5; ionic strength = 2 mM), saturation fluctuations can dramatically affect virus transport through porous media.

7.2 Future Research

The research presented here has answered several questions concerning the fate and transport of viruses during field-scale infiltration. However, many questions remain. Below, I have listed several topics for future studies.

7.2.1 In the Field

1. Recharge experiments conducted at the research field site showed that the reduction of aqueous nitrogen was slightly greater than one-third and the reduction of dissolved organic carbon (DOC) was about one-third, although actual removal rates of aqueous nitrogen varied under different environmental and operational conditions but DOC did not. However, the conditions that would maximize the removal rates of viruses during recharge have not been identified yet.

2. Tracer experiments conducted at the research field site indicated that rapid reduction occurs in the concentration of bacterial viruses released into the environment with recycled water during aquifer recharge. Collision efficiency factors for MS2 and PRD1 confirmed that favorable attachment conditions existed for both bacteriophage, although these values varied between experiments. Therefore, additional studies are needed to identify what factors might contribute to variability in attachment conditions between tracer experiments.

3. As the research presented here has demonstrated, the saturation levels of the porous media has a dramatic effect on the retention and inactivation of viruses. Therefore, field-scale tracer experiments conducted during unsaturated conditions would also provide valuable information to develop ground-water recharge programs.

4. Lastly, conducting several field-scale recharge experiments with surrogates for human viruses would provide large hydraulic and concentration datasets for parameter sensitivity analysis to be performed using the newly developed virus transport model.

7.2.2 In the Laboratory

1. As this research has demonstrated, the electrostatic character of bacteriophage MS2 and PRD1 influences their inactivation and sorption processes in the presence of air-liquid-solid interfaces both in batch and column experiments. Further investigation into this phenomena is recommenced with other commonly used viruses and different types of soils.

2. Natural organic matter (NOM) is present in recycled water and has been suggested to influence the transport behavior of viruses. Experiments conducted to examine the influence of NOM on the transport of viruses in saturated and unsaturated porous media is warranted.

3. Because filed-scale tracer experiments are expensive and difficult to carry out, a comparison of transport parameters for model viruses and microspheres is also a recommenced area of future study. Preliminary work suggests that fluctuations in moisture content effects differently the transport of viruses and microspheres.

4. Most importantly is the possible influence of biofilm growth on the fate and transport of viruses during artificial recharge. The presence of subsurface biofilm during the recharge experiment is evident by the removal of aqueous nitrogen and DOC. Also, biofilm is attributed to the reduction in infiltration rates. However, it is not know how biofilm might influence viruses sorption and inactivation processes during recharge.

Chapter 8

References

Abdel-Salam, A., and C.V. Chrysikopoulos, Modeling of colloid and colloid-facilitated contaminant transport in a two-dimensional fracture with spatially-variable aperture, *Transp. Porous Media*, 20, 197-221, 1995.

Abramowitz, M. and I.A. Stegun, *Handbook of Mathematical Functions*, 1046 pp., Dover, 1972.

Adams, M.H., *Bacteriophages*, 592 pp., Interscience Publishers, New York, 1959.

Anders, R., and C.V. Chrysikopoulos, Evaluation of the factors controlling the time-dependent inactivation rate coefficients of bacteriophage MS2 and PRD1, *Environ. Sci. and Tech.*, submitted.

Anders, R., and C.V. Chrysikopoulos, Virus fate and transport during artificial recharge with recycled water, *Water Resour. Res.*, 41, W10415, doi:10.1029/2004WR003419.

Anders, R. and R.A. Schroeder, Use of water-quality indicators and environmental tracers to determine the fate and transport of recycled water in Los Angeles County, California: U.S. Geological Survey Water-Resources Investigations Report, 104 p., 2003.

Anders, R., W.A. Yanko, R.A. Schroeder, and J.L. Jackson, Virus fate and transport during recharge using recycled water at a research field site in the Montebello Forebay, Los Angeles County,

California, 1997–2000: U. S. Geological Survey Scientific Investigation Report 2004-5161, 65 p., 2004.

Atkins, P.W., *Physical Chemistry, 4^{th} Edition*, 995 pp., Oxford University Press, New York, 1990.

Asano, T., and J.A. Cotruvo, Groundwater recharge with reclaimed municipal wastewater: health and regulatory considerations, *Water Res.*, 38, 1941-1951, 2004.

Auset, M., and A.A. Keller, Pore-scale processes that control dispersion of colloids in saturated porous media, *Water Resour. Res.*, 40, W03503, doi:10.1029/2003WR002800.

Bales, R.C., S.R. Hinkle, T.W. Kroeger, K. Stockling, and C.P. Gerba, Bacteriophage adsorption during transport through porous media: Chemical perturbations and reversibility, *Environ. Sci. Tech.* 25, 2088-2095, 1991.

Bales, R.C., S. Li, T.C.J. Yeh, M.E. Lenczewski, and C.P. Gerba, Bacteriophage and microscope transport in saturated porous media: Forced-gradient experiment at Borden, Ontario, *Water Resour. Res.*, 33, 639-648, 1997.

Barclays California Code of Regulations, Ground water recharge: Title 26, Sect. 22.60320, (loose leaf), 1978.

Bear, J., *Dynamics of Fluids in Porous Media*, Dover Publications, Inc. New York, 1972.

Beck, J.V. and K.J. Arnold, Parameter Estimation in Engineering and Science, 501 pp., Wiley, New York, 1997.

Bookman-Edmonston Engineering, Inc., Hydrologic Assessment and Background Data for Domestic Wells within 500 Feet of the Montebello Forebay Recharge Areas. Bookman-Edmonston Engineering, Inc., 100 North Broad Boulevard, Suite 600, Glendale, CA. 91203-2699, 10 sections, 1994.

California Department of Health Services, Wastewater reclamation criteria, an excerpt from the California Administrative Code, Title 22, Division 4, Environmental Health: Engineering

Section, Berkeley Calif., (loose leaf), 1978.

Cary, J.W., Estimating the surface area of fluid phase interfaces in porous media, *J. Contam. Hydrol.*, 15, 243-248, 1994.

Chrysikopoulos, C.V., Artificial tracers for geothermal reservoir studies, *Environ. Geology*, 22, 60-70, 1993.

Chrysikopoulos, C.V., and K.Y. Lee, Contaminant transport resulting from multicomponent non-aqueous phase liquid pool dissolution in three-dimensional subsurface formations, *J. Contam. Hydrol.*, 31, 1-21, 1998.

Chrysikopoulos, C.V., P.V. Roberts, and P.K. Kitanidis, One-dimensional solute transport in porous media with partial well-to-well recirculation: Application to field experiments, *Water Resour. Res.*, 26, 1189-1195, 1990.

Chrysikopoulos, C.V., and Y. Sim, One-dimensional virus transport in homogeneous porous media with time dependent distribution coefficient, *J. Hydrol.*, 199-219, 1996.

Chrysikopoulos, C.V., and E.T. Vogler, Estimation of time dependent virus inactivation rates by geostatisical and resampling techniques: application to virus transport in porous media, *Stochastic Environ. Res. Risk Assess.*, 18(2), 67-78, 2004.

Chu, Y., Y. Jin, M. Flury, and M.V. Yates. 2000. Virus transport through saturated sand columns as affected by different buffer solutions, *J. Environ. Qual.*, 29, 1103-1110.

Craft, T.F., and G.G. Eichholz, Mechanism of rapid filtration in a uniform filter bed, *Water Resour. Res.*, 6, 527-537, 1970.

Debartolomeis, J., and V.J. Cabelli, Evaluation of an *Escherichia coli* host strain for enumeration of male-specific bacteriophages, *Appl. Environ. Microb.*, 57, 1301-1305, 1991.

Deborde, D.C., W.W. Woessner, Q.T. Kiley, and P. Ball, Rapid transport of viruses in a floodplain aquifer, *Water Res.* 33, 2229-2238, 1999.

Enfield, C.G., G. Bengtsson, and R. Lindqvist, Influence of macromolecules on chemical-transport, *Environ. Sci. Technol.*, 23, 1278-1286,

Faybishenko, B.A., Hydraulic behavior of quasi-saturated soils in the presence of entrapped air: Laboratory experiments, *Water Resour. Res.*, 31, 2421-2435, 1995.

Fogler, H.S., *Elements of Chemical Reaction Engineering*, 2nd ed., Prentice Hall, 1992.

Gerba, C.P., Applied and theoretical aspects of virus adsorption to surfaces, *Adv. Appl. Microb.*, 30, 133-168, 1984.

Gerba, C.P., and B.H. Keswick, Survival and transport of enteric bacteria and viruses in groundwater, *Stud. Environ. Sci.*, 17, 511-515, 1981.

Ginn, T.R., A travel time approach to exclusion on transport in porous media, *Water Resour. Res.*, 38, W01041, doi:10.1029/2001WR000865.

Ginoza, W. Inactivation of viruses by ionizing radiation and by heat, p. 139-209. *In* K. Maramorosch and H. Koprowski (eds.), Methods in virology. Academic Press, Inc., New York, 1968.

Grant, S.B., Virus coagulation in aqueous environments, *Environ. Sci. Tech.*, 28, 928-933, 1994.

Grant, S.B., E.J. List, and M.E. Lidstrom. Kinetic analysis of virus adsorption and inactivation in batch experiments: Virus adsorption, virus inactivation, and equilibrium isotherms, *Water Resour. Res.*, 29, 2067-2085. 2607-2611, 1994.

Grosser, P.W., A one-dimensional mathematical model of virus transport, paper presented at the Second International Conference on Ground-Water Quality Research, Univ. Cent. for Water Res., Okla. State Univ., Tulsa, Okla., March 26-29, 1984.

Guymon, G.L., *Unsaturated zone Hydrology*, Prentice Hall, 1994.

Harter, T., S. Wagner, and E.R. Atwill, Colloid transport and filtration of *Cryptosporidium parvum* in sandy soils and aquifer sediments, *Environ. Sci. Tech.*, 34, 62-70, 2000.

Harvey, R.W., and S.P. Garabedian, Use of colloid filtration theory in modeling movement of bacteria

through a contaminated sandy aquifer, *Environ. Sci. Tech.*, 25, 178-185, 1991.

Harvey, R.W., and J.N. Ryan, Use of PRD1 bacteriophage in groundwater viral transport, inactivation, and attachment studies, *FEMS Microbiol. Eco.*, 49, 3-16, 2004.

Hultquist, R., Reuse of Water for Groundwater Recharge in California, presented at the Water Reuse Foundation Annual Meeting, Manhattan Beach, California, 2002.

Hultquist, R.H., R.H. Sakaji, and T. Asano, Proposed California regulations for ground water recharge with reclaimed municipal wastewater, in: Proceedings of the 1991 Specialty Conference, Environmental Engineering, ASCE, Reno, Nev., pp. 759-764, 1991.

Hurst, C.J., C.P. Gerba, and I. Cech, Effects of environmental variables and soil characteristics on virus survival in soil, *Appl. Environ. Microb.*, 40, 1067-1079, 1980.

IMSL, *IMSL MATH/LIBRARY user's manual, 2.0*, IMSL: Houston, 1991.

Jansons, J., L.W. Edmonds, B. Speight, and M.R. Bucens, Survival of viruses in groundwater, *Wat. Res.*, 23, 301-306, 1989.

Jin, Y., Y. Chu, Y. Li, Virus removal and transport in saturated and unsaturated sand columns, *J. Contam. Hydrol.*, 43, 111-128, 2000.

Jin, Y., M.V. Yates, S. S. Thompson, and W.A. Jury, Sorption of viruses during flow through saturated sand columns, *Environ. Sci. Tech.*, 31, 548-555, 1997.

Keller, A.A., S. Sirivithayapakorn, and C.V. Chrysikopoulos, Early breakthrough of colloids and bacteriophage MS2 in a water-saturated sand column, *Water Resour. Res.*, 40, W08304, doi:10.1029/2003WR002676.

Kinoshita, T., R.C. Bales, K.M. Maguire, and C.P. Gerba, Effect of pH on bacteriophage transport through sandy soils, *J. Contam. Hydrol.*, 14, 55-70, 1993.

Kott, Y. Estimation of low numbers of Escherichia coli bacteriophage by use of the most probable number method, *Appl. Environ. Microb.*, 14, 141, 1966.

Lance, J.C., and C.P. Gerba, Virus movement in soil during saturated and unsaturated flow, *Appl. Environ. Microb.*, 47(2), 335-337, 1984.

Leenheer, J.A., Rostad, C.E., Barber, L.B., II, Schroeder, R.A., Anders, R., and Davisson, M.L., Nature and chlorine reactivity of organic constituents for reclaimed water in groundwater, Los Angeles County, California: Environmental Science and Technology, v. 35, p. 3869-3876, 2001.

Levenberg, K., A method for the solution of certain nonlinear problems in least squares, *Quart. Appl. Math.*, 2, 164-168, 1944.

Logan, B.E., D.G. Jewitt, R. G. Arnold, E. J. Bouwer, and C. R. O'Melia, Clarification of clean-bed filtration models, *J. Environ. Eng.*, 121, 869–873, 1995.

Marquardt, D.W., An algorithm for least-squares estimation of nonlinear parameters, *SIAM J. Appl. Math.*, 11, 431-441, 1963.

Moore, R.S., D.H. Taylor, M.M.M. Reddy, and L.S. Sturman, Adsorption of reovirus by minerals and soils, *Appl. Environ. Microb.*, 44(4), 852-859, 1982.

Morel, F.M.M., and J.G. Hering. *Principles and Applications of Aquatic Chemistry*, Wiley, New York, 588 pp., 1993.

Murray, J.P., and S.J. Laband. Degradation of poliovirus by adsorption on inorganic surfaces, *Appl. Environ. Microbiol.*, 37, 480-486, 1979.

National Research Council, Ground water recharge using waters of impaired Quality: National Academy Press, Washington D.C., 1994.

Nielsen, D.R., M. Th. van Genuchten, and J.W. Biggar, Water flow and solute transport processes in the unsaturated zone, *Water Resour. Res.*, 22(9), 89S-108S, 1986.

Park N.-S., T.N. Blanford, and P.S. Huyakorn, VIRALT: A modular semi-analytical and numerical model for simulating viral transport in ground water, report, Int. Ground Water Model.

Cent., Colo. Sch. of Mines, Golden, 1992.

Parker, J.C., and M. Th. van Genuchten, Flux-averaged and volume-averaged concentrations in continuum approaches to solute transport, *Water Resour. Res.*, 20(7), 866-872, 1984.

Parkinson, J.S., and R.J. Huskey. Deletion mutants of bacteriophage Lambda, 1, Isolation and initial characterization, *J. Mol. Biol.*, 56, 369-384, 1971.

Penrod, S.L., T.M. Olson, and S.B. Grant, Deposition kinetics of two viruses in packed beds of quartz granular media, *Langmuir*, 12, 5576-5587, 1996.

Philip, J.R., The theory of infiltration, in *Advances in Hydroscience*, vol. 5, edited by V.T. Chow, pp. 215-296, Academic, San Diego, Calif., 1969.

Pieper, A.P., J.N. Ryan, R.L. Amy, T.H. Illangasekare, and D.W. Metge, Transport and recovery of bacteriophage PRD1 in a sand and gravel aquifer: Effect of sewage-derived organic matter, *Environ. Sci. Tech.*, 31, 1163-1170, 1997.

Pollard, E.C., and W. Solosko. The thermal inactivation of T_4 and λ bacteriophage, *Biophys. J*, 11, 66-74, 1971.

Powelson, D.K., J.R. Simpson, and C.P. Gerba, Virus transport and survival in saturated and unsaturated flow through soil columns, *J. Environ. Qual.*, 19, 396-401, 1990.

Press, W.H., S.A. Teukolsky, W.T. Vetterling, and B.P. Flannery, *Numerical Recipes in Fortran 77: The Art of Scientific Computing*, 931 pp., Cambridge University Press, New York, 1992.

Preston, D.R., and S.R. Farrah. Activation thermodynamics of virus adsorption to solids, *Appl. Environ. Microbiol.*, 54, 2650-2654, 1988.

Rajagopalan R., and C. Tien, Trajectory analysis of deep-bed filtration with the sphere-in-cell porous media model, *AIChE J.*, 22, 523-533, 1976.

Redman, J.A., S.B. Grant, T.M. Olson, M.E. Hardy, and M.K. Estes, Filtration of recombinant norwalk virus particles and bacteriophage MS2 in quartz sand: Importance of electrostatic

interactions, *Environ. Sci. Tech.*, 31, 3378-3383, 1997.

Rehmann, L.L.C., C. Welty, and R.W. Harvey, Stochastic analysis of virus transport in aquifers, *Water Resour. Res.*, 35, 1987-2006, 1999.

Reichard, E.G., Land, M., Crawford, S.M., Johnson, T., Everett, R.R., Kulshan, T.V., Ponti, D.J., Halford, K.L., Johnson, T.A., Paybins, K.S., and Nishikawa, T., Geohydrology, geochemistry, and ground-water simulation-optimization of the Central and West Coast Basins, Los Angeles County, California: U.S. Geological Survey Water-Resources Investigations Report, 184 p., 2003.

Ryan, J.N., E. Elimelech, R.A. Ard, R.W. Harvey, and P. R. Johnson, Bacteriophage PRD1 and silica colloid transport and recovery in an iron oxide-coated sand aquifer, *Environ. Sci. Tech.* 33, 63-73, 1999.

Ryan, J.N., R.W. Harvey, D. Metge, M. Elimelech, T. Navigato, and A.P. Pieper. Field and laboratory investigations of inactivation of viruses (PRD1 and MS2) attached to iron oxide-coated quartz sand, *Environ. Sci. Technol.*, 36, 2403-2413, 2002.

Schijven, J.K., W. Hoogenboezem, S. M. Hassanizadeh, and J. H. Peters, Modeling removal of bacteriophages MS2 and PRD1 by dune recharge at Castricum, Netherlands, *Water Resour. Res.*, 35, 1101-1111, 1999.

Schijven J.F., H.A.M. de Bruin, S. M. Hassanizadeh, and A.M. de Roda Husman, Bacteriophage and Clostridium spores as indicator organisms for removal of pathogens by passage through saturated dune sand, *Water Res.*, 37, 2186-2194, 2003.

Schroeder, R.A., R. Anders, L.B. Barber, J. A. Leenheer, T.I. Noyes, R.T. Rathbun, K.A. Thorn, and S.J. Younger, Water-quality changes and organic-carbon characterization during recharge with recycled water at a recharge basin in Montebello Forebay, Los Angeles County, California, 1991-1996: U.S. Geological Survey Water-Resources Investigations Report 03–3146, 260 p., 2003.

Sim, Y., and C.V. Chrysikopoulos, Analytical models for one-dimensional virus transport in saturated porous media, *Water Resour. Res.*, 31, 1429-1437, 1995. (Correction, *Water Resour. Res.*, 32, 1473, 1996.)

Sim, Y., and C.V. Chrysikopoulos, One-dimensional virus transport in porous media with time-dependent inactivation rate coefficients, *Water Resour. Res.*, 32, 2607-2611, 1996.

Sim, Y., and C.V. Chrysikopoulos, Three-dimensional analytical models for virus transport in saturated porous media, *Transport in Porous Media*, 30, 87-112, 1998.

Sim, Y., and C.V. Chrysikopoulos, Analytical models for virus adsorption and inactivation in unsaturated porous media, *Colloids Surfaces A: Physicochem. Eng. Aspects*, 1999.

Sim, Y., and C.V. Chrysikopoulos, Virus transport in unsaturated porous media, *Water Resour. Res.*, 36, (1), 173-179, 2000.

Sinton, L.W., R.K. Finlay, and P. A. Lynch, Sunlight inactivation of fecal bacteriophage and bacteria in sewage-polluted seawater, *Appl. Environ. Microb.*, 65, 3605-3613, 1999.

Sirivithayapakorn, S., and A. Keller, Transport of colloids in saturated porous media: A pore-scale observation of the size exclusion effect and colloid acceleration, *Water Resour. Res.*, 39, 1109, doi:10.1029/2002WR001583.

Sobsey, M.D., C.H. Dean, M.E. Knuckles, and R.A. Wagner, Interactions and survival of enteric viruses in soil materials, *Appl. Environ. Microbiol.*, 40, 92-101, 1980.

Taylor, D.H., and H.B. Bosman, The electrokinetic properties of reovirus type 3: Electrophoretic mobility and zeta potential in dilute electrolytes, *J. Colloid Inter. Sci.*, 83, (1), 153-162, 1981.

Thompson, S.S., M. Flury, M.V. Yates, and W.A. Jury, Role of air-water interface in bacteriophage sorption experiments, *Appl. Env. Microb.*, 64(1), 304-309, 1998.

Thompson, S.S., and M.V. Yates. Bacteriophage inactivation at the air-water-solid interface in dynamic batch systems, *Appl. Environ. Microbiol.*, 65, 1186-1190, 1999.

Tim, U.S., and S. Mostaghimi, Model for predicting virus movement through soils, *Ground Water*, 29, 251-259, 1991.

Truesdail, S.E., J. Lukasik, S.R. Farrah, D.O. Shah, and R.B. Dickinson, Analysis of bacterial deposition on metal (Hydr) oxide-coated sand filter media, *J. Colloid Interface Sci.*, 203, 123, 1998.

Tufenkji, N., and M. Elimelech, Correlation equation for predicting single-collector efficiency in physicochemical filtration in saturated porous media, *Environ. Sci. Tech.*, 38, 529-536, 2004.

Tufenkji, N., J.A. Redman, and M. Elimelech, Interpreting deposition patterns of microbial particles in laboratory-scale column experiments, *Environ. Sci. Technol.*, 37, 616-623, 2003.

Valocchi, A.J., Validity of the local equilibrium assumption for modeling sorbing solute transport through homogeneous soils, *Water Resour. Res.*, 21, 808-820, 1985.

van Genuchten, M. Th., F.J. Leij, and S.R. Yates, The RETC Code for Quantifying Hydraulic Functions of Unsaturated Soils, EPA/600/S2-91/065, 1992.

Veerapaneni, S., and M.R. Wiesner., Deposit morphology and head loss development in porous media, *Environ. Sci. Technol.*, 31, 2738-2744, 1997.

Vilker, V.L., and W.D. Burge, Adsorption mass transfer model for virus transfer in soils, *Water Res.*, 14, 783-790, 1980.

Wan, J., and J.L. Wilson, Colloid transport in unsaturated porous media, *Water Resour. Res.*, 30(4), 857-864, 1994.

Wan, J., and T.K. Tokunaga, Film straining of colloids in unsaturated porous media: conceptual model and experimental testing, *Environ. Sci. Technol.*, 31,(8), 2413-2420, 1997.

Wan, J., and T.K. Tokunaga, Measuring partition coefficients of colloids at air-water interfaces, *Environ. Sci. Technol.*, 32, 3293-3298, 1998.

Yahya, M.T., L. Galsomies, C.P. Gerba, and R.C. Bales, Survival of bacteriophage MS-2 and PRD-1

in ground water, *Wat. Sci. Tech.*, 27, 409-412, 1993.

Yamagishi, H., and H. Ozeki. Comparative study of thermal inactivation of phage ϕ80 and Lambda, *Virology*, 48, 316-322, 1972.

Yanko, W.A., J.L. Jackson, F.P. Williams, A.S. Walker, and M.S. Castillo, An unexpected temporal pattern of coliphage isolation in groundwaters sampled from wells at varied distances from reclaimed water recharge sites, *Water Res.*, 33, 53-64, 1999.

Yao, K.M., M.T. Habibian, and C.R. O'Melia, Water and waste water filtration: Concepts and applications, *Environ. Sci. Technol.*, 5, 1105-1112, 1971.

Yates, M.V., Modeling virus survival and transport in the subsurface, *J. Contam. Hydrol.*, 1 , 329-345, 1987.

Yates, M.V., C.P. Gerba, and L.M. Kelly, Virus persistence in groundwater, *Appl. Environ. Microb.*, 49, 778-781, 1985.

Yates, M.V., and Y. Ouyang, VIRTUS, a model of virus transport in unsaturated soils, *Appl. Environ. Microb.*, 58, 1609-1616, 1992.

Yates, M.V. and S.R. Yates, J. Wagner, and C.P. Gerba. Modeling virus survival and transport in the subsurface, *J. Contam. Hydrol.*, 1, 329-345, 1987.

Zerda, K.S., Adsorption of viruses to charge-modified Silica. PhD dissertation, Department of Virology and Epidemiology, Baylor College of Medicine, Houston.

Zevi, Y., A. Dathe, J.F. McCarthy, B.K. Richards, and T.S. Steenhuis, Distribution of colloid particles onto interfaces in partially saturated sand, *Environ. Sci. Technol.*, 39, 7005-7064, 2005.